Partitioning of Acidic Solutes between Water and Supercritical
Carbon Dioxide

by

Meredith S. Curren

A thesis submitted to
the Faculty of Graduate Studies and Research
in partial fulfillment of
the requirements for the degree of

Doctor of Philosophy

Chemistry Department

Carleton University
Ottawa, Ontario
July 7, 1999
© copyright
1999, M. S. Curren

0-612-48326-6

Canada

ABSTRACT

A high pressure stainless steel extraction cell was constructed to measure the solubilities and partitioning coefficients of several acidic and non-polar solutes in water and liquid and supercritical carbon dioxide. On-line analysis of both phases was possible by HPLC.

Solubilities in carbon dioxide were determined as functions of temperature and pressure. The solubilities of all solutes increased with increasing pressure and temperature. Crossovers of isotherms were observed for the solubility of pentachlorophenol in CO_2 as a function of pressure. Analyte solubilities were also measured in water at atmospheric pressure, and in pressurized water for pentachlorophenol. The solubility of pentachlorophenol in water decreased as the pressure was increased, indicating PCP has a positive volume change upon solution in water.

The partitioning of pentachlorophenol between water and CO_2 was measured as a function of pressure, temperature, solute concentration, and pH and ionic strength of the water. Partitioning was higher as the pressure was increased, but increasing the temperature caused the partitioning of PCP to drop significantly. The distribution coefficient (K) increased as the pH was decreased; K was highest for a solution with a high ionic strength.

The partitioning of pentachlorophenol was modeled with the Peng-Robinson equation of state using concentration dependent mixing rules. The interaction parameter between CO_2 and PCP was sensitive to both PCP concentration and temperature.

The partitioning data were compared to the ratio of solubilities in the two phases. K was significantly smaller than the solubility ratio, likely due to the mutual solubilities of CO_2 and water, and to the fact that the partitioning experiments were performed at much lower analyte concentrations.

The results indicate that supercritical CO_2 could be used to extract polar or acidic species from water for analytical or remediative purposes.

ACKNOWLEDGEMENTS

This thesis is dedicated to my parents, Janet Martin and Thomas Curran, to my sister, Kristina Curren, and to my fiancé, Eric Stroud. Thanks are not enough for the unlimited support, time, patience, and understanding they have provided. I looks toward you all!

Bob Burk has been a friend, mentor, and supervisor for many years. Through his example I have learned to strive for the standard of excellence, even in frustrating times when one is tempted to settle for mediocrity. Thanks for forgetting about the many beers I still owe you, for guiding me through the "yellow book", and for reminding me the important things in life are at home and on the water.

Wayne Mullett has listened to my psycho-babble over countless coffees, subs, and visits to the Oasis. He has in turn regaled me with his escapades to every Irish bar in Ottawa and with his memories from the Rock. Thanks for being a courier of partridgeberries and for contributing many ideas to my research.

Robert Kehle provided a hideaway where I could laugh, vent, and howl about the events in my life. He always found time to listen and laugh in between rushing through orders for supplies that "I absolutely had to have yesterday".

Rocio Aranda, Bio Aikawa, Marcin Pawlak, and Victoria Nawaby were always ready to lend a hand. I especially enjoyed the diversity of our backgrounds at potlucks! Group meetings at Mike's Place and on Bob's sailboat will never be forgotten.

Many other people have made the bumpy road of research a little smoother: Keith Bourque, Tony O'Neil, Angela Kiss, and everyone who has laughed and gabbed with me in the hallways over the years.

PUBLICATIONS AND PRESENTATIONS

Portions of this work have been published and presented as follows:

Publications

Meredith S. Curren, Robert C. Burk. Supercritical Fluid Extraction of Acidic, Polar Solutes from Aqueous Matrices: Partitioning Data for Pentachlorophenol between Carbon Dioxide and Water. *J. Chem. Eng. Data* **1998**, 43, 978-982.

Meredith S. Curren, Robert C. Burk. Solubilities of Acidic Pesticides in Water and Supercritical and Liquid Carbon Dioxide. *J. Chem. Eng. Data* **1997**, *42*, 727-730.

Meredith Curren, Robert C. Burk. "Supercritical Fluid Extraction of Acidic, Polar solutes from Aqueous Matrices: Partitioning Data for Pentachlorophenol" in *Proceedings of the Second Biennial International Conference on Chemical Measurement and Monitoring of the Environment*, R. Burk and R. Clement, Eds., **1998**.

Presentations

Annual Meeting of the American Institute of Chemical Engineers, Los Angeles, 1997

*Enviro*Analysis, Ottawa, Canada, 1996/1998

79th Canadian Society for Chemistry Conference and Exhibition, St. John's, Canada, 1996

TABLE OF CONTENTS

LIST OF TABLES

LIST OF FIGURES

LIST OF APPENDICES

CHAPTER ONE

INTRODUCTION

1.1 Supercritical Fluid and Conventional Water Extractions

Over the past decade, supercritical fluid (SF) technologies have been investigated as alternatives to conventional methods for water analyses. Current procedures for extractions from water tend to require multiple steps and frequently consume large volumes of toxic solvents that are hazardous and have high costs of production and disposal.

Sample pretreatment is the most time-consuming step in an analytical method and is crucial to its success. It accounts for about two-thirds of the analysis time and is the primary source of errors and discrepancies between laboratories (Barceló, 1995). During sample pretreatment, solutes are separated from the matrix and further clean-up is needed if interfering solutes have been co-extracted. The analytes must also be concentrated to at least the limit of detection of the method. Traditional liquid-liquid extraction methods have multiple steps and limited sensitivities. They are also compromised by regulations for reducing the use of organic solvents. Solid phase extractions using sorbent disks, cartridges, or pre-columns are useful alternatives. However, multiple steps for sample clean-up, concentration, and derivatization are still needed. The development of rapid and reliable methods requires removing intermediate steps such as transfer, evaporation, and derivatization. Novel technologies such as solid phase microextraction (SPME) strive to minimize the steps and time required for sample preparation. SPME has the potential of extracting and concentrating almost any compound in a single step with the appropriate solid phase. However, selective extractions are not possible if the analytes are similar.

Supercritical fluid methods can extract and concentrate analytes in a single step. As well, selective extractions are possible due to the variable densities of the fluids. Fast extractions result from their low viscosities and hence from the high diffusivities of

both the solvent and solutes. Supercritical fluid methods have the potential for on-line coupling with detection techniques such as supercritical fluid chromatography, gas chromatography, and liquid chromatography. Automated, on-line methods which combine extraction, separation, and detection maximize sample throughput while removing the risk of sample loss or contamination. Supercritical carbon dioxide (SC CO_2) has typically been the fluid of choice for SF extractions as it possesses easily achieved critical parameters (31.1°C; 73.8 bar), is inexpensive, and is a non-toxic gas at atmospheric pressure. Solutes have enhanced solubilities in supercritical fluids; SC CO_2 can extract both nonpolar and moderately polar compounds. Polar solutes can be extracted by combining CO_2 with a polar solvent modifier such as methanol. Supercritical fluid extractions of solid samples are well documented. However, the development of supercritical fluid methods for water extractions is still in its infancy.

1.2 Direct Extractions

The development of supercritical fluid methods for water extractions has had to confront the problems associated with the solubility of water (0.1 - 0.3 %) in CO_2. Researchers have tackled problems such as activation of trapping and/or chromatographic phases, the generation of two phases upon sample collection, and restrictor plugging. As a consequence, diverse and interesting methods have been developed for the direct extraction of water samples.

In 1989, in the first study of its kind, Hedrick and Taylor (1989) extracted a phosphonate directly from water using an extraction vessel which was isolated in an extraction loop. Carbon dioxide was recirculated through the sample until equilibrium was achieved. Adding salt resulted in faster extractions. On-line analysis was performed by supercritical fluid chromatography (SFC). Phenols (Hedrick et al, 1992; Hedrick and Taylor, 1990), polar solutes (triprolidin and pseudoephedrin) (Hedrick and Taylor, 1990), and organic bases (Hedrick and Taylor, 1992) have since been analyzed in water with the same extraction system with SFC or off-line analysis. Bases with greater lipophilicity were more readily extracted with CO_2. A similar apparatus was used by Daneshfar et al (1995) and Combs et al (1996) in both static and dynamic modes to extract phenoxy acids and phenols from water. Ong et al extracted polyaromatic hydrocarbons from wastewater (Ong, 1991). Ramsey et al (1997) interfaced an aqueous extraction vessel to SFC with a multivalve switching system which housed an analyte trap. Phenols were extracted at the 40 ng/mL level. Thiebaut et al (1989) achieved recoveries of over 85% for phenols from water and urine using a phase separator to remove residual water from CO_2 following a direct extraction with on-line SFC analysis. The initial concentration of phenol in water was 5000 ppm; urine was spiked with 120 ppm 4-chlorophenol.

Also in 1989, Roop and Akgerman (1989) and Roop et al (1989) introduced a static extraction vessel which could measure the equilibrium distribution coefficient (K) of a solute between two phases. K is defined as the ratio of the mole fraction of a solute

in the supercritical phase to that in the aqueous phase. The cell design allowed each phase to be sampled independently. The entrainer effects of methanol, chlorobenzene, and benzene on the extraction of 6.8% liquefied phenol in water were explored. The CO_2-rich phase was collected in an organic solvent and both phases were tested with a liquid scintillation counter to determine solute concentration. The vessel has since been used to measure the partitioning of benzene, toluene, naphthalene, and parathion (Yeo and Akgerman, 1990); to extract soil-water slurries (Green and Akgerman, 1996); and to analyze a phenol mixture which was extracted and measured for total organic content (TOC) using a carbon analyzer. The TOC in water was reduced by several thousand parts per million (Roop and Akgerman, 1990). The extraction vessel was plumbed on-line to a liquid chromatograph to measure the partitioning of 2,4-dichlorophenol between CO_2 and water (Akgerman and Carter, 1994). In 1991, Ghonasgi et al (1991a, 1991b) and Gupta et al (1991) developed a different static extraction system to measure the partitioning of benzene and several phenolic solutes. These methods are further reviewed in section 1.6.

Several authors have emphasized means to optimize extraction efficiency and method sensitivity. Brewer and Kruus (1993) increased the water-fluid interfacial area by continuously flowed droplets/bubbles of SC CO_2 through the aqueous phase. An average recovery of 97% was achieved from a sample contaminated with 86 ng/mL pentachlorophenol. A plug of silanized wool was used earlier by Ehntholt et al (1983) to disperse CO_2 as fine bubbles through water. Low phenol recoveries (about 40%) were likely a consequence of the analytes breaking through the trapping system. Barnabas et al (1994a) dispersed carbon dioxide through aqueous organochlorine pesticide samples with a solvent filter. Recoveries were less than 20% despite good analyte solubilities in CO_2. As three different flow rates were used with little change in recoveries, it was concluded that the extractions were diffusion-controlled.

1.3 Indirect Methods

Indirect methods as well as derivatization techniques have been used to extract a variety of solutes from water. Examples of each are briefly reviewed.

Indirect water extractions have been performed by combining solid disk extraction with supercritical fluid elution (Tang and Ho, 1994; Barnabas et al, 1994b). A small volume of water may also be loaded onto a cartridge packed with a suitable inert particulate material (Hawthorne et al, 1992). In a unique approach, Alzaga et al (1994) extracted freeze-dried water samples which had been spiked previously with eight different agrochemicals.

Metals may be removed from water by complexation. Laintz et al (1992) extracted Cu^{2-} from water with CO_2 which contained the ligand lithium bis(trifluoroethyl) dithiocarbamate. A similar approach has been used to chemically derivatize polar analytes in situ. Croft et al (1994) extracted and methylated chlorophenoxyacetic acids from a solid support with a combination of CO_2, tetrahexylammonium hydrogen sulfate, and methyl iodide. Using surfactants, non-volatile and hydrophilic molecules which are insoluble in CO_2 can be extracted from water into aqueous microemulsion droplets in a carbon dioxide phase (Johnston et al, 1996). Fluorinated dendrimers have been used to transport, within their cores, insoluble molecules into CO_2 (Cooper et al, 1997).

1.4 Solubility Measurements

1.4.1 Solubility in CO_2

Designing a novel, viable extraction system requires an understanding of the physical behaviour of a solute in each phase at equilibrium. Parameters such as system temperature and pressure govern the solubility of a solute in a supercritical fluid. These parameters also govern the distribution of a solute between the supercritical fluid and water. Solubility measurements in CO_2 can therefore provide an indication of the ability of SC CO_2 to extract a compound from contaminated water. Knowledge of the solubility of the solute in water is also important as the ratio of solubilities can then be used to predict the magnitude of the distribution coefficient K. Solubility data for phenols and several other compounds are reviewed below.

The solubility of naphthalene in supercritical carbon dioxide has been well defined and is widely reported in the literature. Measurements of the solubility of naphthalene are often used to verify that a new apparatus or methodology can provide good data, by comparison with previously published values. Measurements performed by McHugh and Paulaitis (1980) show the solubility of naphthalene to increase with increasing temperature and pressure to an upper critical end point at about 63 °C and 240 atm. Solubilities were of the order of magnitude of 10^{-2} mole fraction naphthalene. Polynuclear aromatic hydrocarbons with higher molecular weights are less volatile and are less soluble in CO_2. The solubilities of chrysene, fluoranthene, and triphenylene were determined to be between 10^{-6} and 10^{-4} mole fraction solute over the temperature and pressure ranges of 35 to 55 °C and 80 to 250 atm (Barna et al, 1996).

The moderately polar solutes phenol, p-chlorophenol, and 2,4-dichlorophenol have high solubilities in CO_2, likely due to the effects of high analyte volatilities and the potential of interaction with the solvent's quadrupole moment. Solute solubilities are of the order of 10^{-2} mole fraction; 2,4-dichlorophenol was the most soluble species

over the pressure range of 80 to 250 atm at 36 °C (Van Leer and Paulaitis, 1980).

The more polar species 2,4-dichlorophenoxyacetic acid (2,4-D) is less soluble in CO_2 (10^{-5} mole fraction) than its corresponding phenol (Schäfer and Baumann, 1988; Macnaughton and Foster, 1994; Miller et al, 1997). Saturation of carbon dioxide with water gave a solubility enhancement of up to 90% for 2,4-D, indicating the importance of the mutual solubilities of CO_2 and water in a partitioning experiment (Macnaughton and Foster, 1994).

The solubility of pentachlorophenol (PCP) in carbon dioxide is lower than for more volatile phenols having fewer chlorine atoms. However, its solubility in CO_2 is greater than that of polar 2,4-D. Values of the order of magnitude of 10^{-4} mole fraction or higher have been reported over the temperature range of 25 to 140 °C and between 110 to 450 atm (Madras et al, 1993; Miller et al, 1997; Cross and Akgerman, 1998). Replacing the hydroxide group with a sixth chlorine caused the solubility to drop to the order of 10^{-5} mole fraction (Cross and Akgerman, 1998). The solubilities of both analytes were increased at increased temperatures and pressures.

1.4.2 Solubility in water

The solubilities of chlorinated phenols in water tend to decrease as the number of chlorine atoms on the molecule increases. The solubility of phenol in water is 1.5×10^{-2} mole fraction, which drops to 3.8×10^{-3} mole fraction for p-chlorophenol and 4.9×10^{-4} for 2,4-dichlorophenol (Perry and Chilton, 1973). The solubility of pentachlorophenol in water at atmospheric pressure has been reported to be in the range of 9.4×10^{-7} to 1.3×10^{-6} mole fraction (Freiter, 1979) and 1.2×10^{-6} mole fraction at 27 °C (Carswell and Nason, 1938).

In general, molecules which are acidic, polar, and/or can hydrogen bond are soluble in water. Species containing no polar groups are sparingly soluble.

1.5 Analyte Partitioning

1.5.1 Methods

A static system is required to measure the distribution coefficient of a solute between two phases. It is ideal to analyze aliquots by on-line methods to avoid the problems associated with sample collection, especially for the supercritical phase. In addition, it is important to construct calibration curves for the solute in both phases to ensure mass balance has been achieved.

Akgerman et al used a steel extraction cell to measure the partitioning of solutes between water and CO_2 (Roop and Akgerman, 1989; Roop and Akgerman, 1990; Green and Akgerman, 1996; Roop et al, 1989; Yeo and Akgerman, 1990). The contents of the vessel were mixed for 1 hr and a time of 2 hr was determined to be adequate for phase separation. A Jerguson gauge allowed visual confirmation of the number of phases. Each phase was sampled independently through narrow bore tubing for off-line analysis. The CO_2 sample was bled across a restrictor and through an organic solvent trap. A wet test meter monitored the amount of CO_2. Distribution coefficients were calculated based on solute concentration in the aqueous sample. The carbon dioxide phase was sampled in preliminary experiments to confirm the mass balance. No measurable change in volume of the aqueous phase was observed with the addition of compressed CO_2.

This apparatus was also used with on-line detection of the analyte in both phases by high performance liquid chromatography (HPLC) (Akgerman and Carter, 1994). The detector was calibrated using solutions of known concentrations similar to those expected during a partitioning experiment. The methods used to make standards were not further specified. Both water and CO_2 caused HPLC perturbations which eluted at the same time as the solute peaks. These were attributed to either switching of the sampling valves or slight changes in the absorption of the mobile phase in the presence of water or CO_2. The perturbations were small compared to the solute peaks and were subtracted before making a calibration curve.

Ghonasgi et al constructed an apparatus which used a static mixer to attain equilibrium for a water – CO_2 – solute mixture (Ghonasgi et al, 1991a; Ghonasgi et al, 1991b; Gupta et al, 1991). A Jerguson gauge was then used as a windowed cell phase separator. Each phase was sampled separately, then further separated into its vapour and liquid components at atmospheric pressure using a micrometering valve. The liquid samples were weighed and compared to the weight of the original aqueous solution delivered by a metering pump. This allowed closure of water and solute mass balances. The flow rates of the CO_2 samples were measured with a dry test meter. The solute concentrations of the liquid samples were determined by visible spectroscopy of a dye complex of the solute. The system was tested by measuring the CO_2 – water vapour/liquid equilibrium which was in good agreement with the available data of Wiebe and Gaddy (1940; 1941).

Hedrick et al (1992) used an apparatus which recirculated supercritical carbon dioxide upward through a water sample in a closed loop. Flow rates were between 3-5 mL / min. The extraction was allowed to occur for 15 min at which time replicate injections of the supercritical phase were made into an on-line SFC at 10 min intervals to verify that equilibrium was established. The SFC was calibrated by referring to an external phenol calibration curve. The amount of phenol remaining in the aqueous phase was calculated assuming a 100% material balance.

1.5.2 Results

Several measurements have been made of the distribution coefficient for phenol, a solute with a high solubility in both CO_2 and water. Phenol partitions almost equally between water and carbon dioxide as evidenced by K values between 0.2 and 1.5 at temperatures up to 76 °C and at pressures as high as 350 atm (Hedrick et al, 1992; Roop et al, 1989; Ghonasgi et al, 1991b; Chang and Huang, 1995; Brudi et al, 1996). The addition of functional groups to the phenol structure increased K in all reported

cases with the exception of p-methoxyphenol (Green and Akgerman, 1996). K was marginally higher for m-cresol and p-chlorophenol compared with the values measured for phenol (Ghonasgi et al, 1991b; Chang and Huang, 1995). The distribution coefficient for o-methoxyphenol was 10 at about 200 atm (Green and Akgerman, 1996) and was as high as 40 at 25 °C and 200 atm for 2,4-dichlorophenol (Akgerman and Carter, 1994). Similar results were obtained for 2,6-dimethylphenol (Green and Akgerman, 1996). In all cases, at moderate pressures, K was equal or higher in magnitude at the lowest temperatures as a function of pressure. Crossover regions were observed for phenol and m-cresol at higher pressures (Ghonasgi et al, 1991b).

Several authors have examined the ratio of a solute's solubility in water to that in CO_2. Ghonasgi et al (1991b) determined that the partitionings of benzene, m-cresol, p-chlorophenol, and phenol are dependent on their solubilities in both phases. At 40 °C, although it is less soluble in water, m-cresol had a smaller K than p-chlorophenol because it is also less soluble in CO_2. Only solubilities in water at atmospheric pressure were considered. The solubility ratio was also considered by Akgerman and Carter (1994) for the partitioning of phenol, p-chlorophenol, and 2,4-dichlorophenol in water. The distribution coefficient was highest for 2,4-dichlorophenol, which had the lowest solubility in water and the highest in CO_2.

The distribution coefficient depends on the combined concentration of a solute in the water and supercritical phases at equilibrium in addition to its solubility in both phases. Non-dilute solutions will deviate from ideal behaviour due to the effects of attractive and repulsive molecular interactions. Starting concentrations reported in the literature have typically been in excess of 100 μg analyte / mL solvent (Hedrick et al., 1992; Roop and Akgerman, 1990). Concentrations of interest to the analytical chemist are typically three or more orders of magnitude smaller. No significant influence of concentration was found by Brudi et al on the partitioning of phenol to supercritical CO_2 from solutions with high initial concentrations of 0.2 to 10 wt % (Brudi et al, 1996). To date, no other studies have investigated the effect of solute

concentration on the partitioning of phenols.

Interactions among solutes can enhance the extraction of a target compound. Distribution coefficients between water and CO_2 were measured for a mixture composed of phenol, 2-methyl-phenol, 2-methoxy-phenol, 2,3-dimethyl-phenol, and methoxy-methyl-phenol at 25 and 50 °C and at pressures up to 275 atm. Values as high as 6 were obtained and partitioning was favoured at the lower temperature (Roop and Akgerman, 1990). Partitioning was slightly improved for the mixture of phenol, p-methoxyphenol, o-methoxyphenol, and 2,6-dimethylphenol compared with partitioning of the pure solutes (Green and Akgerman, 1996). Distribution coefficients were also higher for each component in a mixture of benzene, toluene, naphthalene, and parathion compared with each separate ternary system (Yeo and Akgerman, 1990).

Entrainers, or solvent modifiers, have been employed to enhance the partitioning of a solute between phases. Roop and Akgerman (1989) investigated the entrainer effects of methanol, chlorobenzene, and benzene for the CO_2 extraction of phenol from water. Methanol was found to slightly decrease K for phenol while chlorobenzene caused the formation of a third, separate phase. Benzene, however, increased the distribution coefficient of phenol by as much as 50 %. This result was also obtained for a mixture of phenols (Roop and Akgerman, 1990).

1.6 Purpose and Plan of Research

The implementation of supercritical carbon dioxide methods for the direct extraction of water samples requires a complete characterization of the solute – water – CO_2 system. With this knowledge, suitable chemical and physical parameters can be determined for efficient and sensitive extractions.

Polar compounds are difficult to extract from water samples due to their high boiling points and low solubilities in traditional, nonpolar solvents. The polar nature of water and its potential for hydrogen bonding combine to promote the retention of many solutes. The partial dissociation of weakly acidic compounds make water extractions particularly difficult. The dissolution of carbon dioxide in water is expected to affect the partitioning of acidic analytes due to the formation of carbonic acid.

The purpose of this research was to characterize and interpret the partitioning of polar and acidic solutes between water and supercritical carbon dioxide. The primary solute of interest was pentachlorophenol (PCP) which is still found in natural water resources and food products due to its past abundant use as a wood preservative.

The research had the following objectives:

(1) To construct a high-pressure extraction apparatus for performing solubility and partitioning experiments in water and CO_2 with on-line HPLC analysis of each phase.

(2) To measure solute solubilities in CO_2 and water as a function of system temperature and pressure.

(3) To measure the distribution coefficients for PCP and other solutes between water and carbon dioxide as a function of system temperature and pressure as well as solute concentration, pH, and ionic strength. These results will provide

information on what parameters need to be optimized for water extractions. Information will also be obtained on the potential of supercritical CO_2 for the extraction of polar and acidic solutes.

(4) To compare distribution coefficients with solubility ratios and thus to recognize the molecular interactions which govern solute solubilities in water and carbon dioxide and to interpret how these interactions affect solute partitioning between the two phases.

(5) To comment on the viability of supercritical CO_2 extractions for water samples contaminated with pentachlorophenol and other organic species.

CHAPTER TWO
THEORY

2.1 Supercritical Fluids

2.1.1 The CO_2 Phase Diagram

The phase diagram in Figure 2.1.1 defines the regions corresponding to the gas, liquid, and solid states of carbon dioxide. Points along the sublimation, melting, and boiling lines define the equilibria between the phases. A single-phase fluid having gas- and liquid-like properties exists in the supercritical region, that is, above the critical temperature (T_c) and pressure (P_c). The critical point for carbon dioxide occurs at $31.1°C$ and 73 atm.
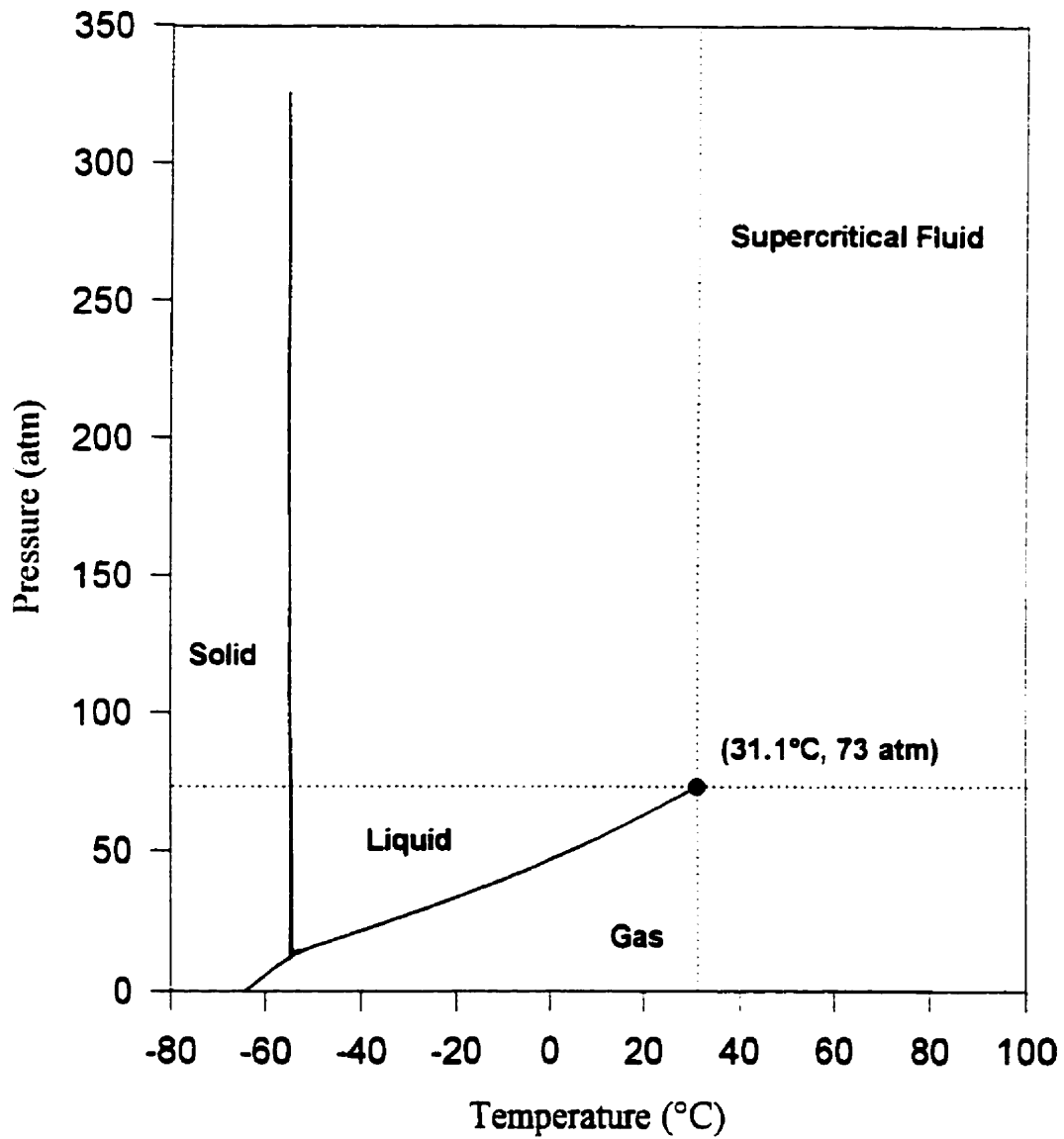
Figure 2.1.1. Phase diagram for carbon dioxide

2.1.2. Thermodynamic Properties: Equations of State

The physical properties of a pure substance are defined by any three of volume (V), pressure (P), temperature (T), or the number of moles (n) of pure substance. Each variable may be expressed as a function of the other three in an equation of state. Ideal gases obey the perfect gas equation of state at low pressures:

$$PV = nRT \qquad (2.1.1)$$

The gas constant R has the value 0.082 L atm K^{-1} mol^{-1}. Real gases obey equation (2.1.1) exactly in the limit of zero pressure. Under this condition Boyle's Law ($PV =$ constant) and Gay-Lussac's Law ($V \propto T$) are defined. Similarly, ($P \propto T$) by holding the amount and volume constant.

The compression factor, Z, demonstrates how real gases deviate from Boyle's law due to the effects of attractive and repulsive molecular interactions

$$Z = \frac{PV_m}{RT} \qquad (2.1.2)$$

where V_m is the molar volume of the gas. For a perfect gas $Z = 1$. At very high pressures $Z > 1$, indicating real gases are difficult to compress due to dominating repulsive forces. For a compressible fluid, $Z < 1$ due to the effects of attractive forces.

The virial equation of state is used to describe the behaviour of real gases under pressure. The ideal gas law is treated as the first term in a power series; at high temperatures and large molar volumes perfect and real gas isotherms do not differ greatly:

$$PV_m = RT(1 + B'P + C'P^2 + ...) \qquad (2.1.3)$$

The second and third virial coefficients (B', C') are dependent on temperature. The virial equation of state may also be expressed in terms of the molar volume of a gas:

$$PV_m = RT(1 + B/V_m + C/V_m^2 + ...)$$ (2.1.4)

The virial equation demonstrates that not all properties of a real gas will coincide with the perfect gas law at low pressures, except at the Boyle temperature T_B where $B = 0$. For a perfect gas $dZ/dP = 0$, but for a real gas $dZ/dP \to B'$ as $P \to 0$. Similarly, $dZ/d(1/V_m) \to B$ as $V_m \to \infty$ in equation (2.1.4).

Consideration of the physical behaviour of real gases has resulted in many approximate equations of state which do not require the insertion of specific virial coefficients. The van der Waals equation of state assumes repulsive interactions cause molecules to behave as small but impenetrable spheres. Molecules are restricted to a volume ($V - nb$) where nb is approximately the volume taken up by the molecules themselves. Attractive forces reduce the pressure exerted by a real gas. The strength of these forces is proportional to the molar concentration n/V of molecules in the sample. The consequent reduction in pressure is written as $-a(n/V)^2$. Combining the effects of repulsive and attractive forces gives:

$$P = \frac{nRT}{V - nb} - a\left(\frac{n}{V}\right)^2$$ (2.1.5)

The constants a, b are specific for each gas.

The critical constants can be calculated by setting the first and second derivatives of equation (2.1.5) with respect to V to zero. The critical molar volume, pressure, and temperature are then defined in terms of the constants a and b:

$$V_c = 3b; P_c = \frac{a}{27b^2}; T_c = \frac{8a}{27Rb} \qquad (2.1.6)$$

The critical compression factor, Z_c, is therefore predicted to be equal to

$$Z_c = \frac{P_c V_c}{RT_c} = \frac{3}{8} \qquad (2.1.7)$$

for all gases.

The principle of corresponding states was first proposed by van der Waals. The definition of reduced variables gives a relative scale of comparison for real gases based on their critical constants. All gases therefore exert the same reduced pressure at the same reduced molar volume and temperature:

$$P_r = \frac{P}{P_c}; V_r = \frac{V_m}{V_c}; T_r = \frac{T}{T_c}; \rho_r = \frac{\rho}{\rho_c} \qquad (2.1.8)$$

Reduced isotherms are plotted in terms of P_r and V_r in Figure 2.1.2. This approximation is obeyed by gases composed of spherical molecules. The principle fails for non-spherical or polar molecules.

Van der Waals' equation may be rewritten in terms of reduced variables:

$$P_r = \frac{8T_r}{3V_r - 1} - \frac{3}{V_r^2} \qquad (2.1.9)$$
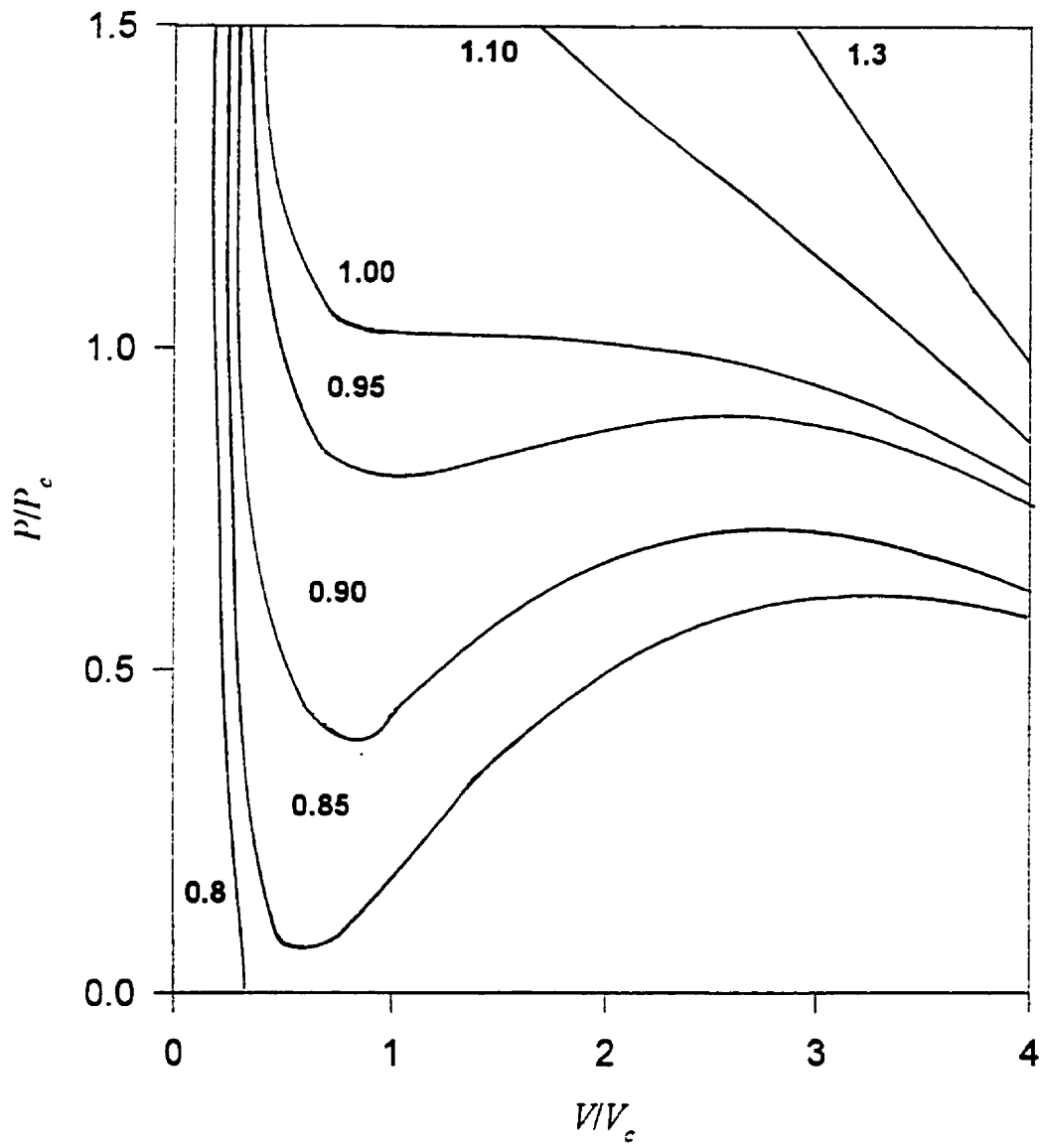
Figure 2.1.2. The van der Waals isotherms at several values of T_r

The van der Waals loops seen in Figure 2.1.2 are unrealistic as they suggest that under some conditions an increase in pressure results in an increase in volume. In these regions liquids and gases coexist. The critical isotherm ($T/T_c = 1$) shows an almost flat inflection at the critical point, demonstrating a fluid's almost infinite compressibility in this region. Figure 2.1.3 further illustrates the compressibility of a supercritical fluid at the critical point (CP). The density (ρ) can be varied almost an order of magnitude, from 0.1 to 0.9 g mL^{-1}, with small changes in pressure at $T_r = 1.0$ − 1.2.

The density increases as the pressure is increased, but decreases with an increase in temperature. Outside the critical region (at $T_r > 1.2$, say), only small changes in fluid density will result from changes in pressure. Carbon dioxide is almost incompressible in the liquid region at $T_r < 1$; however, the density of liquid CO_2 is greater than that of supercritical CO_2 under easily attainable conditions.

A successful variation of the van der Waals equation was proposed by Peng and Robinson (1976):

$$P = \frac{RT}{(V-b)} - \frac{a(T)}{V(V+b)+b(V-b)}$$

(2.1.10)

In this case, the value of a is dependent on temperature and on the acentric factor. The latter is a measure of the non-sphericity of the molecule. The repulsive term also produces more realistic values of the critical compressibility, Z_c.

Density versus pressure curves are compared at the critical temperature for ideal, van der Waals, Peng-Robinson, and experimental values for CO_2 in Figure 2.1.4. The ideal gas law appears useful only at low pressures of several bar while the van der Waals equation fails at high pressures. The Peng-Robinson equation of state provides reasonably accurate results over a wide range of pressure.
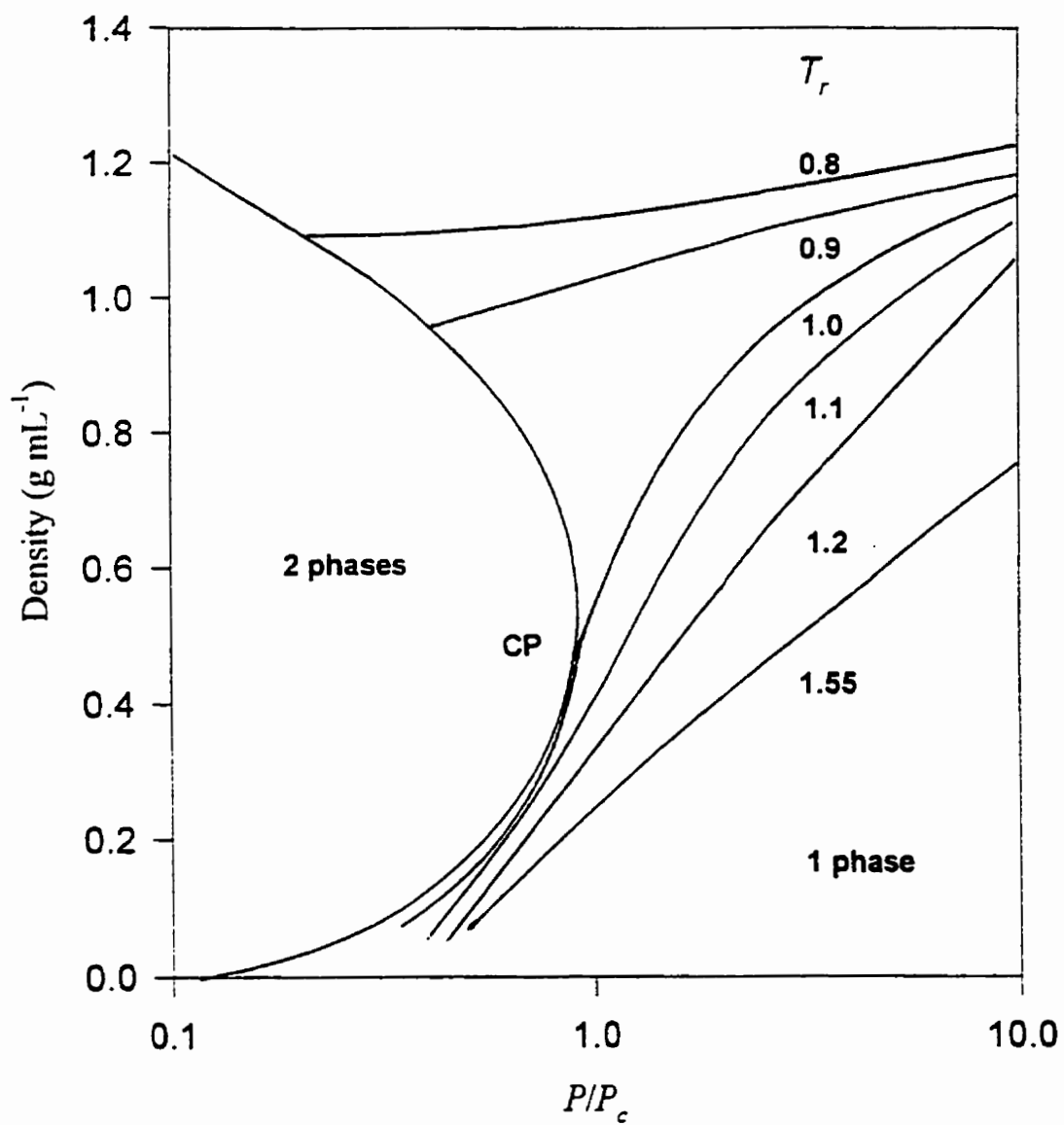
Figure 2.1.3. Density of carbon dioxide versus reduced pressure
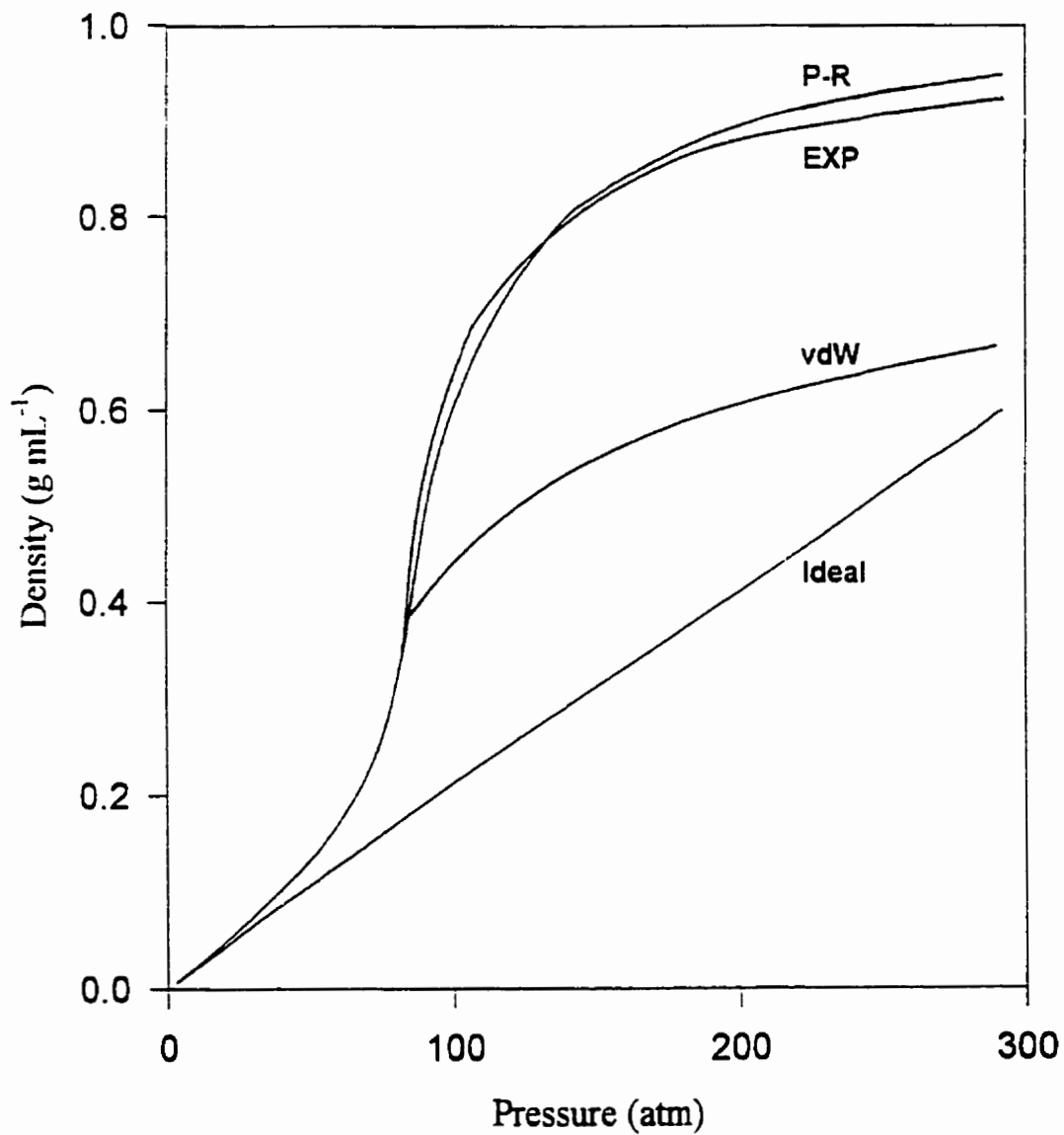
Figure 2.1.4. Comparison of CO_2 density from the ideal, van der Waals (vdW), and Peng-Robinson (PR) equations of state with experimental data

2.1.3 Transport Properties: Viscosity and Diffusivity

The physicochemical properties of supercritical fluids lie between those of a liquid and a gas. In addition to their high, liquid-like densities which afford good solvent power, rapid mass transfer occurs in supercritical fluids relative to liquids. As shown in Table 2.1.1, the dynamic viscosities of supercritical fluids are 10 - 100 times lower than liquid values while their diffusion coefficients are 1 to 2 orders of magnitude higher.

Table 2.1.1 Orders of Magnitude of Viscosity and Diffusivity for Gaseous, Supercritical Fluid, and Liquid States

	Dynamic Viscosity $(g\ cm^{-1}\ s^{-1})$	Diffusion Coefficient $(cm^2\ s^{-1})$
Gas (ambient)	0.0001 – 0.003	0.1 – 0.4
Supercritical fluid (T_c, P_c)	0.0001 – 0.0003	0.0007
Liquid (ambient)	0.002 – 0.03	0.000002 – 0.00002

The diffusivity of supercritical CO_2 varies between 10^{-4} and 10^{-13} $cm^2\ s^{-1}$ at pressures between 50 and 500 atm.

Both the viscosity and diffusivity of supercritical fluids approach values for liquids as pressure is increased. Conversely, an increase in temperature will increase a fluid's diffusivity while decreasing its viscosity. This effect on viscosity is generally associated with the behaviour of liquids, not gases. Changes in both properties are most pronounced in the region near the critical point as illustrated in Figures 2.1.5 and 2.1.6.
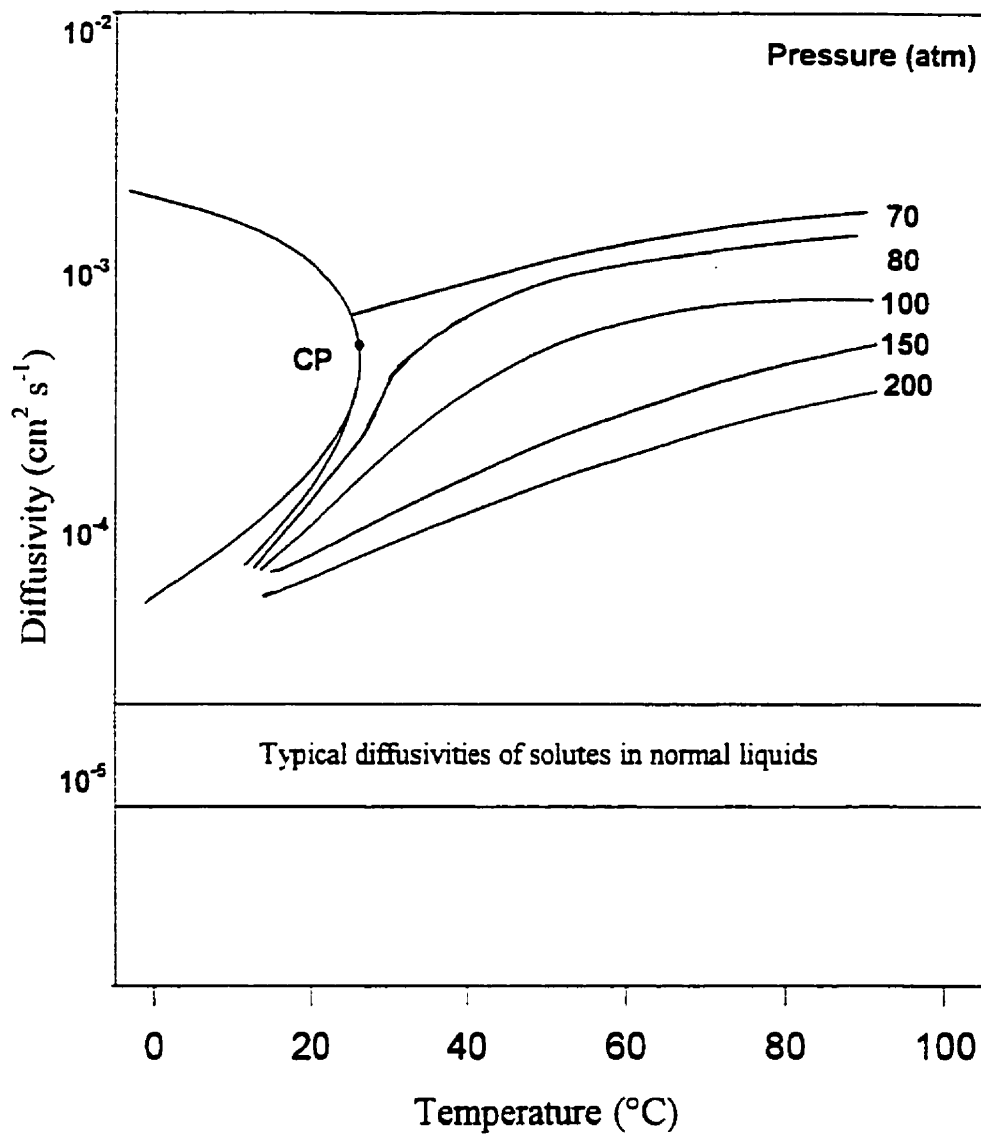
Figure 2.1.5. Diffusivity of CO_2 versus temperature at various pressures (from Taylor, 1996)
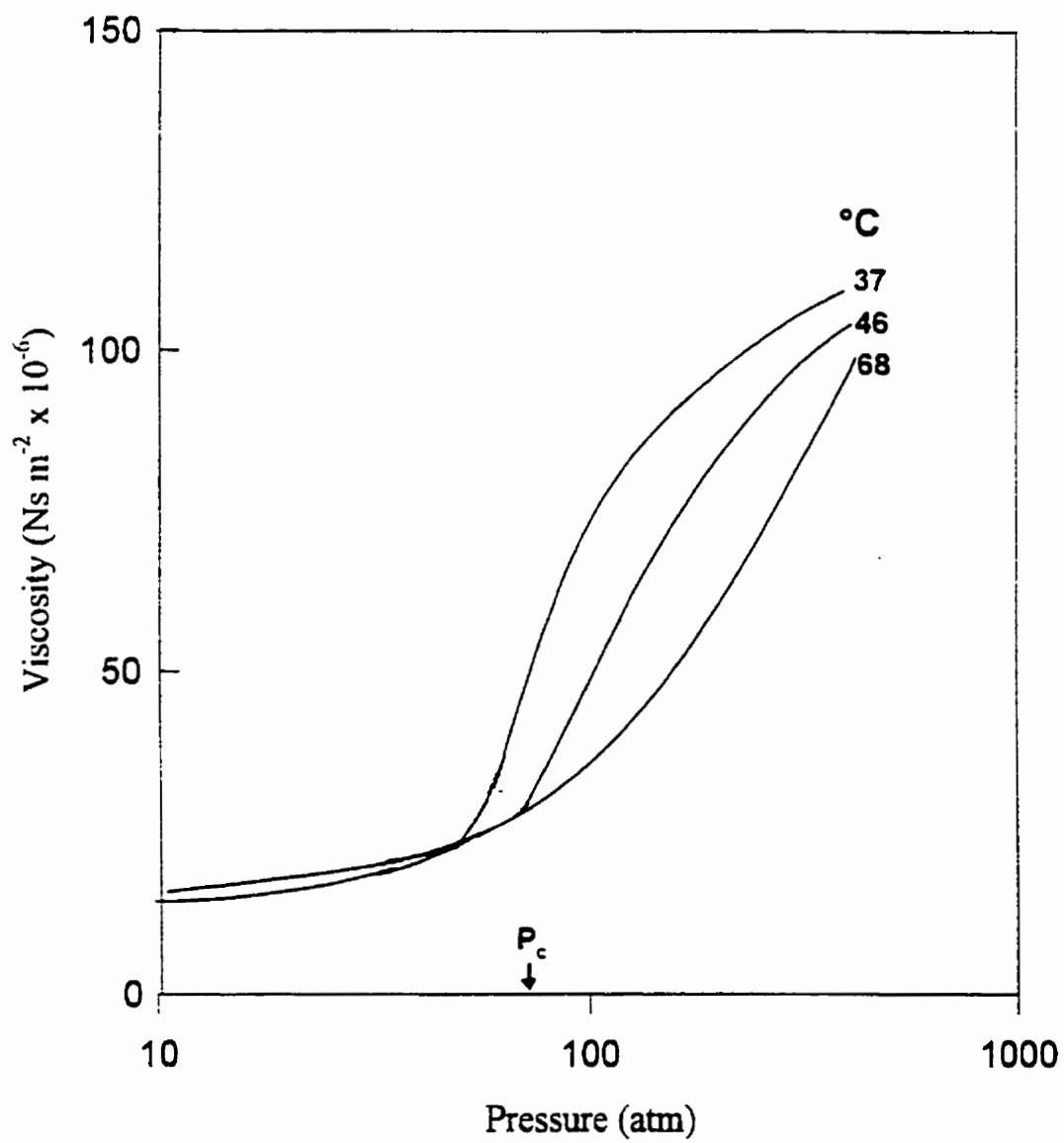
Figure 2.1.6. Viscosity of CO_2 versus pressure at various temperatures

The diffusion coefficients $\mathcal{D}_{AB}$ of infinitely dilute solutes in supercritical solvents are a function of the thermodynamic properties of the system. The coefficients $\mathcal{D}_{AB}$ in Table 2.1.2 are larger at higher temperatures and lower pressures, that is, at low values for fluid density and viscosity. Increasing fluid density increases the number of molecular collisions and reduces the mean free paths of the solutes. However, at constant density, $\mathcal{D}_{AB}$ values for less polar solutes seem to be relatively independent of temperature. The data in Table 2.1.2 were taken from the review by Suárez et al (1998).

Table 2.1.2 Diffusion Coefficients of Several Compounds in Supercritical CO_2

Compound	Pressure (atm)	Temperature (°C)	$\mathcal{D}_{AB}$ ($\times 10^{-9}$ m^2 s^{-1})
Benzene	108.5	40.0	18.6
	246.8	40.0	10.5
	108.5	50.0	21.6
Naphthalene	108.5	40.0	15.6
	246.8	40.0	9.5
	106.8	55.0	22.5
Phenol	114.3	40.0	15.2
	115.4	55.0	22.7
	142.3	55.0	18.2

Solute diffusion coefficients are also functions of the chemical properties of the solute and solvent. The $\mathcal{D}_{AB}$ value decreases with increasing molar volume of the solute, which is generally directly related to the solute molecular mass. Molecular mobility

is also hindered if the solute and solvent molecules are significantly different in size.

.

2.2 Intermolecular Interactions

At moderate to high pressures, molecular interactions cause real gases to deviate from the perfect-gas surface. Physical forces between ions, dipoles, induced dipoles, and higher poles contribute to molecular behaviour in solution. The potential energy of each type of interaction can be predicted.

The potential energy of interaction of point charges q_1 and q_2 may be defined in terms of the permittivity of the medium, ε, and the distance of separation of the charges, r:

$$V = \frac{q_1 q_2}{4\pi\varepsilon r}$$

(2.2.1)

The relative permittivity, or dielectric constant, of the medium is the more common indicator used for non-vacuum systems:

$$\varepsilon_r = \frac{\varepsilon}{\varepsilon_0}$$

(2.2.2)

The permittivity in a vacuum, ε_0, has the value $8.854 \times 10^{-12} \, J^{-1} \, C^2 \, m^{-1}$.

The potential energy of interaction between a dipole $\mu_1 = q_1 l$ and the point charge q_2 is the sum of a repulsion and an attraction, and is reduced to:

$$V = -\frac{\mu_1 q_2}{4\pi\varepsilon_0 r^2}$$

(2.2.3)

The separation, r, is now the distance between the centre of the dipole of length l and the ion.

Polar molecules will not rotate with complete freedom in solution since lower energy orientations are marginally favoured, resulting in an overall non-zero interaction. Relative molecular orientations depend on the field established by the polar molecules, which tends to line up the dipoles, as well as on the kinetic (thermal) energy causing the molecules to move in a random manner. At moderate to high temperatures, orientations leading to negative potential are preferred statistically. At low to moderate temperatures the contribution of polarity to the interaction potential is significant. The potential energy between dipoles is dependent on a higher power of r as well as on the thermal motion of the molecules

$$V = -\frac{2(\mu_1\mu_2 : 4\pi\varepsilon_0)^2}{3kTr^6} \quad (2.2.4)$$

where k is Boltzmann's constant and T is the absolute temperature.

A polar molecule with dipole moment μ_1 may induce a dipole μ_2^* in a polarizable molecule. The magnitude of μ_2^* will depend on the field generated by the polar molecule, that is, on the molecular separation and the magnitude of μ_1. Thermal effects are not considered as the induced dipole is committed to following the direction of the inducing dipole. The potential of the system is directly proportional to the polarizability volume, α_2', of the induced dipole:

$$V = -\frac{\mu_1^2 \alpha_2}{4\pi\varepsilon_0 r^6} \quad (2.2.5)$$

Interactions between non-polar molecules can exist due to the instantaneous transient dipoles all molecules possess. An instantaneous dipole moment μ_1^* in a given molecule may polarize a second molecule to create the induced dipole moment μ_2^*. The two dipoles are correlated in direction as each dipole changes in direction and magnitude. The strength of this "dispersion" interaction depends on the polarizability of the initiating molecule. The polarizability of the induced molecule in part

determines how readily the induction will occur. A reasonable approximation to the potential energy of interaction is given by the London formula and includes the ionization potentials, I, of the two molecules:

$$V = -\frac{3\alpha_1\alpha_2(I_1I_2(I_1+I_2))}{2r^6} \qquad (2.2.6)$$

Molecules such as carbon dioxide possess quadrupole moments, Q, due to a separation of charge into two back-to-back dipoles:

+ -	- + + -
or	or
- +	+ - - +

<u>Dipole</u>	<u>Quadrupole</u>
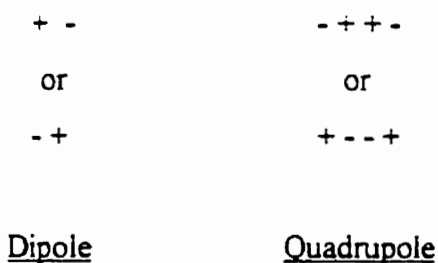
Q for CO_2 is given by the first example (- + + -), since O is more electronegative than C. For a linear molecule, Q is defined by the sum of the second moments of the charges:

$$Q = \sum_i q_i d_i^2 \qquad (2.2.7)$$

The charge q_i is located at a point (on an axis common to all charges) a distance d_i from some arbitrary origin. The quadrupole moment is independent of the position of the origin so long as the molecule has no net charge and no dipole moment. The potential energy of interaction between a dipole-i and a quadrupole-j, or two quadrupoles, is a function of the intermolecular distance, the angles of mutual orientation, and random thermal motion:

$$V = -\frac{\mu_i^2 Q_j^2}{kTr^8} \qquad (2.2.8)$$

Similarly, the interaction energy between quadrupoles-i,j is:

$$V = -\frac{7Q_i^2 Q_j^2}{40kTr^{10}}$$

(2.2.9)

Dispersion interactions may also be initiated by permanent quadrupole moments. Their potential energies are typically smaller in magnitude than for quadrupole-dipole or quadrupole-quadrupole interactions:

$$V = -\frac{3(\alpha_i Q_j^2 + \alpha_j Q_i^2)}{2r^8}$$

(2.2.10)

2.3 Ideal and Real Gases

A perfect gas is in its standard state when $P^\theta = 1$ bar and T = 298 K; the Gibbs function is then G^θ. At any other pressure P its Gibbs function G is

$$G = G^\theta + nRT \ln \frac{P}{P^\theta} \qquad (2.3.1)$$

where R is the gas constant and T is the absolute temperature. The chemical potential of a pure substance is defined as:

$$\mu = \left(\frac{\delta G}{\delta n} \right)_{P,T} \qquad (2.3.2)$$

The chemical potential μ describes how G changes as the composition of a system changes. It follows that for a perfect gas:

$$\mu = \mu^\theta + RT \ln \frac{P}{P^\theta} \qquad (2.3.3)$$

The chemical potential of real gases is pressure-dependent as shown in Figure 2.3.1. As $P \rightarrow 0$, μ approaches the value for a perfect gas. Attractive forces dominate at intermediate pressures making the chemical potential less than for a perfect gas. As a consequence, molecules have a lower "escaping tendency" or fugacity. At high pressures, repulsive forces dominate and both the chemical potential and fugacity are greater than for a perfect gas. Equation (2.3.4) is the real gas equivalent of equation (2.3.3). The pressure P is replaced by the fugacity, f:

$$\mu = \mu^\theta + RT \ln \frac{f}{P^\theta} \qquad (2.3.4)$$
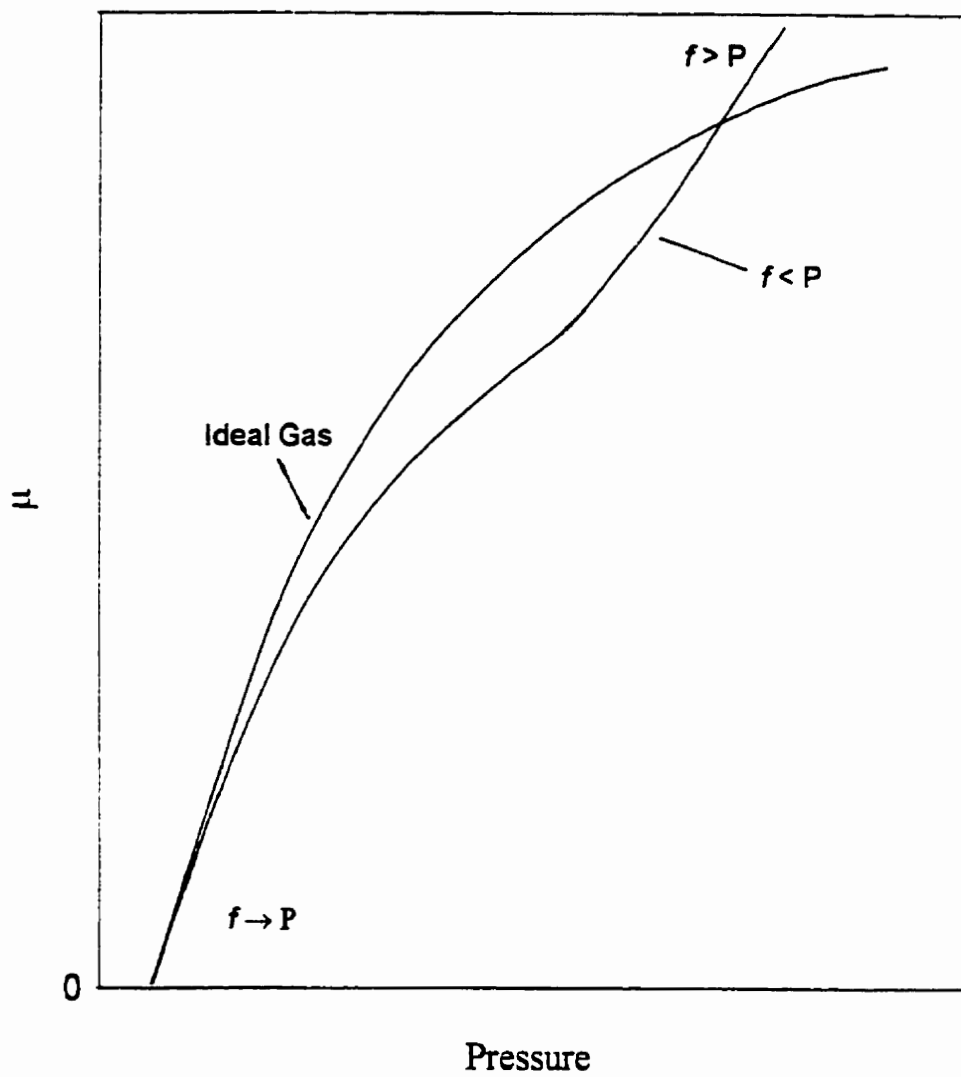
Figure 2.3.1. Chemical potential as a function of pressure

Fugacity can be related to pressure with a dimensionless fugacity coefficient φ which is dependent on the gas as well as the system temperature and pressure (i.e. φ can be calculated with an equation of state):

$$f = \varphi P \qquad (2.3.5)$$

Equation (2.3.4) can now be rewritten as:

$$\mu = \mu^\theta + RT \ln \frac{P}{P^\theta} + RT \ln \varphi \qquad (2.3.6)$$

The third term $(RT \ln \varphi)$ expresses the effect of all intermolecular forces. Since $f \to P$ as $P \to 0$, then $\varphi \to 1$ as $P \to 0$.

2.4 Ideal and Real Liquids

2.4.1 Solvents

The chemical potential of a solvent depends on its composition. At equilibrium, the chemical potential μ^* of a pure liquid is equal to the chemical potential of its vapour:

$$\mu^*(l) = \mu^\theta - RT \ln \frac{P^*}{P^\theta} \qquad (2.4.1)$$

P^* is the vapour pressure of the pure liquid at temperature T and P^θ is equal to 1 bar. If another substance is also present, the chemical potential is defined without the (*) notation. Combining these two relations gives an equation dependent on the ratio of vapour pressures:

$$\mu(l) = \mu^*(l) - RT \ln \frac{P}{P^*} \qquad (2.4.2)$$

For ideal solutions, $P/P^* = x$ which is the mole fraction of solvent. This is Raoult's Law. Ideal solutions obey the law throughout the entire composition range. For real solutions, the law is obeyed closely for the component in excess as it approaches purity, that is, for the solvent. When a real solution does not obey Raoult's Law an activity term is used instead:

$$\mu(l) = \mu^*(l) + RT \ln a \qquad (2.4.3)$$

The activity a accounts for the effect of molecular interactions and approaches the mole fraction as $x \to 1$. This convergence is expressed with an activity coefficient such that $a = \gamma x$ and $\gamma \to 1$ as $x \to 1$. The chemical potential of the solvent is then:

$$\mu(l) = \mu^{\bullet}(l) + RT \ln x + RT \ln \gamma \qquad (2.4.4)$$

2.4.2 Solutes

The vapour pressure of a volatile solute is proportional to its mole fraction in real solutions at low concentrations. However, a plot of solute vapour pressure versus mole fraction does not give the pure solute's vapour pressure as its slope. Using Henry's Law ($P = xH$), the slope is equal to Henry's constant, H. Henry's constant is chosen so that the plot in Figure 2.4.1 is tangent to the experimental curve at $x = 0$.

Real solutes approach ideal dilute behaviour at low concentrations. The chemical potential for an ideal solute is written as

$$\mu = \mu^{\dagger} + RT \ln x \qquad (2.4.5)$$

with

$$\mu^{\dagger} = \mu^{\bullet} + RT \ln \frac{H}{P^{\bullet}} \qquad (2.4.6)$$

The chemical potential for a real solute substitutes an activity term for the mole fraction term in (2.4.5):

$$\mu = \mu^{\dagger} + RT \ln a \qquad (2.4.7)$$

The activity coefficient reflects the magnitude of molecular interactions which cause the solute to deviate from ideal behaviour, such that $a = \gamma x$; $a \rightarrow x$ and $\gamma \rightarrow 1$ as $x \rightarrow 0$.
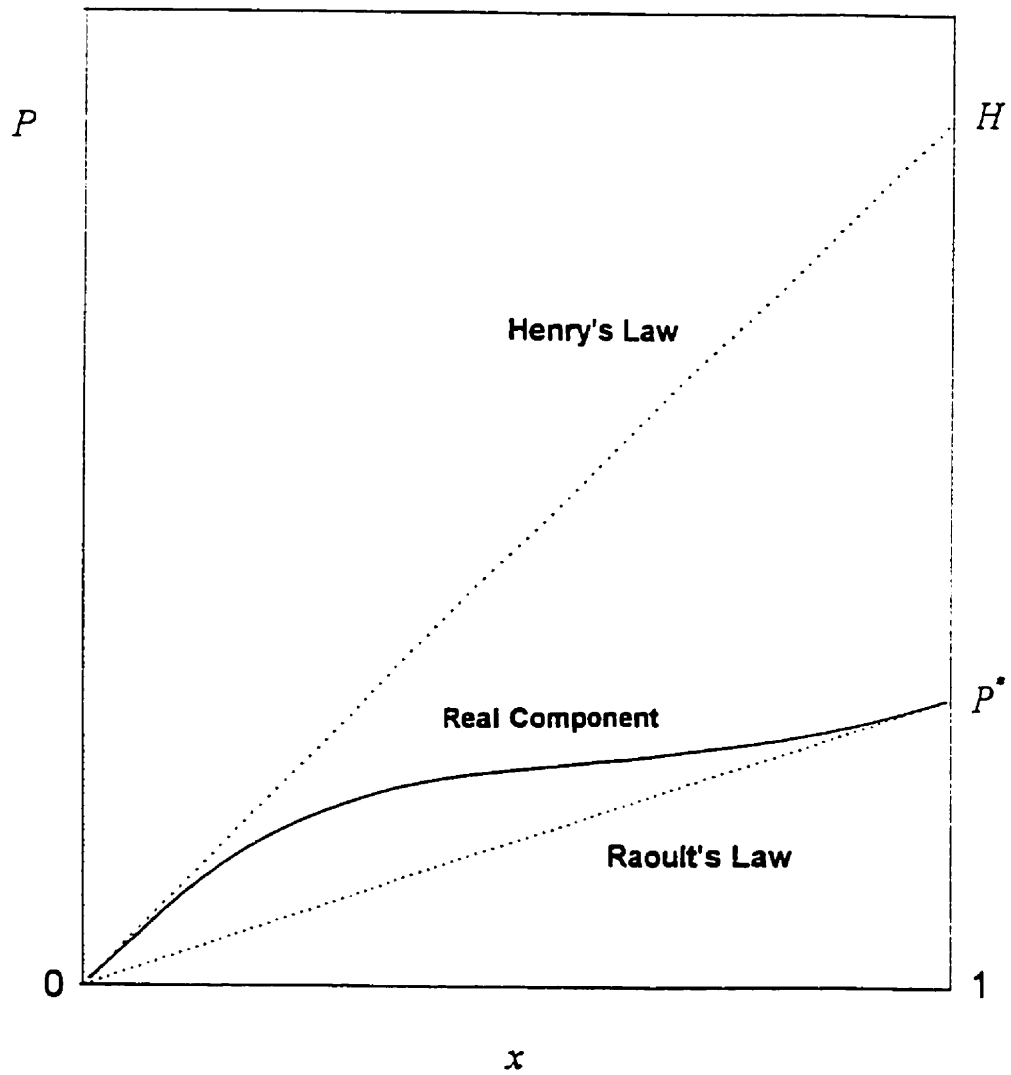
Figure 2.4.1. Pressure versus composition for Raoult's and Henry's Laws

2.5 Solubilities

2.5.1 Thermodynamics of Dissolution

A solid solute is assumed to be in be equilibrium with a saturated solution of it according to the simple reaction:

$$Solute_{(solid)} \rightleftharpoons Solute_{(solution)} \tag{2.5.1}$$
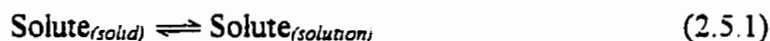
The Gibbs function for the reaction is defined by the change in chemical potential upon dissolution:

$$\Delta G_r = \mu_{(solution)} - \mu_{(solid)} \tag{2.5.2}$$

This function can also be expressed in terms of the standard Gibbs function and the ratio of partial pressures $P_{(solution)} / P_{(solid)}$. $P_{(solution)}$ is the partial pressure of the dissolved solid and $P_{(solid)}$ is the partial pressure of the solid solute. Assuming ideality:

$$\Delta G_r = \Delta G^{\theta} + RT \ln \frac{P_{(solution)}}{P_{(solid)}} \tag{2.5.3}$$

At equilibrium $\Delta G_r = 0$ and the ratio of partial pressures is replaced by the equilibrium constant K:

$$\Delta G^{\theta} = -RT \ln K \tag{2.5.4}$$

For an ideal solution, the mole fraction x can be used in place of K. Since $\Delta G^{\theta} = \Delta H^{\theta} - T\Delta S^{\theta}$, (2.5.4) becomes:

$$\ln x = \frac{-\Delta H^{\theta}{}_{solution}}{RT} + \frac{\Delta S^{\theta}{}_{solution}}{R} \qquad (2.5.5)$$

If the mole fraction of a saturated solution is measured as a function of temperature, the enthalpy and entropy of solution can be determined from the slope $-\Delta H^{\theta}{}_{solution} / R$ and the intercept $\Delta S^{\theta}{}_{solution} / R$.

The solubility of a compound is a strong function of the intermolecular forces between solute and solvent. The forces between chemically similar species cause the enthalpy of solution to be more negative than between dissimilar species. As dissolution is accompanied by a decrease in the Gibbs energy, a more negative enthalpy is more favourable than a large one.

The molar volume change of a solute upon solution, ΔV, is the difference between its partial molar volume at infinite dilution, $V_m{}^{\infty}$, and the molar volume of the pure crystal, V_c, (Sawamura et al., 1993):

$$\Delta V = V_m^{x} - V_c \qquad (2.5.6)$$

It is assumed the degree of mutual solubility is small for an infinitely dilute solution.

Using the relationship,

$$\Delta V = -RT\left(\frac{\delta \ln x}{\delta P}\right)_T \qquad (2.5.7)$$

the volume change of a solute upon solution can be determined by plotting $\ln x$ as a function of pressure.

2.5.2 Solids in Compressed Gases

A discussion of the solubility of a solid or liquid in a compressed gas requires a relation describing the effect of pressure on the fugacity

$$RT\ln\varphi_i = RT\ln\frac{f_i}{x_iP} = \int_0^P\left[\bar{v}_i - \frac{RT}{P}\right]dP \tag{2.5.8}$$

where $\bar{v}_i$ is the partial molar volume of substance i. For a pure component, the molar volume v_i is used and the above equation simplifies to:

$$RT\ln\left(\frac{f}{P}\right)_{pure,i} = \int_0^P\left[v_i - \frac{RT}{P}\right]dP \tag{2.5.9}$$

To calculate the fugacity of a pure liquid or pure solid, the integral in equation (2.5.9) is separated into two parts. The first part gives the fugacity of the saturated vapour at T and P^s, the saturation pressure. The second part of the integral gives the correction due to the compression of the condensed phase, c, to pressure P. At P^s, the fugacity of the saturated vapour is equal to the fugacity of the saturated liquid (or solid) because the phases are in equilibrium. Equation (2.5.9) is rewritten to define the fugacity f_i^c of i in the compressed, condensed phase:

$$RT\ln\frac{f_i^c}{P} = \int_0^{P^s}\left(v_i - \frac{RT}{P}\right)dP + \int_{P^s}^P\left(v_i^c - \frac{RT}{P}\right)dP \tag{2.5.10}$$

The first term on the right-hand side gives the fugacity of the saturated vapour, that is, the fugacity of the condensed phase. Equation (2.5.10) therefore becomes

$$RT\ln\frac{f_i^c}{P} = RT\ln\frac{f_i^s}{P_i^s} + \int_{P_i^s}^P v_i^c dP - RT\ln\frac{P}{P_i^s} \tag{2.5.11}$$

which can be rearranged to yield

$$f_i^c = P_i^s \varphi_i^s \exp\left(\int_{P_i^s}^{P} \frac{v_i^c dP}{RT}\right)$$

(2.5.12)

This result shows that the fugacity of a pure condensed component is, to a first approximation, equal to the saturation or vapour pressure. The fugacity coefficient φ_i^s corrects for deviations of the pure saturated vapour from ideal gas behaviour. The exponential correction, or Poynting correction, takes into account that the condensed phase is at a pressure different from its vapour pressure. As the Poynting correction is an exponential function of pressure, it is small at low pressures but can become large at high pressures or at low temperatures.

When considering an equilibrium between a compressed gas and a solid, it is generally assumed that the solubility of the gas in the solid is negligible. The condensed phase is therefore considered to be pure and all non-ideal behaviour can be attributed to the vapour phase. The vapour (V) phase fugacity coefficient in the high pressure mixture is given by:

$$\varphi_i^V = \frac{f_i^V}{x_i P}$$

(2.5.13)

Substituting and solving for x_i, the solubility of a solid is expressed as its mole fraction in the gas phase:

$$x_i = \left(\frac{P_i^s}{P}\right) E$$

(2.5.14)

The enhancement factor, E, is a measure of the extent to which pressure enhances the solubility of a solid solute in a compressed gas:

$$E = \frac{\varphi_i^s \exp\left(\int_{P_i^s}^{P} \frac{v_i^c \, dP}{RT}\right)}{\varphi_i^V} \tag{2.5.15}$$

The enhancement factor is nearly always greater than unity, except at low pressures. Therefore, as $P \rightarrow P_i^s$, $E \rightarrow 1$.

Of the three correction terms, φ_i^V is the most important. It can produce large enhancement factors in excess of 10^3. As the saturation pressure P_i^s is usually small, φ_i^s is nearly equal to unity. The Poynting correction is not negligible but is rarely more than 2 or 3.

The review in section 1.4 reported solubility data for phenols, pesticides, and PAH's in CO_2 at 10^{-6} mole fraction or several orders of magnitude higher. Enhancement factors for chrysene, fluoranthene, and triphenylene were 10^6 or more. Solubilities in CO_2 were improved at increased pressures for all solutes due to an increase in fluid density. Solubilities also increased with increasing temperature, although there were cross-over regions for several solutes. Raising the temperature has a dual effect. The fluid density and solvent power are decreased, however, there is a positive effect on solute vapour pressure.

2.5.3 Liquids in Compressed Gases

A discussion of the solubility of a liquid in a compressed gas is more difficult as gases can be appreciably soluble in liquids.

The equilibrium between a high-boiling liquid (A) and a sparingly soluble gas (B) is considered at conditions remote from critical. The "y" term is used for mole fraction values in the gas (or less dense) phase; "x" is used for the liquid (or more dense) phase. The equation of equilibrium between the two phases is

$$f_A^L = f_A^V = \varphi_A y_A P \qquad (2.5.16)$$

where φ_A is the vapour-phase fugacity coefficient of component A in the gaseous mixture. To calculate φ_A, the fugacity of component A in the liquid phase is considered. If the gas is only sparingly soluble, the liquid phase fugacity of A can be calculated by assuming the solubility of component B in the liquid is described by a pressure-corrected form of Henry's Law. The fugacity f_B^L of component B in the liquid phase is related to the mole fraction x_B by:

$$f_B^L = H_{B,A} x_B \exp\left(\int_{P_A^s}^{P} \frac{\overline{v}_B^\infty}{RT} dP \right) \qquad (2.5.17)$$

From the Gibbs-Duhem equation, it can be shown that for pure liquid A:

$$f_A^L = (1 - x_B) P_A^s \varphi_A^s \exp\left(\int_{P_A^s}^{P} \frac{v_A^L}{RT} dP \right) \qquad (2.5.18)$$

Substituting the above equation into (2.5.16), an equation for y_A is obtained:

$$y_A = \frac{(1 - x_B) P_A^s \varphi_A^s \exp\left(\int_{P_A^s}^{P} \frac{v_A^L dP}{RT} \right)}{\varphi_A P} \qquad (2.5.19)$$

The mole fraction x_B is calculated from:

$$x_B = \frac{y_B \varphi_B P}{H_{B,A} \exp\left(\int_{P_A^s}^{P} \frac{\overline{v}_B^\infty dP}{RT} \right)} \qquad (2.5.20)$$

The solution of equation (2.5.19) requires a trial-and-error calculation because the values for x_B, φ_B, and φ_A depend on the composition of the vapour. It is the fugacity coefficient φ_A which accounts for the nonideal behaviour of liquid solubility in compressed gases.

2.5.4 Gases in Liquids: Effect of Pressure

A discussion on the solubility of gases in liquids is important in this work because the dissolution of CO_2 in water gives carbonic acid. The consequent drop in pH (to about 3) is predicted to increase the distribution coefficient of acidic solutes between water and carbon dioxide (Toews et al, 1995). The effect of the nature of a solute on its partitioning is further discussed in section 2.7.

The dependence of Henry's constant on pressure can be obtained using the equation:

$$\left(\frac{\delta \ln f_B^L}{\delta P} \right)_{T,x} = \frac{\bar{v}_B}{RT} \tag{2.5.21}$$

The thermodynamic definition of Henry's constant for a gas B in a particular solvent is, at constant temperature:

$$H_{B,solvent} \equiv \lim_{x_B \to 0} \frac{f_B^L}{x_B} \tag{2.5.22}$$

Substituting (2.5.22) into (2.5.21) gives

$$\left(\frac{\delta \ln H_{B,solvent}}{\delta P} \right)_T = \frac{\bar{v}_B^\infty}{RT} \tag{2.5.23}$$

where the partial molar volume of solute B is specified at infinite dilution. This equation is integrated to obtain a more general form of Henry's Law, assuming that the fugacity of B at constant temperature and pressure is proportional to the mole fraction x_B:

$$\ln \frac{f_B}{x_B} = \ln H_{B,solvent}^{(P')} + \frac{\int_{P'}^{P} \bar{v}_B^{\infty} dP}{RT} \tag{2.5.24}$$

Henry's constant is evaluated at an arbitrary reference pressure P'. As $x_B \to 0$, the total pressure is P_A^s, the saturation or vapour pressure of the solvent A. It is therefore convenient to set $P' = P_A^s$.

If the solution temperature is well below the critical temperature of the solvent, it is reasonable to assume that the partial molar volume of the solvent is independent of pressure. Equation (2.5.24) becomes:

$$\ln \frac{f_B}{x_B} = \ln H_{B,A}^{(P_A^s)} + \frac{\bar{v}_B^{\infty}(P - P_A^s)}{RT} \tag{2.5.25}$$

This is the Krichevsky-Kasarnovsky equation. It represents well the solubilities of sparingly soluble gases to very high pressures. It is assumed that the activity coefficient does not change noticeably over the range of x_B being considered (x_B is small) and that the infinitely dilute solution is essentially incompressible.

2.5.5 Gases in Liquids: Effect of Temperature

The solubility of a gaseous solute in a liquid phase has a temperature derivative that is directly related to either the partial molar enthalpy or the partial molar entropy of the solute. For a nonvolatile solvent where the gas solubility is sufficiently small to make the activity of the solute independent of the mole fraction, the following are true

$$\left(\frac{\delta \ln x_B}{\delta 1/T}\right)_P = -\frac{\Delta \overline{H}_B}{R} \qquad (2.5.26)$$

and

$$\left(\frac{\delta \ln x_B}{\delta \ln T}\right)_P = \frac{\Delta \overline{S}_B}{R} \qquad (2.5.27)$$

where x_B is the mole fraction of gaseous solute at saturation.

Considering equation (2.5.26), the solubility will increase with rising temperature if the partial molar enthalpy is positive. Conversely, if the partial molar enthalpy is negative the solubility will fall as the temperature increases. Equation (2.5.27) indicates that if the partial molar entropy change of the solute is positive, then the solubility increases with rising temperature; otherwise, it falls.

2.5.6 The Carbon Dioxide and Water System

The solubility of water in compressed CO_2 is illustrated in Figure 2.5.1. The amount of water dissolved increases as the pressure and temperature are increased. The solubility of water in CO_2 is less than 0.7 mole % (0.3% v/v) at the experimental conditions used in this work.

Solubility data for carbon dioxide in water are presented in Figure 2.5.2. The solubility increases as pressure is increased but decreases as a function of temperature. The dissolution of carbon dioxide in water reaches saturation once the following equilibria are achieved at a given temperature and pressure:

$$CO_{2\,(g)} + H_2O_{\,(l)} \rightleftharpoons CO_{2\,(aq)} \tag{2.5.28}$$

$$CO_{2\,(g)} \rightleftharpoons H_2CO_{3\,(aq)} \tag{2.5.29}$$

$$H_2CO_{3\,(aq)} \rightleftharpoons H^-_{\,(aq)} + HCO_3^-{}_{\,(aq)} \tag{2.5.30}$$

$$HCO_3^-{}_{\,(aq)} \rightleftharpoons H^-_{\,(aq)} + CO_3^{-2}{}_{\,(aq)} \tag{2.5.31}$$
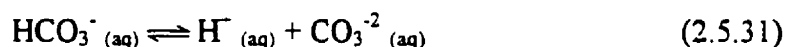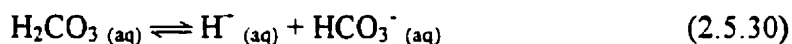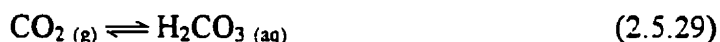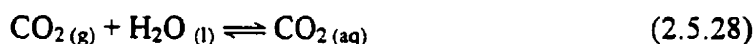
At 25°C and 1 atm, Henry's constant for CO_2 is 3.4×10^{-2} mol L^{-1} atm^{-1}. H decreases to 2.4×10^{-2} mol L^{-1} atm^{-1} at 40°C (Harned and Davis, 1943). The first and second dissociation constants of carbonic acid are $K_1 = 4.5 \times 10^{-7}$ and $K_2 = 4.7 \times 10^{-11}$ at 25°C and 1 atm. The relative amounts of each carbonate species are shown in Figure 2.5.3 as a function of pH.

The value for K_1 increases to 5.1×10^{-7} at 40°C (Harned and Davis, 1943). The first dissociation constant also increases with pressure. Its value is about 5.4×10^{-7} at 200 bar at 25°C (Read, 1975). The data for K_1 indicate the concentration of protons in the water phase increases as the temperature and pressure are increased. This is important for a water extraction as a decrease in pH is predicted to increase the distribution coefficient of acidic solutes between the two phases.
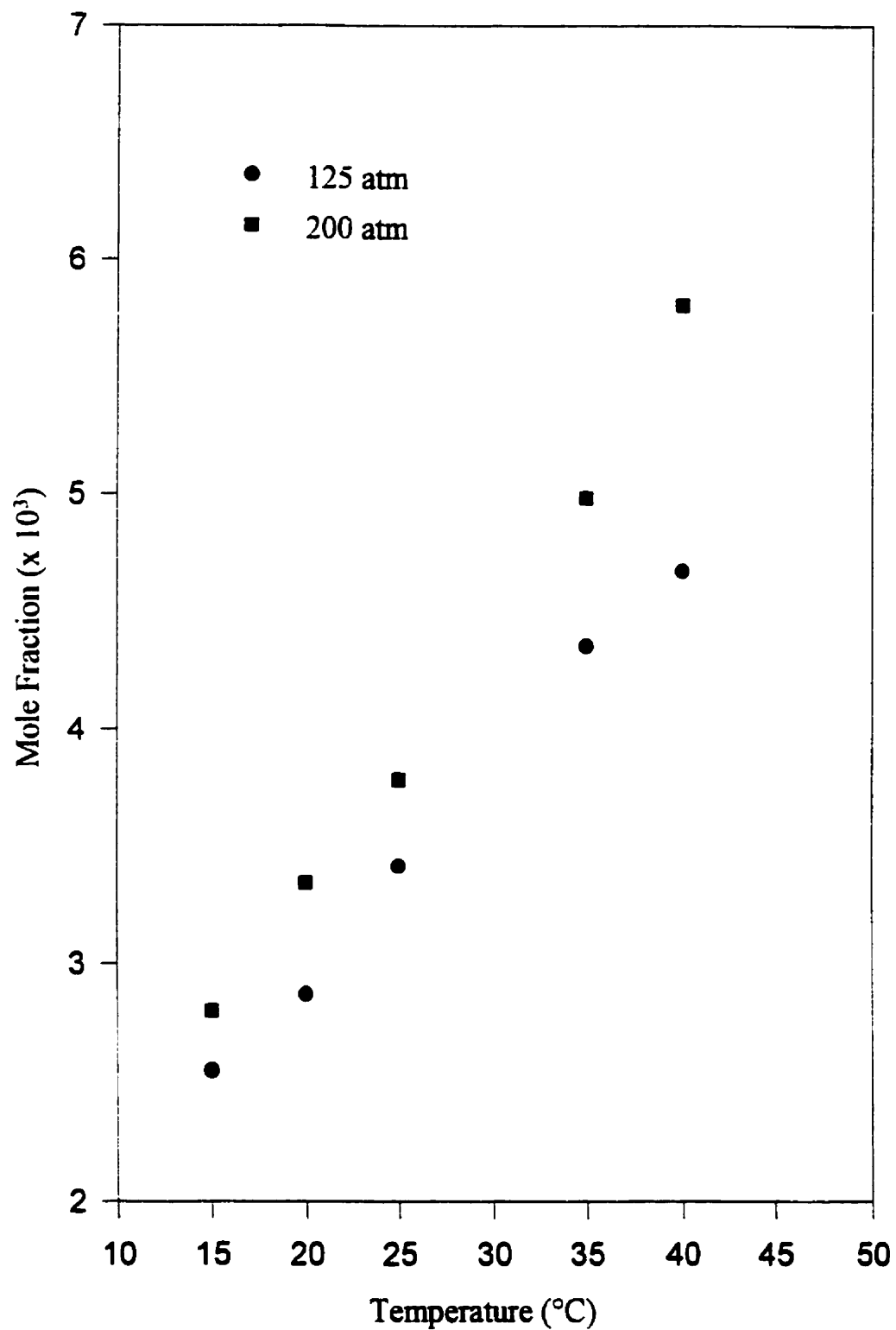
Figure 2.5.1. Solubility of water in CO_2 as a function of temperature and pressure (data from King et al, 1992)
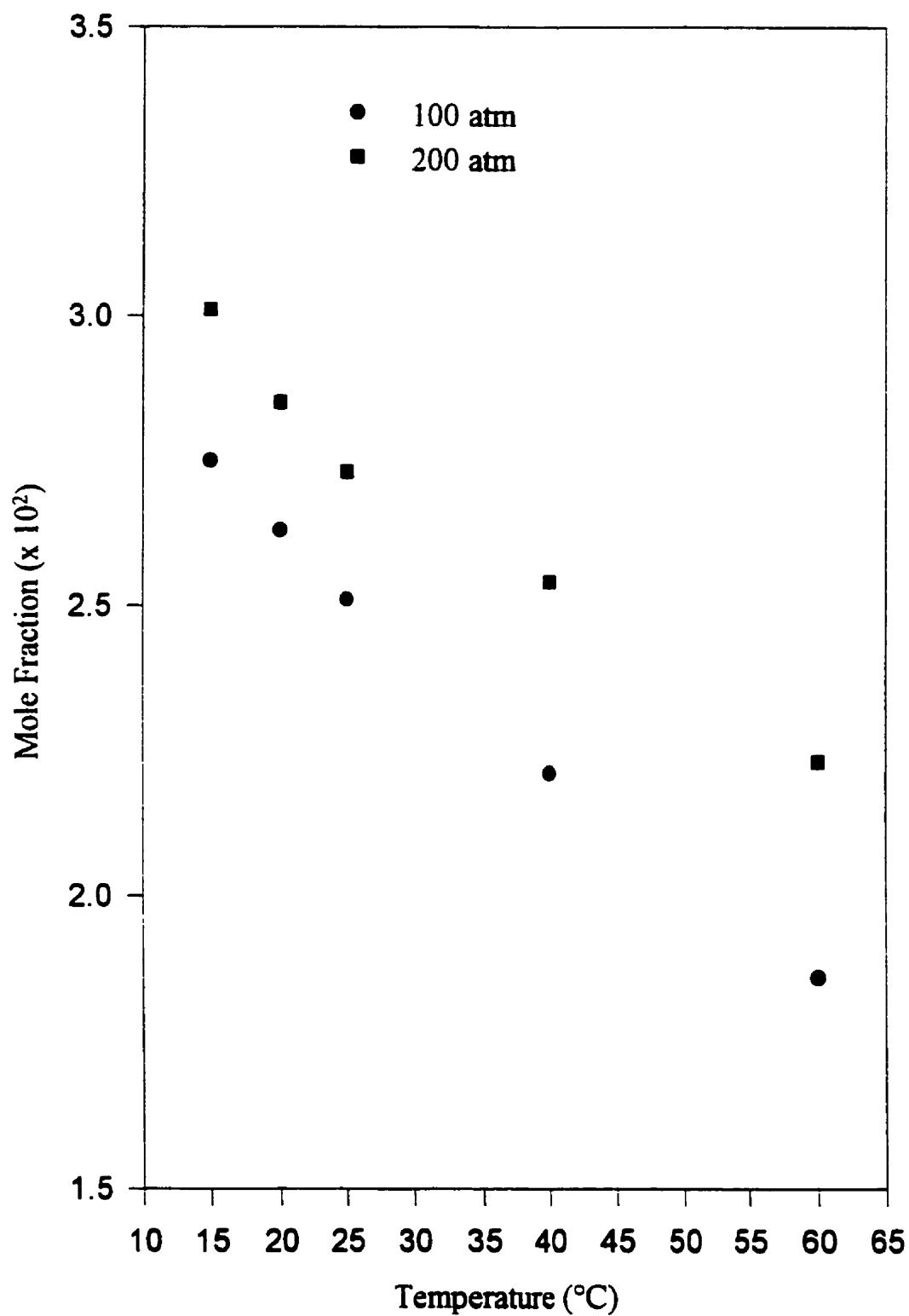
Figure 2.5.2. Solubility of CO_2 in water as a function of temperature and pressure (data from King et al, 1992; Wiebe and Gaddy, 1940; Wiebe, 1941)
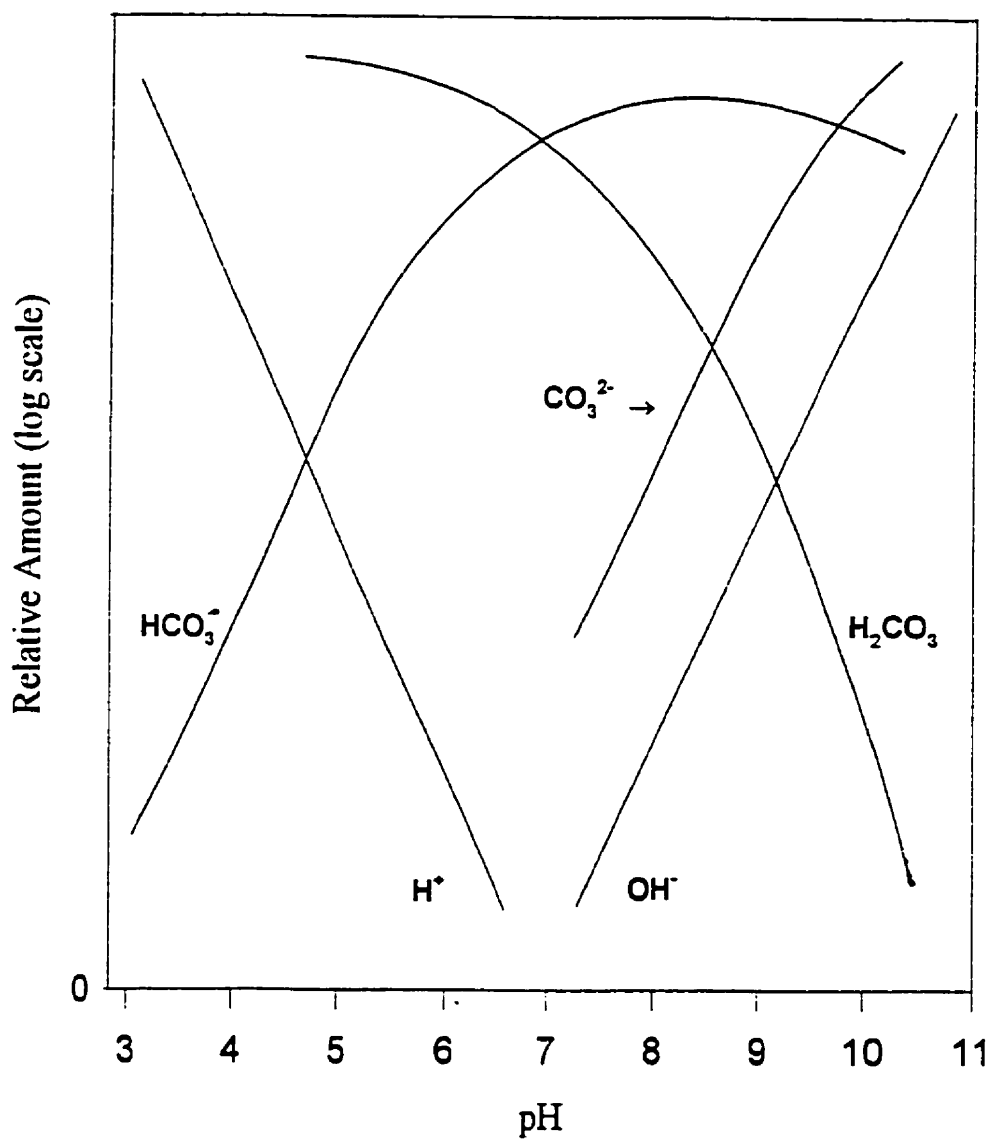
Figure 2.5.3. Variation of carbonate species with pH

The pH of water in contact with carbon dioxide varies between 2.80 to 2.95 over the pressure range of 70 to 200 atm and between 25 and 70°C (Toews et al, 1995). The pH decreases slightly as the pressure is increased due to the increased solubility of CO_2 and thus increased concentration of H_2CO_3, as well as the increase in K_1. However, the pH increases marginally with increases in temperature. This result contradicts the effect predicted by the increase in K_1 as a function of temperature. The decrease in CO_2 solubility in water as a function of temperature evidently has a greater effect on pH than the magnitude of the first dissociation constant.

2.6 Mixtures

2.6.1 Thermodynamics of Mixing

The total Gibbs function of a gaseous system with components A and B is

$$G = n_A \mu_A + n_B \mu_B \qquad (2.6.1)$$

where μ_A and μ_B are the chemical potentials at the composition of the mixture n_A and n_B. After mixing, each gas exerts a partial pressure. For the simplest case, the Gibb's function of mixing is written as:

$$\Delta G_{mix} = nRT(x_A \ln x_A + x_B \ln x_B) \qquad (2.6.2)$$

Since mole fractions are never greater than 1, the logarithms will be negative and $\Delta G_{mix} < 0$ for perfect gases in all proportions.

It follows that $\Delta S_{mix} > 0$ according to:

$$\Delta S_{mix} = -nR(x_A \ln x_A + x_B \ln x_B) \qquad (2.6.3)$$

As well,

$$\{\Delta H_{mix} = 0; \Delta V_{mix} = 0; \Delta U_{mix} = 0\}_{P,T} \qquad (2.6.4)$$

as there are no interactions between gas particles.

The driving force for mixing ideal gases therefore comes from the increase in entropy of the system. The mixing functions defined in equations (2.6.2), (2.6.3), and (2.6.4) are the same for an ideal liquid mixture. In this case interactions occur

but the average *A-B* interactions in the mixture are the same as the average *A-A* and *B-B* interactions in the pure liquids.

In real solutions, the interactions between *A* and *B* are different for each solute-solvent pair. Real mixtures are characterized by an enthalpy change and there can be an additional contribution to the entropy change. If the enthalpy change is large and positive, or if the entropy change is negative, the Gibbs function may be positive, making the two fluids only partially miscible. Real solutions are described by excess functions (G^E, S^E, etc.) to compensate for deviations from the ideal mixing functions. For instance,

$$S^E = \Delta S_{mix} + nR(x_A \ln x_A + x_B \ln x_B) \qquad (2.6.5)$$

Deviations of the excess functions from zero indicate the extent to which the solutions are non-ideal.

2.6.2 Phase Behaviour at High Pressures

A variety of phase behaviours are observed for binary systems at high pressures (20 - 1000 atm). Six classes of binary systems are illustrated in Figure 2.6.1. The simplest case is a class I mixture. The pressure - temperature diagram for this mixture shows the liquid - vapour curves for the pure components 1 and 2. The curves terminate at the critical points for each component, at C_1 and C_2. The dashed line joining these points is the critical locus. Each point on this line is the critical point for a mixture of fixed composition. The critical locus may or may not show a maximum or minimum. The plots in Figure 2.6.1 are actually *p-T* projections of a *P-T-x* surface, shown in Figure 2.6.2 for the class I mixture.
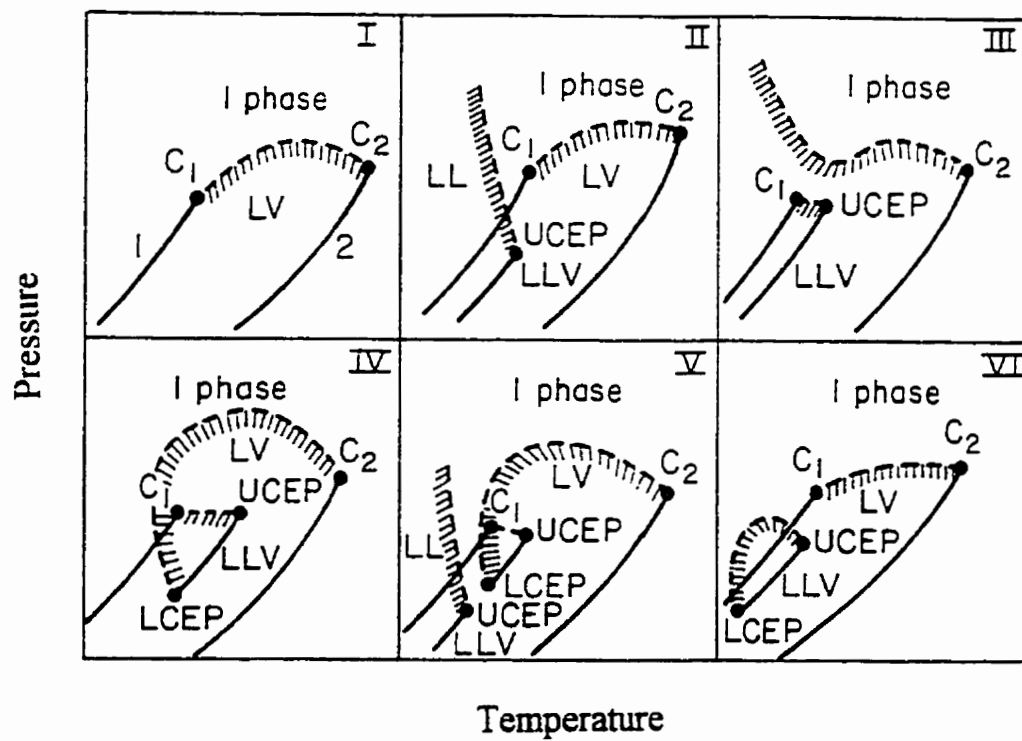
Figure 2.6.1. Six types of phase behaviour in binary fluid systems
(from Prausnitz, 1986)
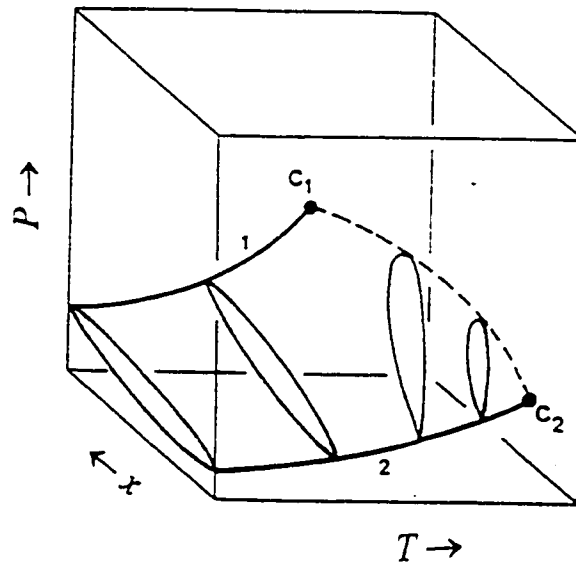
Figure 2.6.2. *P-T-x* surface for a class I mixture

(from Prausnitz, 1986)

Class II mixtures of components 1 and 2 are not miscible in all proportions at low temperatures, but are otherwise similar to class I mixtures. The line labeled LLV describes a three-phase equilibrium of one vapour phase with two liquid phases. This locus ends at the upper critical end point ($UCEP$) where the two liquid phases merge into one liquid phase. The dashed line curving upward from this point indicates that the $UCEP$ depends on temperature. In this case the line has a negative slope but it may be initially positive and become negative at higher pressures.

The class III case illustrates how the vapour-liquid critical locus is not necessarily a continuous line connecting C_1 and C_2. It has two branches, one branch going from C_1 to the $UCEP$, the second starting at C_2 and rising with pressure with a positive or negative slope. The critical line starting at C_2 with a positive slope indicates the existence of a gas-gas equilibria. In this circumstance, two phases are at equilibrium at a temperature larger than the critical temperature of either pure component. In class IV, the second branch from C_2 terminates at the lower critical end point ($LCEP$).

Class V is similar to class IV except that the LLV locus is broken into two parts indicating that there is limited liquid miscibility at low temperatures. The second region of limited miscibility starts at the $LCEP$. Both end at a distinct $UCEP$. In the last case, class VI, there are two critical curves: One connects C_1 and C_1 while the other connects the $UCEP$ to the $LCEP$.

Figures 2.6.3 and 2.6.4 give pressure-composition plots of carbon dioxide and water at isotherms above and below the critical point of CO_2. Both plots approximate class I phase behaviour as neither shows evidence of the LLV line which typically parallels the vapour-liquid curve for pure component 1. In both plots, water is component A and CO_2 component B. Two phases exist at most compositions above the critical pressure for carbon dioxide. Single phases only exist at about $x_B < 0.03$

or $x_B > 0.99$. The CO_2 / water experiments performed in this research were in the two-phase region as x_B was typically between 0.1 and 0.3.
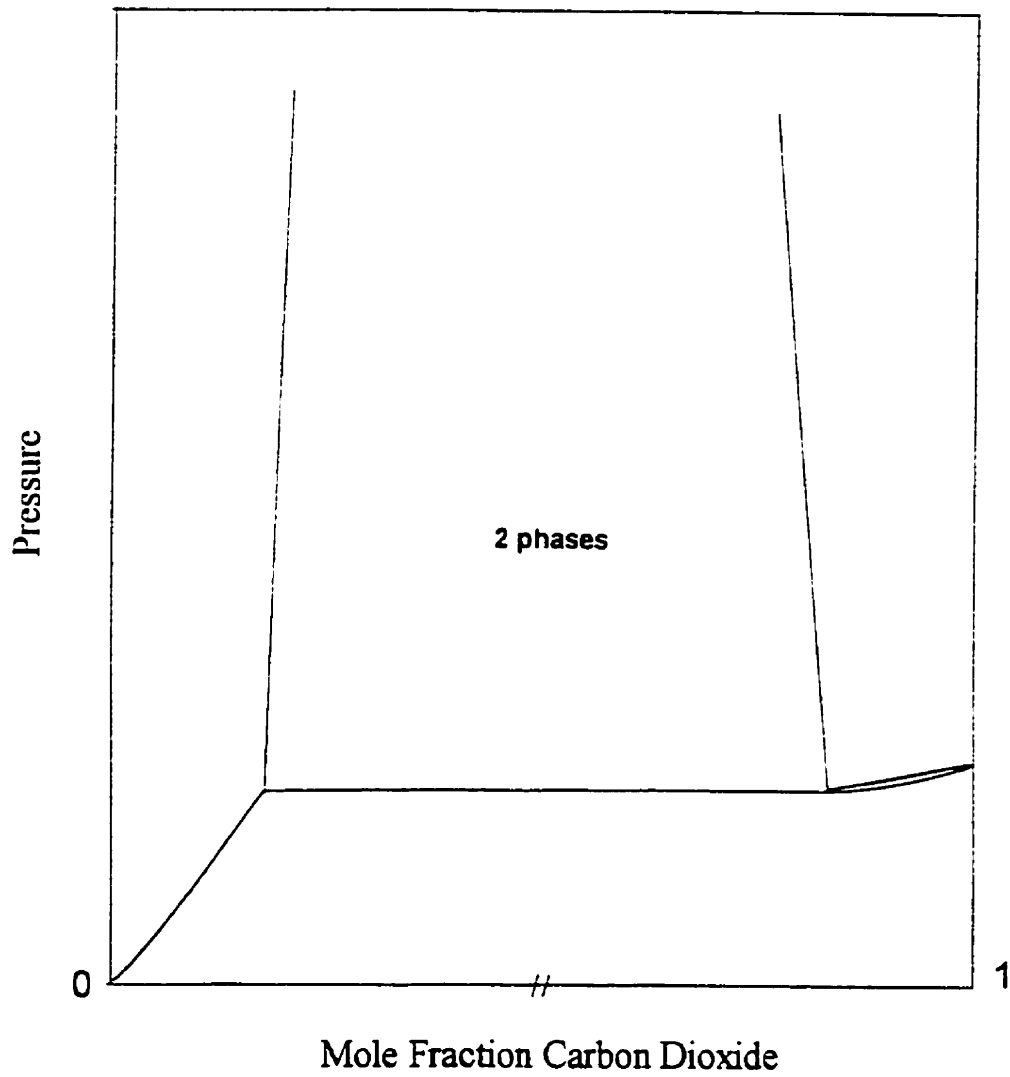
Figure 2.6.3. A typical pressure-composition diagram for the CO_2-water system at temperatures below T_c for carbon dioxide (from King et al, 1992)
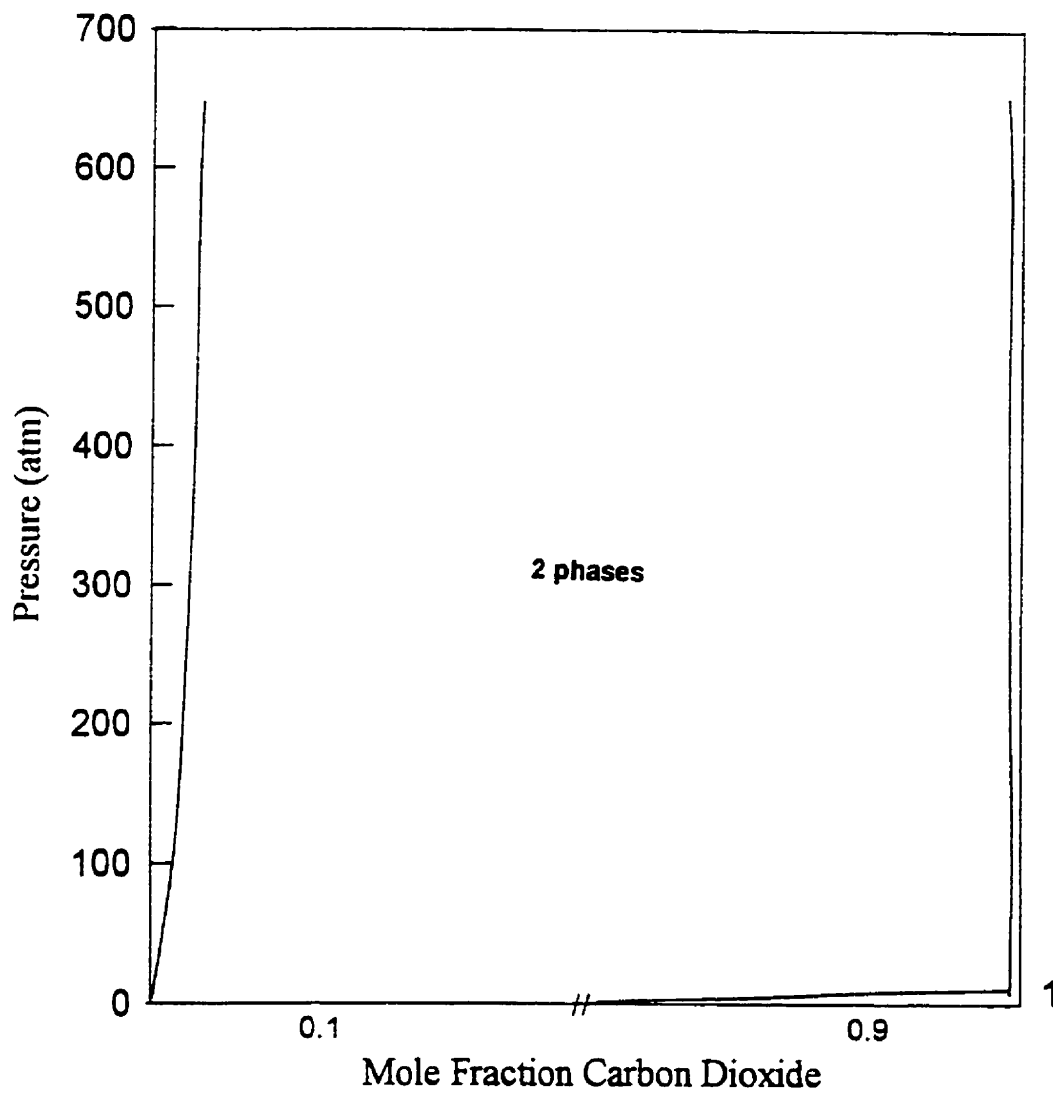
Figure 2.6.4. A typical pressure-composition diagram for the CO_2-water system at temperatures above T_c for carbon dioxide (from Wenzel and Rupp, 1978)

2.7 Partitioning

2.7.1 Distribution Coefficient

At equilibrium, solute i will be distributed between two phases, A and B. In the simplest case, the mole fraction of solute in either phase is very small and it is assumed that the two phases are ideal dilute solutions. The solute activities in the two phases are:

$$a_i^A = \gamma_i^A x_i^A \tag{2.7.1}$$

$$a_i^B = \gamma_i^B x_i^B \tag{2.7.2}$$

The distribution coefficient K between between two immiscible solvents is defined by equating the activities of component i in the two phases:

$$K = \frac{x_i^B}{x_i^A} = \frac{\gamma_i^A}{\gamma_i^B} \tag{2.7.3}$$

At constant temperature and pressure, the partition coefficient is a true constant independent of composition for ideal dilute solutions. Equation (2.7.3) is frequently called the Nernst distribution law.

2.7.2 Distribution of a Solid Solute

The solubility ratio of a solid solute between two phases provides a good prediction of its partitioning behaviour and has been considered in the literature reviewed in section

1.3. However, for non-ideal solutions, partitioning also depends on solute concentration.

The distribution of solid solute i between two immiscible liquids is described at equilibrium:

$$\gamma_i^A x_i^A = \gamma_i^B x_i^B \qquad (2.7.4)$$

Activity coefficients γ_i^A and γ_i^B are, respectively, functions of the mole fractions x_i^A and x_i^B. If the solutions are only moderately non-ideal, these functions can be expressed by

$$\ln \gamma_i^A = \alpha^A (1 - x_i^A)^2 \qquad (2.7.5)$$

$$\ln \gamma_i^B = \alpha^B (1 - x_i^B)^2 \qquad (2.7.6)$$

where α^A and α^B are interaction constants which depend only on temperature for a given solute-solvent pair. Substitution of equations (2.7.4), (2.7.5), and (2.7.6) into (2.7.3) gives:

$$\ln K_i = \alpha^A (1 - x_i^A)^2 - \alpha^B (1 - x_i^B)^2 \qquad (2.7.7)$$

This relation shows that, in general, the distribution coefficient is not a constant but depends on composition as defined by x_i^A or x_i^B.

The interaction constant α^A can be found from the solubility of the solute in solvent (A), $x_{i,sat}^A$. The equation of equilibrium for pure solid (S) and the saturated solution (L) of it is:

$$f_i^S = x_{i,sat}^A \gamma_{i,sat}^A f_i^L \qquad (2.7.8)$$

Substituting equation (2.7.5) and solving for α^A gives:

$$\alpha^A = \frac{\ln \dfrac{f_i^S}{f_i^L x_{i,sat}^A}}{(1 - x_{i,sat}^A)^2}$$

(2.7.9)

Similarly,

$$\alpha^B = \frac{\ln \dfrac{f_i^S}{f_i^L x_{i,sat}^B}}{(1 - x_{i,sat}^B)^2}$$

(2.7.10)

The fugacity ratio f_i^S / f_i^L can be obtained from the thermodynamic properties of the pure solute. Once the interaction constants are known, the relationship between x_i^A and x_i^B is given by (2.7.7) (Prausnitz et al, 1986).

2.7.3 Thermodynamic Models of Partitioning

A model based on the Peng-Robinson equation of state has been shown to work well for the partitioning of 2,4-dichlorophenol between water and supercritical CO_2 (Akgerman and Carter, 1994). From section 2.1, the Peng-Robinson equation of state is:

$$P = \frac{RT}{(V - b)} - \frac{a(T)}{V(V + b) + b(V - b)}$$

(2.7.11)

For a pure fluid, constant b is given by

$$b = 0.07780\frac{RT_c}{P_c} \qquad (2.7.12)$$

while $a(T)$ is given by

$$a(T) = a(T_c)\alpha(T_r,\omega)$$

$$a(T_c) = 0.45724\frac{R^2T_c^2}{P_c} \qquad (2.7.13)$$

$$\alpha = [1 + \beta(1 - T_r^{1/2})]^2$$

(note this is not the same α as in equations (2.7.5) to (2.7.10). Here, T_r is the reduced temperature and β depends on acentric factor ω according to $\beta = 0.37464 + 1.54226\omega$ - $0.26992\omega^2$. The acentric factor is a macroscopic measure of the extent to which the force field around a molecule deviates from spherical symmetry and is given by the empirical relation

$$\omega = -\log 10\left(\frac{P^s}{P_c}\right)_{T/T_c=0.7} - 1.0000 \qquad (2.7.14)$$

where P^s is the saturation (vapour) pressure. The acentric factor is essentially zero for spherical, nonpolar molecules (such as the heavy noble gases) and for small, highly symmetric molecules (such as methane).

The following equation defines the fugacity coefficient for a component in a mixture in terms of the independent variables V and T:

$$RT\ln\gamma_i = RT\ln\frac{f_i}{x_iP} = \int_V^\infty\left[\left(\frac{\partial P}{\partial n_i}\right)_{T,V,n_j} - \frac{RT}{V}\right]dV - RT\ln z \qquad (2.7.15)$$

Equation (2.7.15) can be used to calculate the fugacity of a component in a mixture provided the volumetric data is available. The Peng-Robinson equation of state, which is pressure-explicit, can provide the volumetric data at the temperature under consideration and as a function of composition and density. Applying the integral to the Peng-Robinson equation of state gives the following expression as shown by Panagiotopoulos and Reid (1986) for highly polar asymmetric systems (such as those investigated in this work)

$$\ln \gamma_i = \frac{b_i}{b_m}(Z-1) - \ln(Z-B) - \frac{A}{2\sqrt{2}B}$$

$$\left[\frac{\sum_k x_k(a_{ik} + a_{ik})}{a_m} - \frac{\sum_k \sum_j x_k^2 x_j (k_{kj} - k_{jk})(a_k a_j)^{1/2} - x_i \sum_k x_k (k_{ik} - k_{ki})(a_i a_k)^{1/2}}{a_m} - \frac{b_i}{b_m} \right]$$

$$\ln\left(\frac{Z+(1+\sqrt{2})B}{Z+(1-\sqrt{2})B} \right)$$ (2.7.16)

with

$$a_m = \sum_i \sum_j x_i x_j a_{ij}$$ (2.7.17)

$$b_m = \sum_i x_i b_i$$ (2.7.18)

$$a_{ij} = (1 - k_{ij} + (k_{ij} - k_{ji})x_i)(a_i a_j)^{1/2}$$ (2.7.19)

$$B = \frac{b_m P}{RT}$$ (2.7.20)

$$A = \frac{a_m P}{R^2 T^2}$$ (2.7.21)

$$Z = \frac{PV}{RT}$$ (2.7.22)

The constants a_m and b_m are defined by concentration dependent mixing rules for each phase in the mixture. The constant b_m is proportional to the size of the molecules and is related to the average of the molecular volumes. a_m reflects the strength of attraction between two molecules and is expressed by averaging over all molecular pairs. The interaction coefficients k_{ij} and k_{ji} must be evaluated from experimental data or taken from the literature.

Evaluating equation (2.7.16) is done for the solute in each phase. The interaction parameters are adjusted until the measured value of K matches the predicted ratio of fugacity coefficients in equation (2.7.3).

2.7.4 Nature of the Solute

Most solutes of interest to partitioning experiments between water and carbon dioxide have been acidic due to the anticipated effect pH will have on the distribution coefficient. These weak acids ($pK_a > 3.5$) partially hydrolyze in water to their corresponding anions and proton. Analyte dissociation is expected to have a negative effect on method efficiency and sensitivity as ionic species are almost insoluble in CO_2 due to its low dielectric constant (compared with $\varepsilon_r = 78$ for water at 1 atm and 25°C). ε_r for carbon dioxide increases from about 1 to 1.8 as the pressure is increased from 1 to 2000 bar (Schneider, 1994). However, the dissolution of carbonic acid should cause acidic solutes to be almost completely associated in the water-phase at pH 3 (Toews et al, 1995), thus facilitating their extraction:

$$A^- + H_3O^+ \rightarrow HA + H_2O \qquad (2.7.23)$$

The affinity of a solute for either phase depends in part on the same parameters governing its solubility, that is, on temperature, pressure, fluid density, solute vapour pressure, solute fugacity, and solute molar volume. The molecular interactions

between solute and solvent are also important. Ions, acids, bases, and polar species dissolve well in water due to the strength of ion-dipole and dipole-dipole interactions, hydrogen bonding, and hydrolysis reactions. Phenol is highly soluble in water because it forms strong hydrogen bonds with the water. Pentachlorophenol, on the other hand, is sparingly soluble since hydrogen bonding is minimized by the proximity of chlorine atoms in both ortho positions to the phenol group. Intramolecular hydrogen bonding occurs between the phenol group and the ortho chlorine atoms (Blackman et al, 1955).

The potential for molecular interactions in quadrupolar CO_2 is weak as dipole-quadrupole, quadrupole-quadrupole, and quadrupole dispersion interactions depend on $1/r^8$ or $1/r^{10}$. However, these interactions still occur and are the principle interactions between CO_2 and a solute.

CHAPTER THREE
EQUIPMENT AND METHODS

3.1 Equipment

3.1.1 Supercritical Fluid Apparatus

The supercritical fluid extraction apparatus used in all experiments consisted of a high pressure cell coupled to a liquid chromatograph. Samples could be taken from each of the CO_2 and water phases and injected directly to the HPLC. The apparatus was modified as required to measure the temperature inside the cell as well as the electrical resistance of each phase.

A schematic diagram of the extraction vessel and the on-line plumbing to an HPLC unit using three six-port valves (Valco) is shown in Figure 3.1.1. A photograph of the extraction cell is shown in Figure 3.1.2. An engineering schematic is shown in Appendix 1. The vessel was designed and constructed at the *Science Technology Centre* at Carleton University (Ottawa). The body was made of AISI 316 stainless steel; the cap was made of 17-4-PR hardenable stainless steel hardened to Rockwell C 50. An O-ring groove was drilled on the inside surface of the cap fitted with a Teflon seal. All fittings and tubing were made of ANSI 316 stainless steel. Unless specified, all tubing was 1/16" with a 0.03" i.d. The total internal volume of the system from the entrance Valco two-port shut-off valve to the exit shut-off valves of the same type was 105 mL.

A 1/16" Swagelok - 1/8" universal pipe thread union was screwed into a threaded opening on one side of the vessel. The centre of the union was drilled out such that a 1/16" steel thermocouple could be fed through and swaged in place. Temperature was monitored with an Omega microprocessor thermometer (model HH22) capable of 0.1°C precision. A magnetic stir bar was placed inside the cell and the apparatus
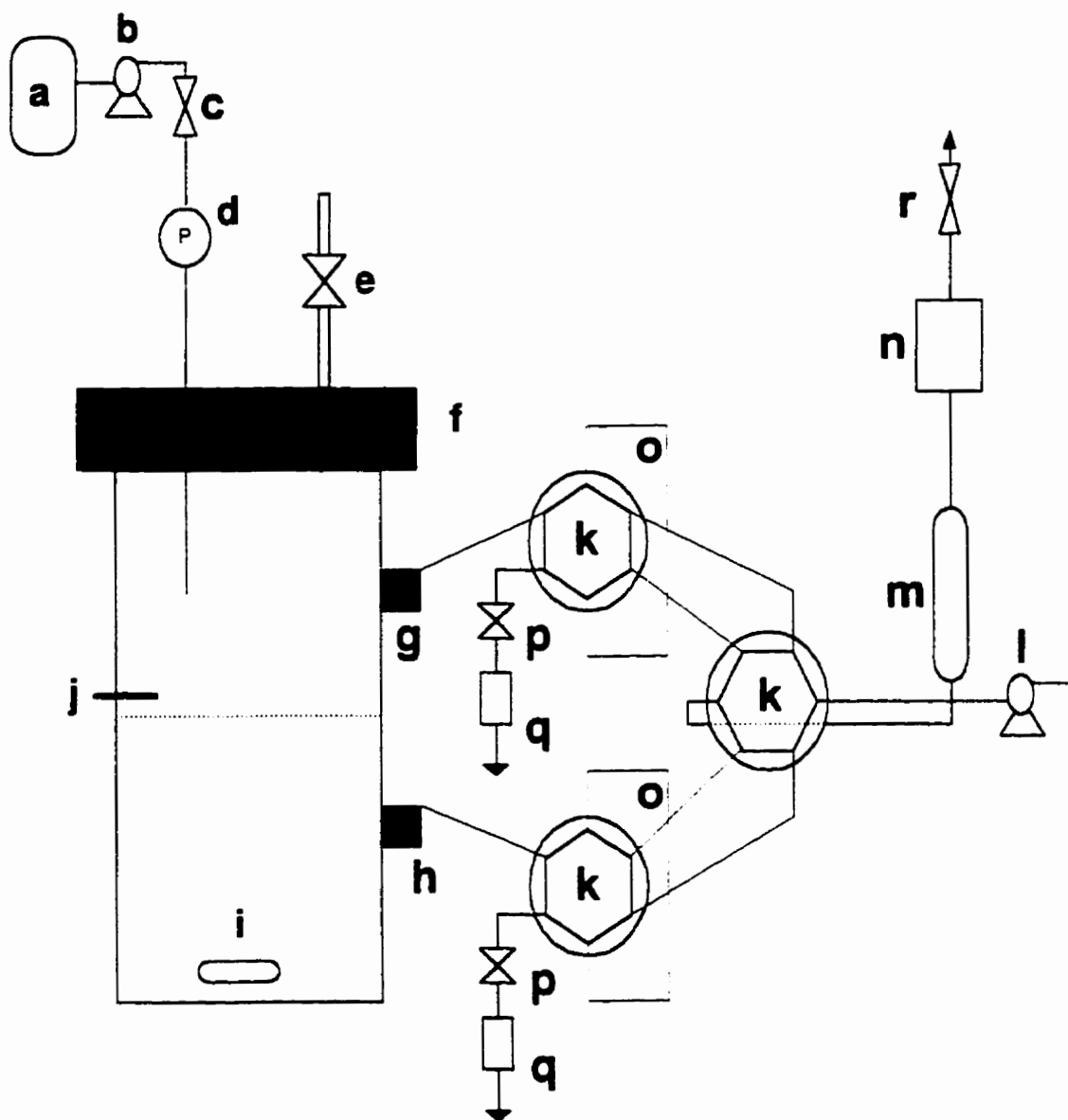
Figure 3.1.1. Experimental apparatus: (a) Liquid CO_2, (b) Pump, (c) Entrance Valve, (d) Pressure Gauge, (e) 1/4" Ball Valve, (f) Screw Cap, (g) Upper Sample Port, (h) Lower Sample Port, (i) Stir Bar, (j) Thermocouple, (k) Six-Port Valve, (l) HPLC Pump, (m) HPLC Column, (n) UV Detector, (o) Sample Loop, (p) Exit Valve, (q) Restrictor, (r) Back-Pressure Regulator
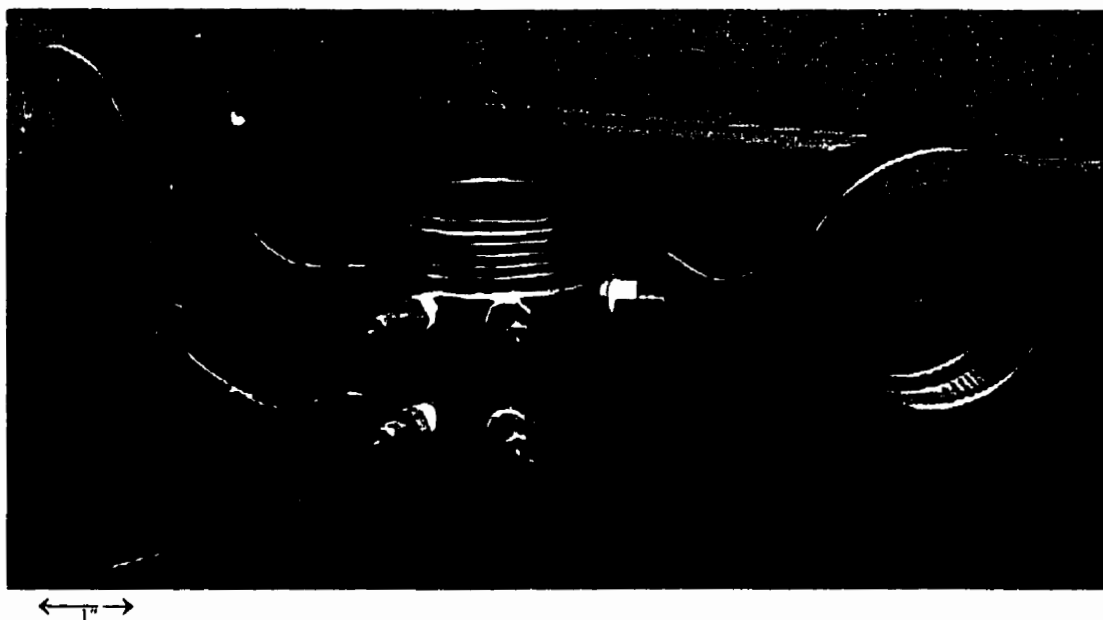
Figure 3.1.2. Supercritical fluid extraction cell

placed over a magnetic stirrer for solution mixing. The pressure was continually monitored using a Bourdon gauge (Span Instruments) with a (0 - 6000) psi range and 25 psi precision. The ¼" ball valve (Whitey) in the cap allowed access to the interior of the vessel without having to dismantle the apparatus. The sample ports were made by welding sections of 1/16" tubing to one side of the vessel. A frit downstream from the upper sample port was sometimes used to trap solid particles during solubility tests. Miscellaneous zero-volume and Swagelok stainless steel fittings, unions, and reducers were used as required.

For chrysene and 2,4-D solubility experiments, the vessel, transfer lines, switching valves, and upper sample loop were thermostated in a water bath heated electrically. A Tenney Junior oven enclosing the entire apparatus was used for all other experiments.

Two different high pressure pumps were used. A packed plunger pump (Milton Roy MiniPump) delivered CO_2 through a section of 1/8" stainless steel tubing welded to the vessel cap for chrysene and 2,4-D solubility measurements. The pump head was cooled with a heat exchanger carrying a solution of 20% ethylene glycol in water to prevent vaporization of the CO_2. A Suprex SFE-50 syringe pump was used for all other experiments, in which case carbon dioxide with a pressurized helium headspace was used. It is possible helium in the carbon dioxide caused solute solubilities to be smaller than in pure CO_2 (King et al, 1995). However, helium was not expected to affect the distribution coefficient K as the supercritical phase was not saturated with solute. The syringe pump was also used for delivery of pressurized water.

3.1.2 HPLC Hardware

A Varian LC Star System with a 250 x 4.6 mm 5 μM C_{18} column (Zorbax), ternary pump (Varian 9010), and variable wavelength ultraviolet detector (Varian 9050; 190 – 700 nm) was used to analyze sample aliquots of chrysene and 2,4-D using the

configuration shown in Figure 3.1.1. The ternary pump was replaced with a Waters 6000A or Waters 501 pump for the analysis of all other solutes. A back-pressure regulator set at 3 atm prevented vaporization of the mobile phase in the detector. Standard aliquots were injected using a needle guide screwed into either the upper or lower six-port valve. In this manner, the same sample loop could be used for both standard and sample injections.

The HPLC methods are listed in Table 3.2.1, section 3.2.6.

3.2 Methods

3.2.1 Sample and Standard Preparation

The sources and purities of all chemicals used are listed in Table 3.2.2, section 3.2.7.

Saturated aqueous solutions were prepared by stirring excess solid solute in flasks of distilled, deionized (DDI) water for several hours to several days. Undissolved solid particles remained in the solutions upon saturation, indicating the solubility limit had been reached. Saturated acid, base, and salt solutions were made in the same manner by first diluting different amounts of HCl, Na_2CO_3, or NaCl in water. The saturated solutions were diluted as required after first filtering them through glass wool to remove solid particulates.

Analyte standards with low concentrations (0.1 – 10 μg / mL) were prepared by doping organic or aqueous solvents with small amounts of concentrated stock solution (~1000 μg / mL organic solvent). Standards of all solutes except chrysene were also prepared in pure carbon dioxide or CO_2 saturated with water. Two methods were used to make pure CO_2 standards. For the first, a very small, concentrated aliquot of the solute was placed inside the cell and the solvent was allowed to evaporate prior to pressurization. Although the cell contents were thoroughly mixed with the stir bar, poor precision was obtained with this method possibly because of partial evaporation of the solute. The alternative was to pass CO_2 from the pump through a sample loop filled with a known volume of stock solution. The syringe pump was programmed to maintain a constant pressure with the result that the standard was carried into the cell when the exit valve on the upper sample port was opened. After a sufficient amount of time, the valve was closed and the cell contents mixed before sampling. The latter method was also used to prepare standards in water-saturated CO_2. Carbon dioxide was first bubbled through water using the "drubbler" developed by Brewer and Kruus (1993) (see section 1.1) before travelling through the loop containing the stock solution.

3.2.2 Determination of Analyte pK$_a$

The dissociation constants of several weak acids were measured at ambient temperature and pressure. A saturated solution of each analyte was titrated against 0.01 M NaOH. The solution pH was measured with an Accumet pH meter (model 910) at the start of the titration and after each NaOH aliquot was added (about 0.05 mL). The meter was calibrated with a buffer solution at pH 7.

Solution pH was plotted as a function of titrant volume using the spreadsheet program SigmaPlot, v.101. It was assumed for the titration of weak acids that at the midpoint [HA] ≈ [A⁻] and

$$K_a = \frac{[H_3O^-][A^-]}{[HA]} = [H_3O^-] \qquad (3.2.1)$$

or pK$_a$ = pH at this midpoint. The derivative of the titration curve in Figure 3.2.1(a) was calculated to find the volume of NaOH added at the endpoint, that is, at the point of maximum slope as shown in (b). From (a), the pH corresponding to half this volume gives the solute pK$_a$.
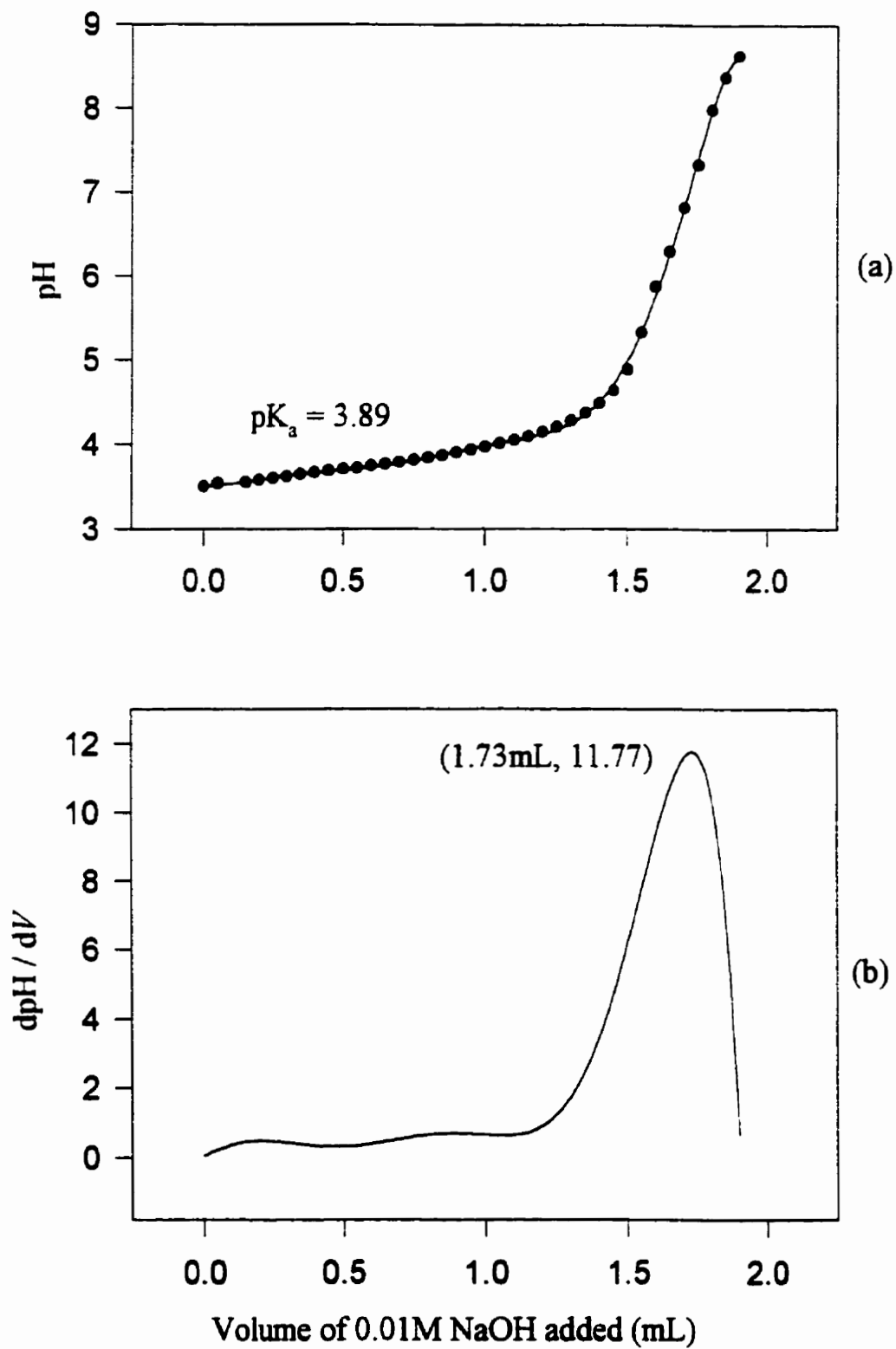
Figure 3.2.1. (a) pK$_a$ titration curve for 2,4-D (b) Differential curve for (a)

3.2.3 Solubility Measurements

To determine analyte solubilities in carbon dioxide, 2-3 g of solid solute were placed in the extraction vessel. Prior to pressurization, the apparatus was purged of ambient air by flushing gaseous CO_2 through the access valve in the cap or through the upper sample port. At each pressure increment the cell was isolated for equilibration by closing the entrance and exit shut-off valves and stirring was started. For sampling, the upper exit valve was opened and the saturated CO_2 or water filled a 2 or 10 μL sample loop before depressurizing through a stainless steel restrictor or open-ended piece of tubing into a hot water collection bath. To ensure saturation of the fluid, the stirring rates, equilibration times, flow rates, and sampling times were varied. For 2,4-D, PCP, pentachlorophenol sodium salt, and chrysene, the typical equilibration and sampling times were 5 - 30 min and 20 - 180 s, respectively. Naphthalene solubility experiments required equilibration times between 15 - 20 hr. In these cases, the entrance shut-off valve was left open to allow the syringe pump to maintain CO_2 pressure. All solutions were accepted as saturated when further increases in equilibration times did not yield higher apparent solubilities.

The previous method was also used to measure the solubility of PCP in water under pressure. In this case, the apparatus was purged of ambient air by flushing water through the access valve. Equilibration times from 5 hr to several days were required.

The solubility of pentachlorophenol was measured in CO_2-saturated water and water-saturated CO_2 by placing 2-3 g PCP in the cell with 50 mL DDI water and letting the two phases equilibrate for up to 24 hr. Pentachlorophenol solubility was also measured in CO_2 bubbled through water prior to contact with the PCP.

To determine analyte solubility in aqueous solution at ambient pressure and temperature, aliquots of the saturated solutions were analyzed by HPLC using the appropriate chromatographic method. The saturated solutions were diluted with water for analysis as required.

3.2.4 Partitioning Measurements

For the partitioning experiments, saturated or dilute aqueous solutions were placed in the cell. The solution volume was either 40.0 or 50.0 mL. Prior to pressurization, the vessel headspace was purged of ambient air by flushing gaseous CO_2 out through the ball valve or upper sample port. At each pressure increment the cell was isolated for equilibration by closing the entrance and exit valves and turning on the stirrer. Before sampling, the stirring was stopped and the phases were allowed to settle and separate. To ensure system equilibration, the stirring times, settling times, flow rates, and sampling times were varied. It was determined through replicate injections that a minimum of 40 min stirring and a 15 min settling period were required for phase equilibration and separation for the partitioning of PCP between CO_2 and water.

To sample each phase, the upper and lower exit valves were simultaneously opened and the CO_2 and water were collected in separate sample loops (2, 10, 112, or 254 μL). The larger loop sizes were used for the water fraction as it was almost depleted of solute at equilibrium. Small loops had to be used for the CO_2 phase. The amount of CO_2 which could be introduced to the chromatographic system was limited as it caused baseline perturbations. The water fraction was collected each time so that the amount removed from the bulk solution could be determined by weighing. The CO_2-rich fraction was immediately injected into the HPLC. Once the chromatography was complete, the mobile phase was re-directed through the lower sample loop for the analysis of the water-rich fraction.

3.2.5 Impedance Measurements

Impedance measurements were made for CO_2 by placing stainless steel wires (0.5 mm o.d.) insulated in PEEK tubing sleeves (0.530 mm i.d.) (Upchurch Scientific) in the cell through 1/16" Swagelok - 1/8" universal pipe thread unions which were drilled out and screwed into threaded openings on one side of the vessel. The resistance across the two wires was measured with a Fluke Digital Multimeter (model 8050A). The cell constant was determined using 0.1M NaCl.

3.2.6 HPLC Methods

Table 3.2.1 Experimental HPLC Methods

SOLUTE	HPLC METHOD
2,3,4,5-tetrachlorophenol	90% MeOH +10% H_2O to pH 3 with H_3PO_4; 1.2 mL/min; 224nm
2,4-D	80% MeOH +20% H_2O to pH 3 with H_3PO_4; 1.2 mL/min; 286nm
Chrysene	100% Dichloromethane; 1.2mL/min; 304nm
Naphthalene	95% MeOH +5% H_2O to pH 3 with H_3PO_4; 1.2 mL/min; 320nm
PCP	95% MeOH +5% H_2O to pH 3 with H_3PO_4; 1.2 mL/min; 224nm & 280nm
Pentachlorobenzene	100% Isopropanol; 0.6mL/min; 224nm
Pentachlorophenol sodium salt	95% MeOH +5% H_2O to pH 3 with H_3PO_4; 1.2 mL/min; 224nm & 280nm

Two wavelengths were used for the analysis of pentachlorophenol and pentachlorophenol sodium salt. The wavelength 224 nm was the most sensitive and was used for the analysis of PCP during partitioning experiments. The wavelength 280 nm was used for solubility experiments in carbon dioxide due to the high amounts of PCP being detected.

3.2.7 Chemicals

Table 3.2.2 Chemical Sources and Purity

CHEMICAL	SOURCE AND PURITY
Buffer Solution, pH 7	Anachemia
Carbon Dioxide	BOC (99.5%); Air Products (SFC-SFE grade pressurized with helium)
2,3,4,5-tetrachlorophenol	Supelco, 98+%
2,3,5,6-tetrachlorophenol	Supelco, 98+%
2,3-dichlorophenol	Supelco, 98+%
2,4,5-trichlorophenol	Supelco, 98+%
2,4-D (2,4-dichlorophenoxyacetic acid)	Aldrich, 98%
Chrysene	Kodak
Dichloromethane	Fisher, HPLC or Optima grade
H_3PO_4	Anachemia
HCl	Anachemia
Isopropanol	Fisher, HPLC or Optima grade
Methanol	Fisher, HPLC or Optima grade
Na_2SO_4	Anachemia, Reagent grade
NaCl	Anachemia, Reagent grade
$NaHCO_3$	Anachemia, Reagent grade
NaOH	Anachemia, Reagent grade
Naphthalene	Fisher, Scintanalyzed
Pentachlorobenzene	Aldrich, 98%
Pentachlorophenol (PCP)	Aldrich, 99% +
Pentachlorophenol sodium salt (Na-PCP)	TCI America, 89%
Water (DDI)	Distilled, deionized Millipore 18 $M\Omega$·cm

3.2.8 Other Analyses

Proton NMR spectra were obtained for pentachlorophenol samples with a Bruker AMX400 nuclear magnetic resonance spectrometer. Effluents containing PCP or pentachlorophenol sodium salt were analyzed for sodium content by atomic emission spectroscopy with a LECO-PLASMARRAY diode array spectrometer (330.237 nm).

The densities of carbon dioxide were determined using the SF-Solver Program distributed by Isco, Inc..

CHAPTER FOUR

RESULTS AND DISCUSSION

4.1 Measurement of Dissociation Constants

The acid dissociation constant K_a (then pK_a) was determined for several chlorinated phenols and acidic pesticides. The experimental data as well as data previously reported in the literature are summarized in Table 4.1.1. The experimental method used was based on solute concentration rather than solute activity. Depending on the method used, pK_a values can vary by a factor of 2 or more (Skoog and West, 1982); however, it is frequently unclear in the literature which method was used for reporting data. As it was important to know the relative acidities of the solutes of interest to this work, all solutes of interest were analyzed by the titration method described in section 3.2.2.

Table 4.1.1 pK_a of Chlorinated Phenols and Pesticides

Solute	pK_a (experimental)	pK_a (literature)
Phenol	Not determined	10.0
2,3-dichlorophenol	7.47	7.44 (HCP, 1977)
2,4,5-trichlorophenol	6.69	7.4 (Bunce, 1991)
2,3,4,6-tetrachlorophenol	Not determined	5.4 (Bunce, 1991)
2,3,5,6-tetrachlorophenol	5.37	---
PCP	4.74	4.9 (Bunce, 1991)
		4.35 (Arcand et al, 1995)
2,4-D	3.89	---

The most acidic solute investigated was 2,4-D. The most acidic chlorinated phenol was pentachlorophenol; the weakest was 2,3-dichlorophenol. Both the experimental and literature data in Table 4.1.1 indicate that phenols with fewer chlorine atoms are

less acidic. The electron-withdrawing effect decreases as each chlorine atom is removed from PCP. Removing all chlorines gives phenol a reported pK_a of 10.0.

4.2 Solubilities

4.2.1 Solubility in CO_2

Vapour pressures as reported in the literature are listed in Table 4.2.1 for solutes whose solubilities were measured in this work.

Table 4.2.1 Solute Vapour Pressures

Compound	T (°C)	P (atm)	Reference
Naphthalene	25	1.1×10^{-4}	Mackay and Shiu, 1981
Chrysene	35	4.11×10^{-11}	Barna et al, 1996
Pentachlorophenol	20	2.2×10^{-7}	Carswell and Nason, 1938
	25	3.5×10^{-7}	
	40	1.5×10^{-6}	
	60	9.2×10^{-6}	

The vapour pressures for pentachlorophenol at 25, 40 and 60°C were taken from a plot of vapour pressure versus temperature.

4.2.1.1 Non-Polar Solutes

The solubility of naphthalene was measured in SC CO_2 at 34.7 °C and at pressures up to about 240 atm. The results plotted in Figure 4.2.1 were compared with literature values to ensure correct functioning of the apparatus. The close proximity of these
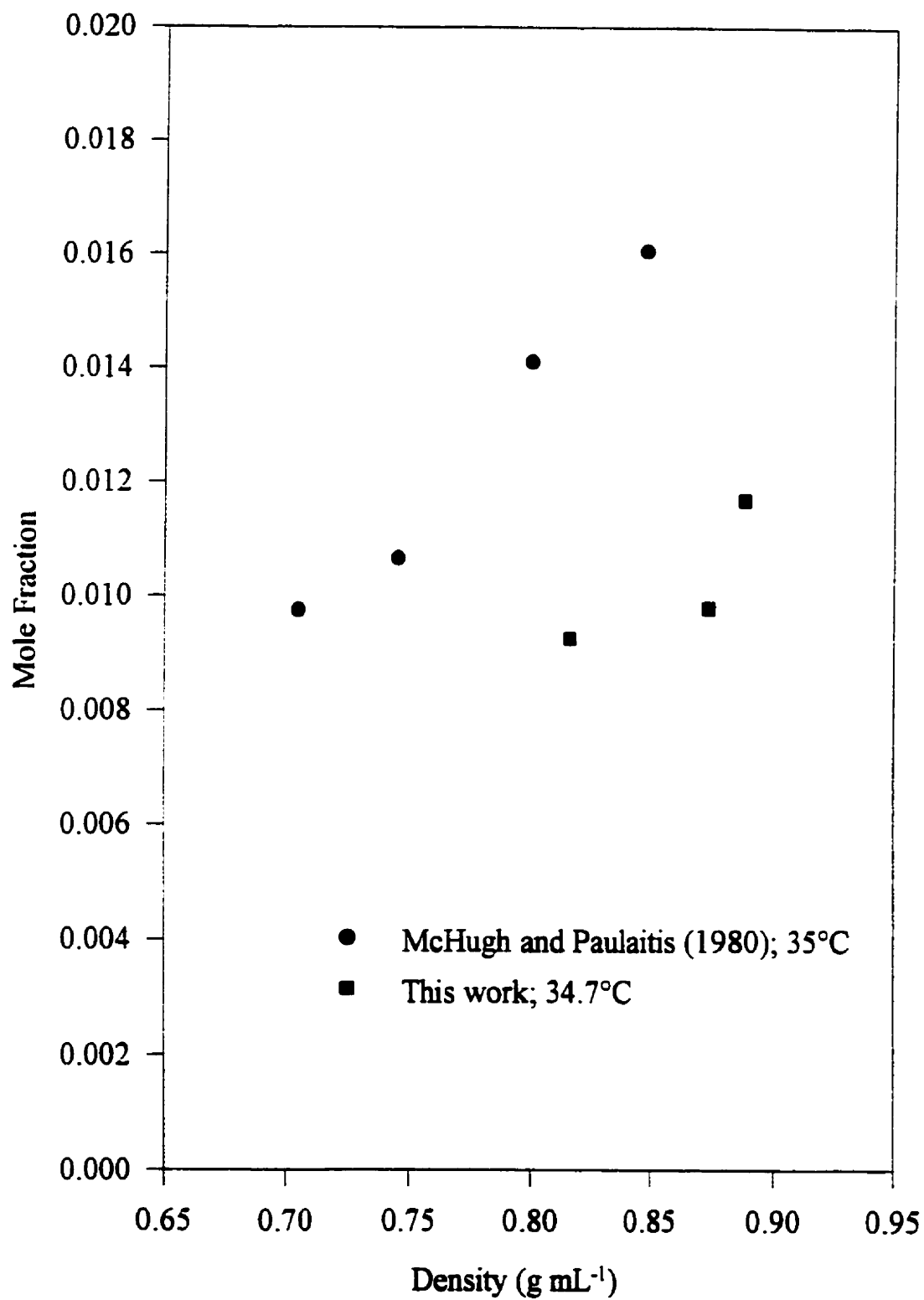
Figure 4.2.1. Solubility of naphthalene in CO_2 as a function of density

results to those obtained by McHugh and Paulaitis (1980) validated continued use of the apparatus for solubility and partitioning experiments. Both sets of data show that, at constant temperature, the solubility of naphthalene increases when CO_2 is compressed to a higher density. This effect of pressure is consistent with the theory presented in section 2.5.2. The enhancement factor E for the solubility of a solid solute in a compressed gas increases as the pressure is increased; the solute mole fraction is a function of E. Pressure had the same positive effect on the solubilities of all other solutes measured in this work.

Naphthalene has a high solubility in carbon dioxide as dispersion interactions between solute and solvent are strong (or numerous) compared with solute-solute interactions. Naphthalene has a high vapour pressure, indicating that the interactions between solute molecules are easily disrupted.

The solubility of chrysene was measured in CO_2 at sub- and supercritical conditions. Figure 4.2.2 illustrates the results for isotherms at 21.5 and 36.0 °C. The error bars are given as the standard deviation of 3 or more measurements. Higher solubilities were obtained at the higher temperature despite the decrease in fluid density. This was expected, as raising the temperature increases the vapour pressure of a solute. This temperature effect was observed for the solubility all other solutes in this work and for the solutes reviewed in the literature in section 1.4.1. The effect of temperature on a solute's vapour pressure has useful practical consequences in supercritical fluid technology. In general, more solute can be dissolved in carbon dioxide by raising the system temperature slightly at constant pressure.

Data obtained by Barna et al (1996) for the solubility of chrysene in CO_2 at 35°C are included in Figure 4.2.3 with the data measured in this work at 36.0°C. The measurements by Barna et al were made coincidentally with this thesis. It is difficult to explain the difference in the two sets of data. Barna et al employed a dynamic system tested by measuring the solubility of a known solute. However, it can be difficult to ensure solute-solvent equilibrium in a dynamic system. The authors had
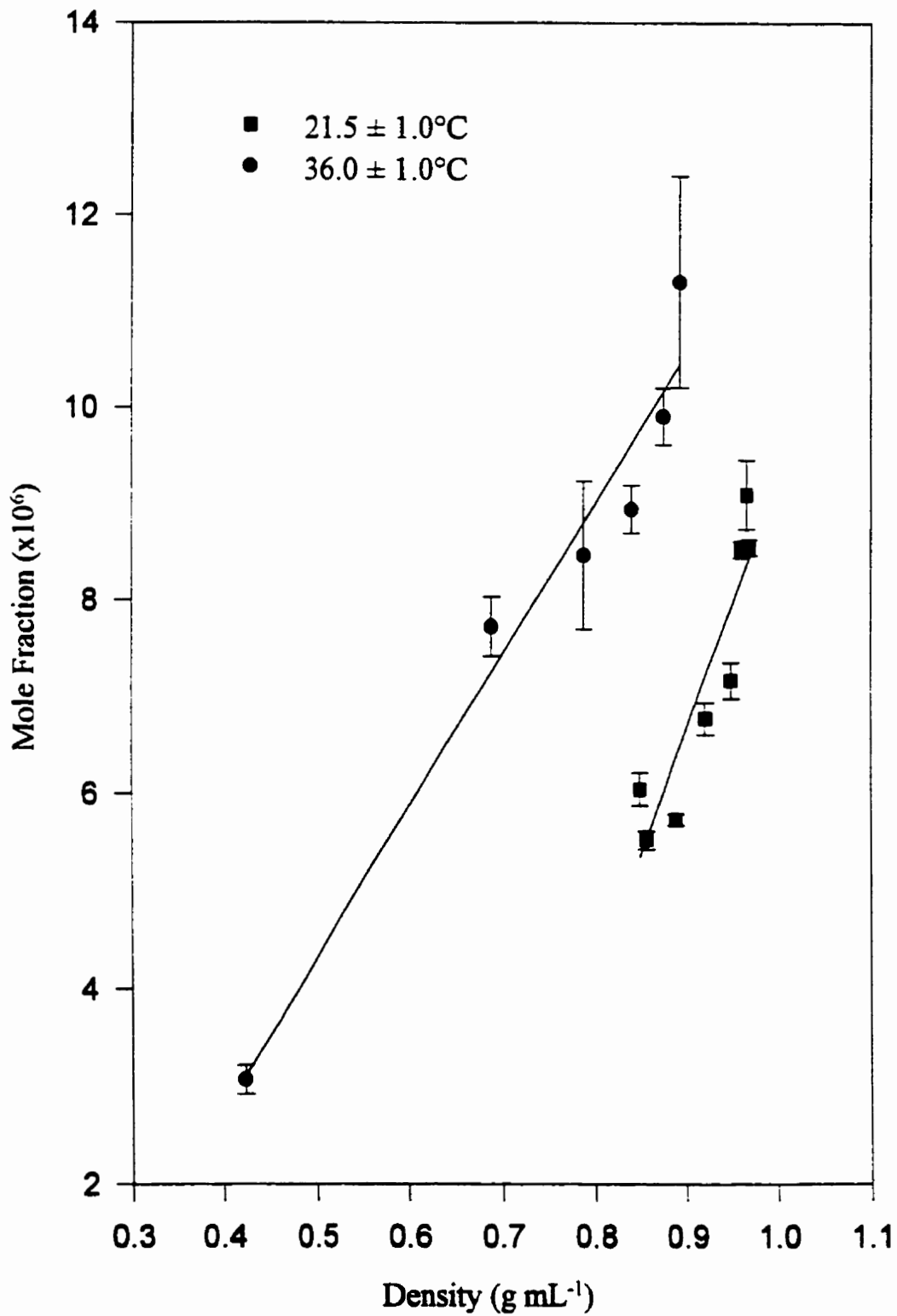
Figure 4.2.2. Solubility of chrysene in CO_2 as a function of density
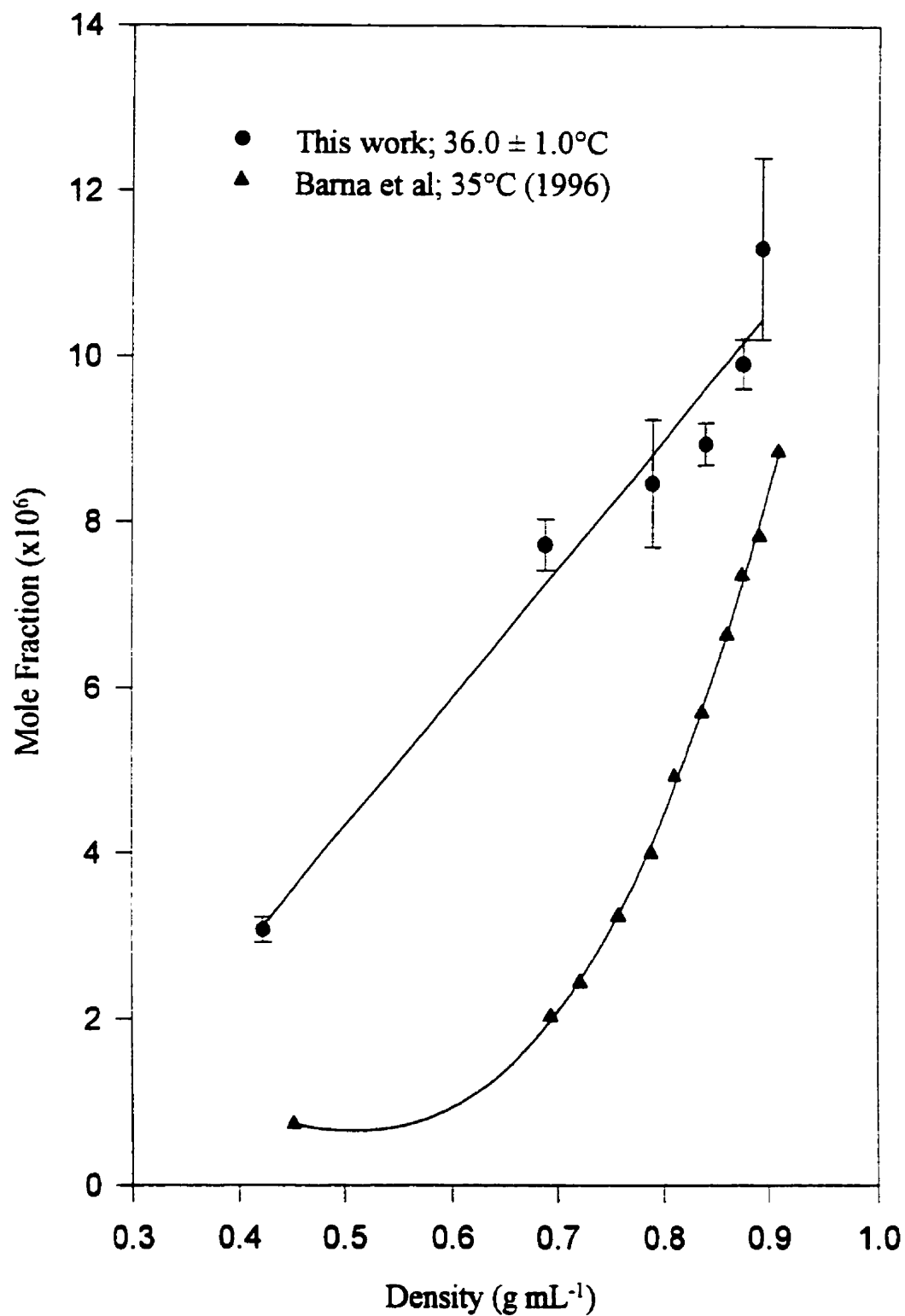
Figure 4.2.3. Experimental and reported solubilities of chrysene in CO_2

to modify the CO_2 flow rate and adjust the quantity and position of the solute in the extraction cell. Although on-line analysis was performed by liquid chromatography, the system had to be decoupled and the eluent collected at the column output if the analytical system became saturated. This extra step was a source of potential sample loss. The static system employed in this work used on-line monitoring by HPLC to accurately determine the solute-solvent equilibrium. As well, on-line detection allowed for direct measurement of solute concentration without sample loss or interference from impurities. It is unlikely the measurements made in this work are too high due to the entrainment of solid chrysene in the sampling process, since in-line frits were used to prevent this problem.

Chrysene and naphthalene are both polynuclear aromatic hydrocarbons. However, chrysene is a larger molecule with four aromatic rings (compared to only two for naphthalene) and its molecular weight is about 100 amu higher. As a consequence, chrysene is less volatile and its solubility in CO_2 is four orders of magnitude less than naphthalene's.

4.2.1.2 Polar solutes

Solubility isotherms are shown in Figure 4.2.4 for 2,4-D in liquid and SC CO_2 at 21.0, 26.3, and 34.8°C at pressures up to about 250 bar. The errors are expressed as the standard deviation of several measurements. Each isotherm demonstrates an increase in 2,4-D solubility with increasing density, that is, with increasing pressure at constant temperature. The solubility of 2,4-D is three orders of magnitude lower than that of naphthalene. Although dipole-quadrupole interactions occur between 2,4-D and CO_2, this solute has a higher molecular weight than naphthalene. As well, the forces between 2,4-D solute molecules are strong as dipole interactions and hydrogen bonding can occur. The vapour pressure and solubility of 2,4-D are lower as a consequence.
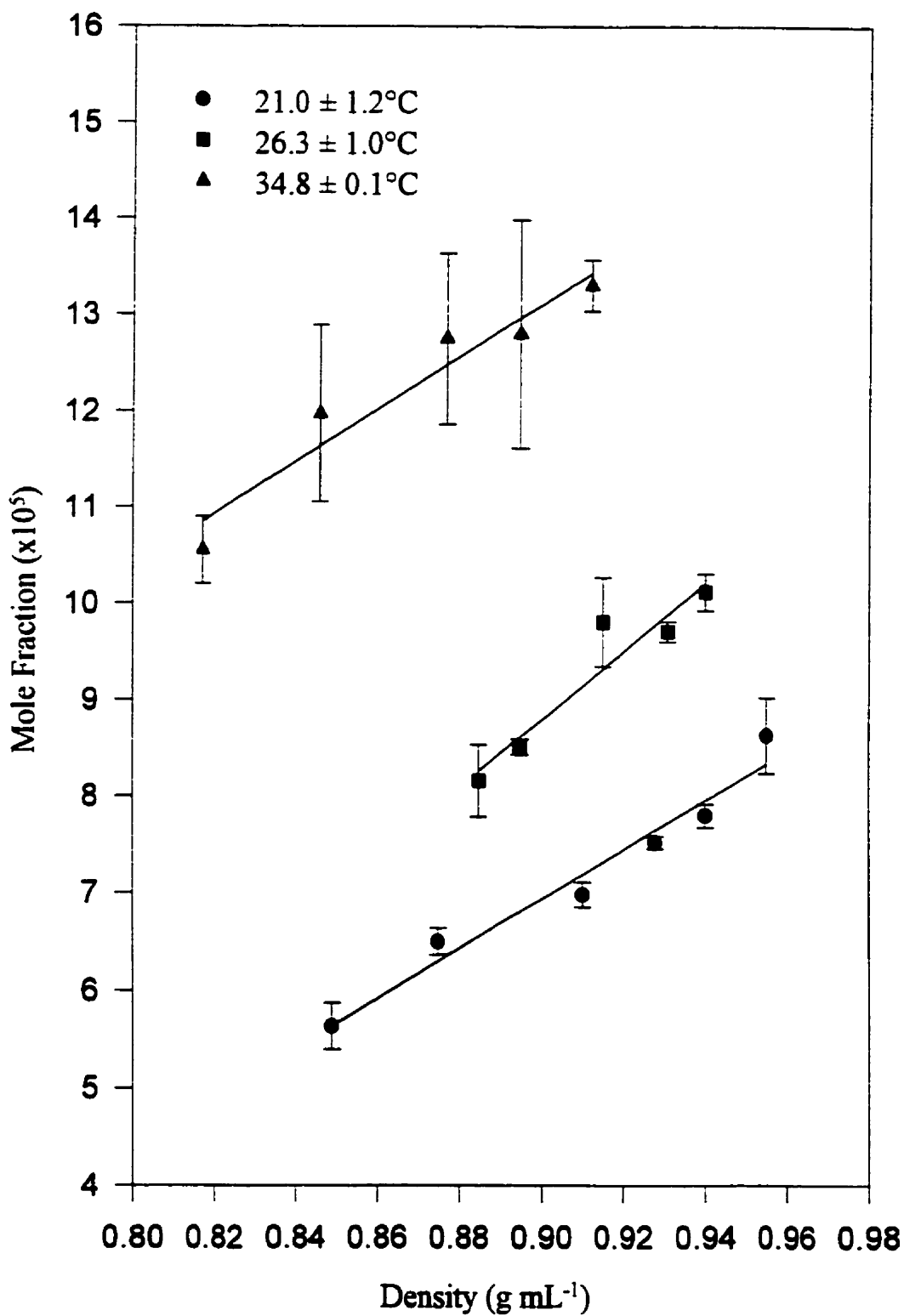
Figure 4.2.4. Solubility of 2,4-D in CO_2 as a function of density

The measurements obtained by Schäfer and Baumann (1988), Macnaughton and Foster (1994), and Miller et al (1997) are presented in Figure 4.2.5 at 40°C with the data in this work at 34.8°C. The measurements made in this work agree well with the data obtained by Schäfer and Baumann and are significantly higher than those of the other two groups. Note the measurements made by all three of the other groups were made using dynamic saturation systems. The fact that the measurements in this work are generally higher may be a reflection of this.

Previously, differences in solubility were attributed by Macnaughton and Foster to a lack of solute purification which would cause the measurements by Schäfer and Baumann to be inordinately high due to the dissolution of impurities. The 2,4-D was not purified for the solubility experiments in this thesis. However, no impurities were observed in the 2,4-D sample or standard aliquots using the HPLC method specified in section 3.2.6.

The solubilities of pentachlorophenol were determined in liquid and supercritical CO_2 at 20.0, 41.0, and 59.5°C. Each isotherm in Figure 4.2.6 shows an increase in PCP solubility with increasing density. The error is expressed either as the standard deviation of 3 or more points, or as the spread between two values. Included in this figure is the data point obtained by Madras et al (1993) at 25°C. This single measurement is only slightly lower than the values measured in this work at 20.0°C. The vapour pressure for PCP is not significantly different at these two temperatures.

The isotherms measured by Miller et al (1997) and by Cross and Akgerman (1998) for the solubility of PCP in CO_2 appeared very recently in the literature, during the time this work was being performed. For clarity, the data are presented in Figure 4.2.7 with the data obtained in this work at 41.0°C. Dynamic systems were used in both cases. The data obtained in this thesis correlate reasonably well with the solubility trends determined by Cross and Akgerman with respect to temperature.
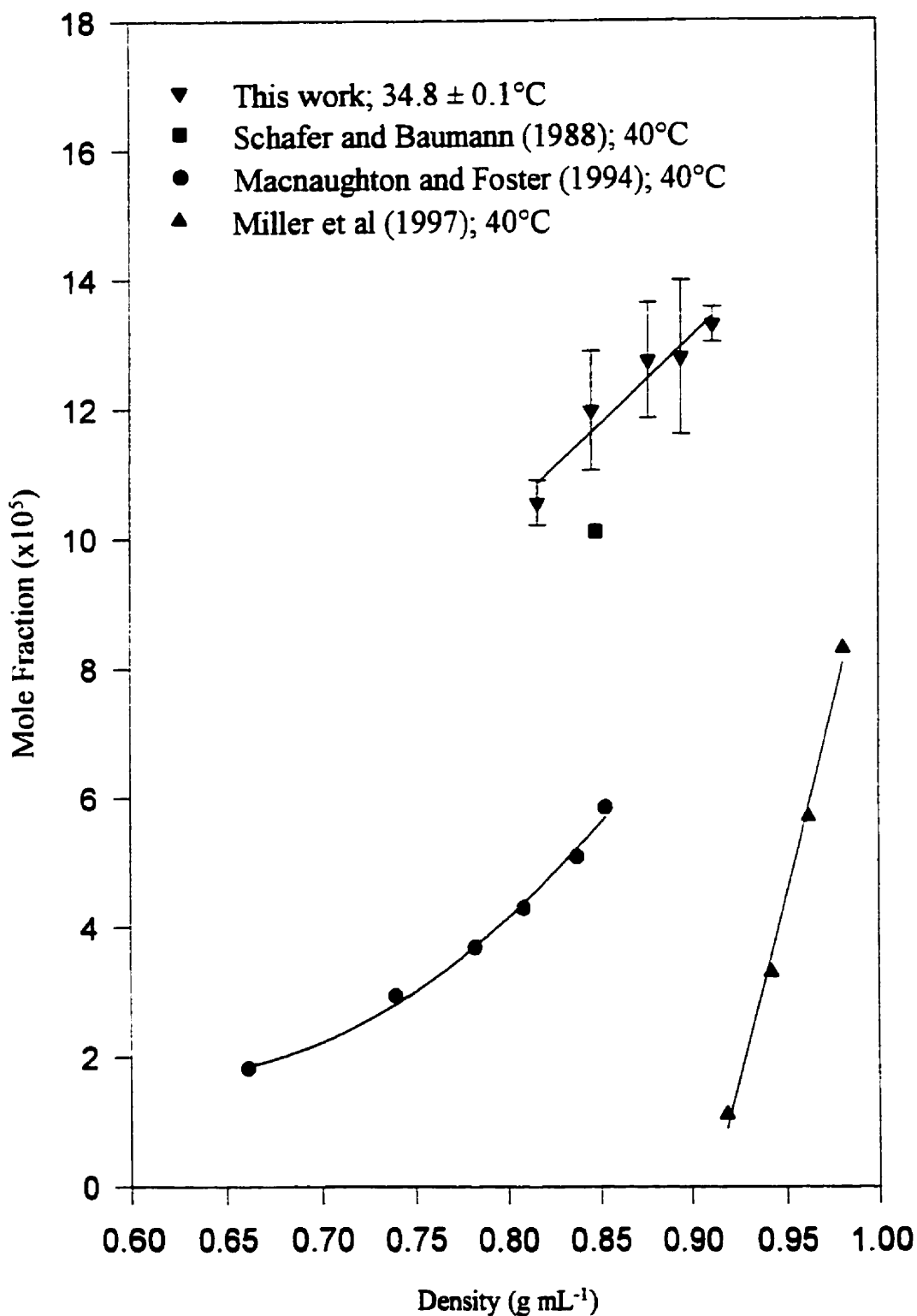
Figure 4.2.5. Experimental and reported solubilities of 2,4-D in CO_2 as a function of density
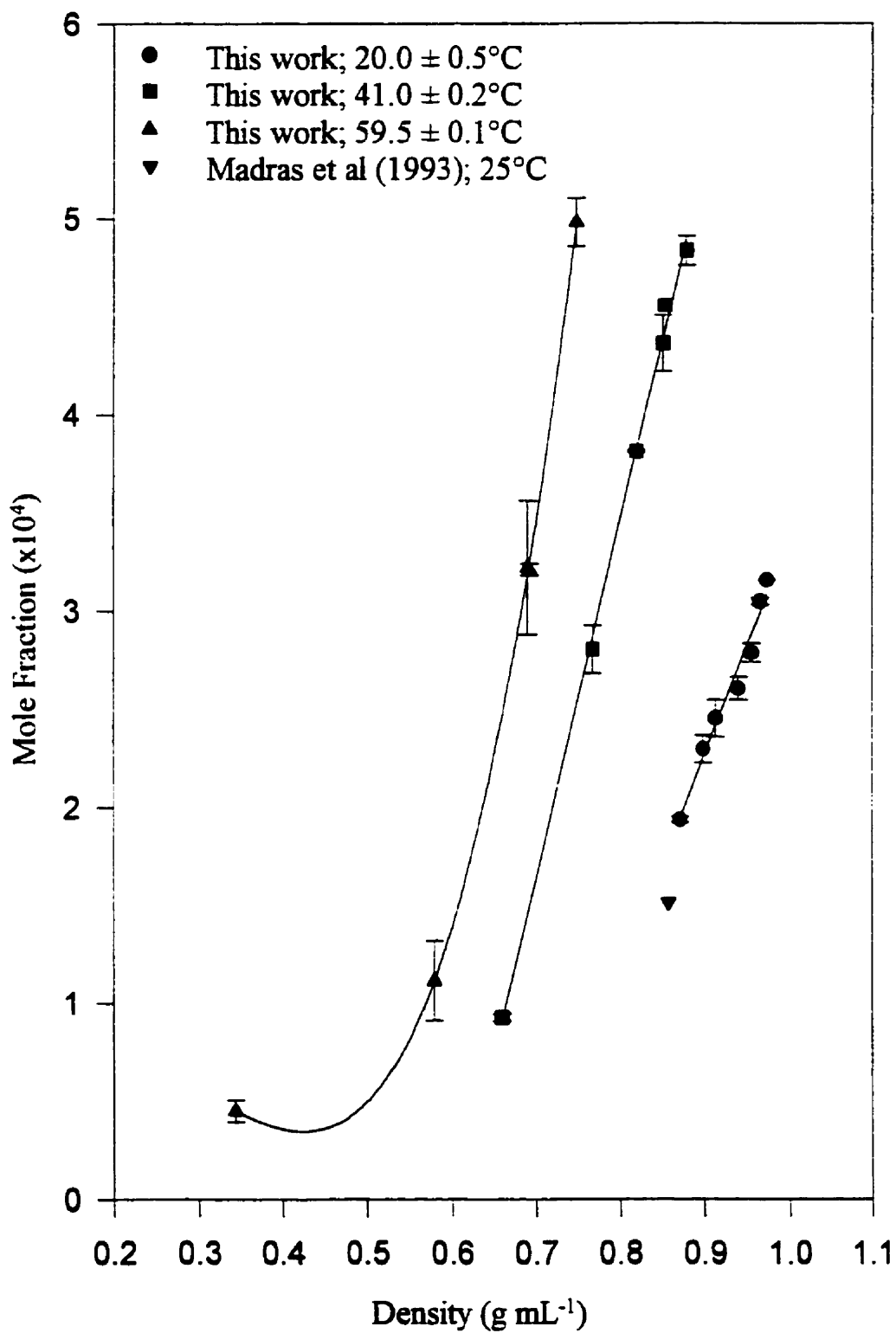
Figure 4.2.6. Solubility of PCP in CO_2 as a function of density
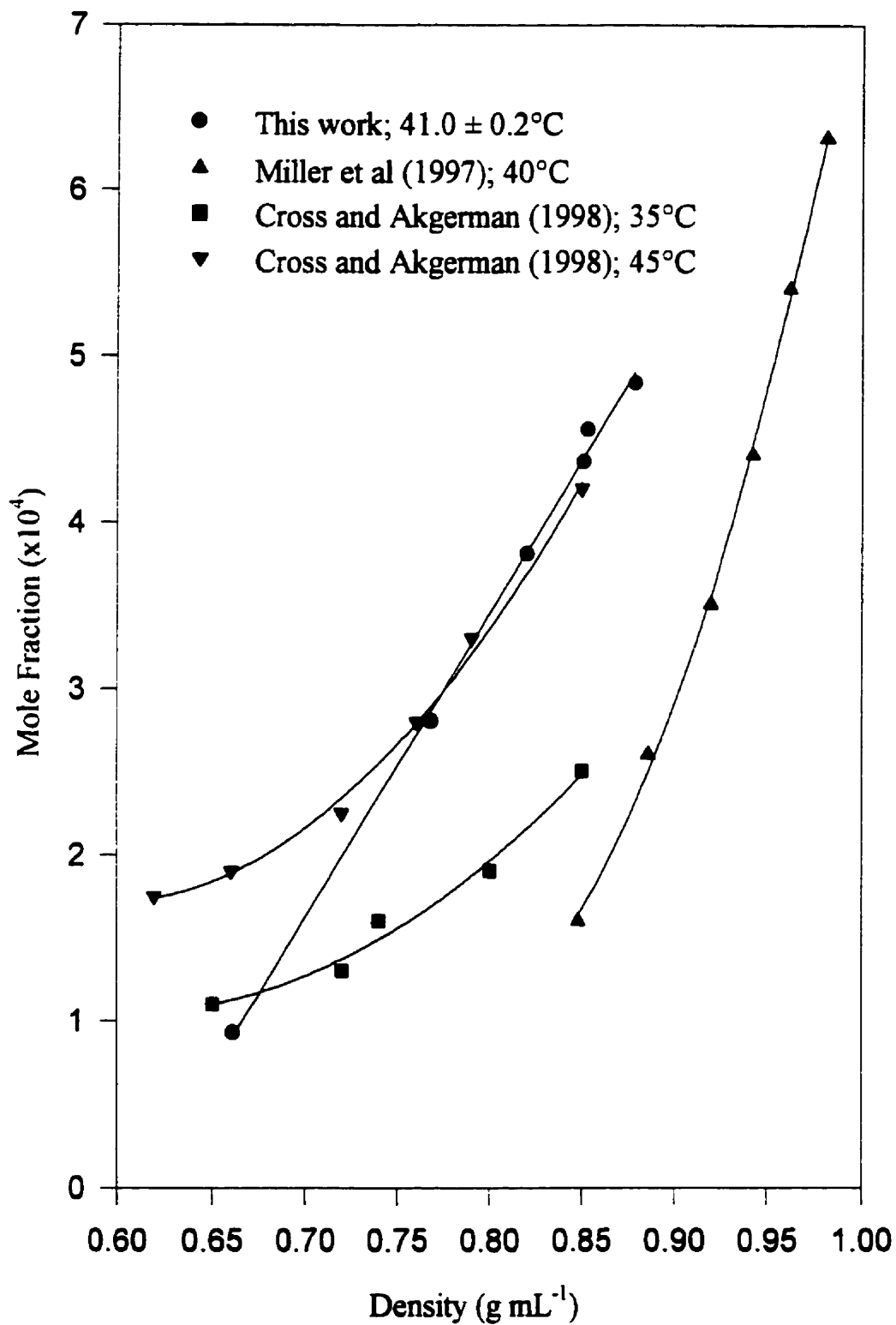
Figure 4.2.7. Experimental and reported solubilities of PCP in CO_2 as a function of density

The measurements made by Miller et al at 40°C are noticeably lower than the other isotherms.

The solubility data are also plotted as a function of pressure in Figure 4.2.8. Several cross-over regions are observed. At pressures up to about 130 atm PCP is less soluble in CO_2 at 41.0°C than at 20.0°C as the solvent density is higher at the lower temperature. However, above this pressure, temperature has greater effect on solute vapour pressure and PCP is more soluble in CO_2 at 41.0°C despite the decrease in fluid density. A cross-over region also occurs at about 190 atm for the isotherms 41.0 and 59.5°C. The density effect causes PCP to be more soluble in CO_2 at 41.0°C than at 59.5°C over a wide range of pressure.

The isopycnic solubilities of PCP were calculated at 0.70, 0.80, and 0.90 g mL^{-1} CO_2 using the regressions for the isotherms in Figure 4.2.6. The data were plotted as ln Mole Fraction versus $1/T$ in Figure 4.2.9. The resulting enthalpies and entropies of solution of pentachlorophenol in carbon dioxide are listed in Table 4.2.2. The heat of solution of pentachlorophenol varies from a high of 90 kJ mol^{-1} at 0.70 g mL^{-1} to 26 kJ mol^{-1} at 0.90 g mL^{-1}. As the density of CO_2 is increased, the solvation of PCP is increased, and hence the process of solution is less endothermic.

Table 4.2.2 Enthalpies and Entropies of Solution in CO₂ for Pentachlorophenol

Density (g mL^{-1})	$\Delta H_{solution}$ (kJ mol^{-1})	$\Delta S_{solution}$ (J K^{-1} mol^{-1})
0.70	90 ± 25	207 ± 81
0.80	34 ± 5	40 ± 15
0.90	26 ± 3	20 ± 10
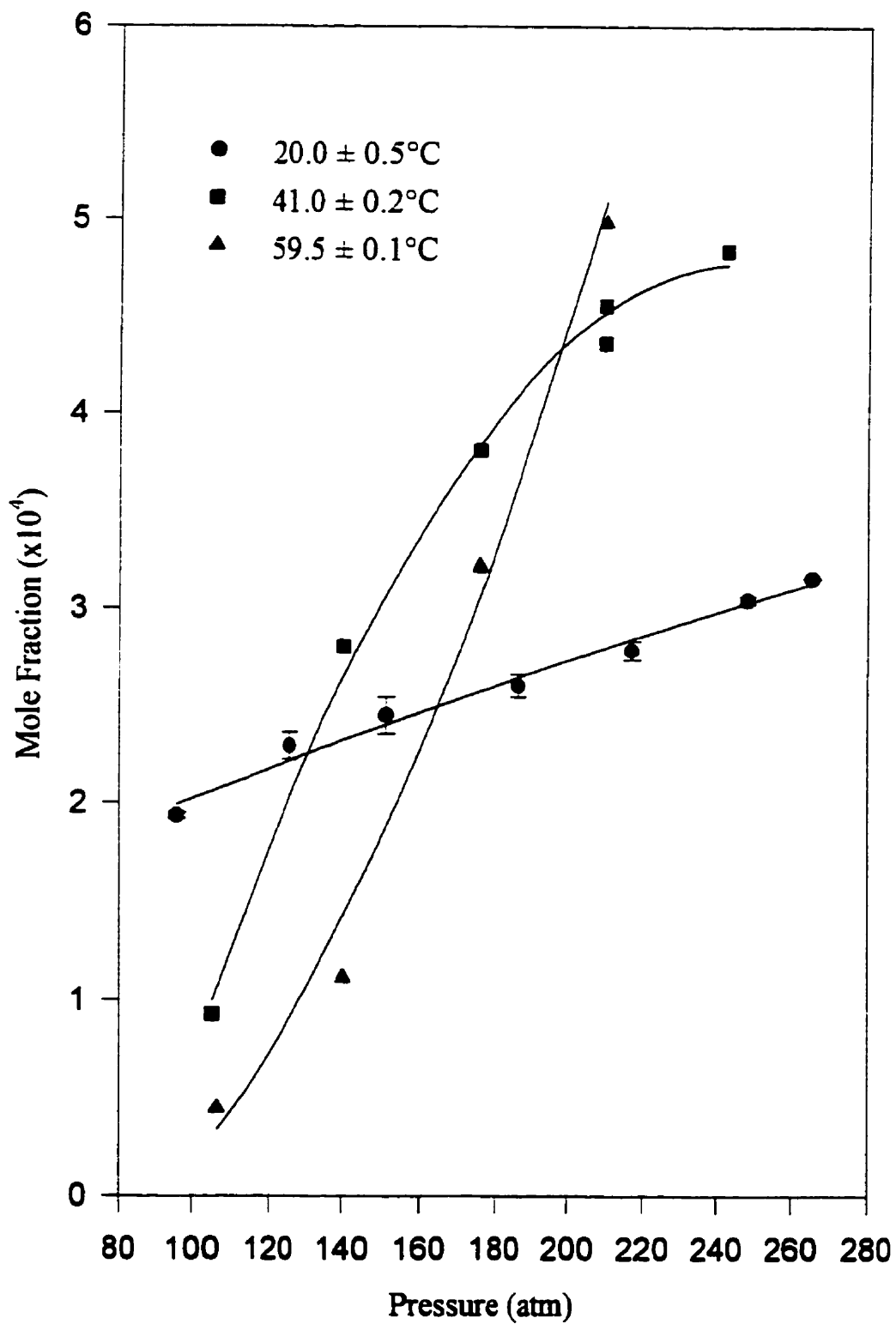
Figure 4.2.8. Solubility of PCP in CO_2 as a function of pressure
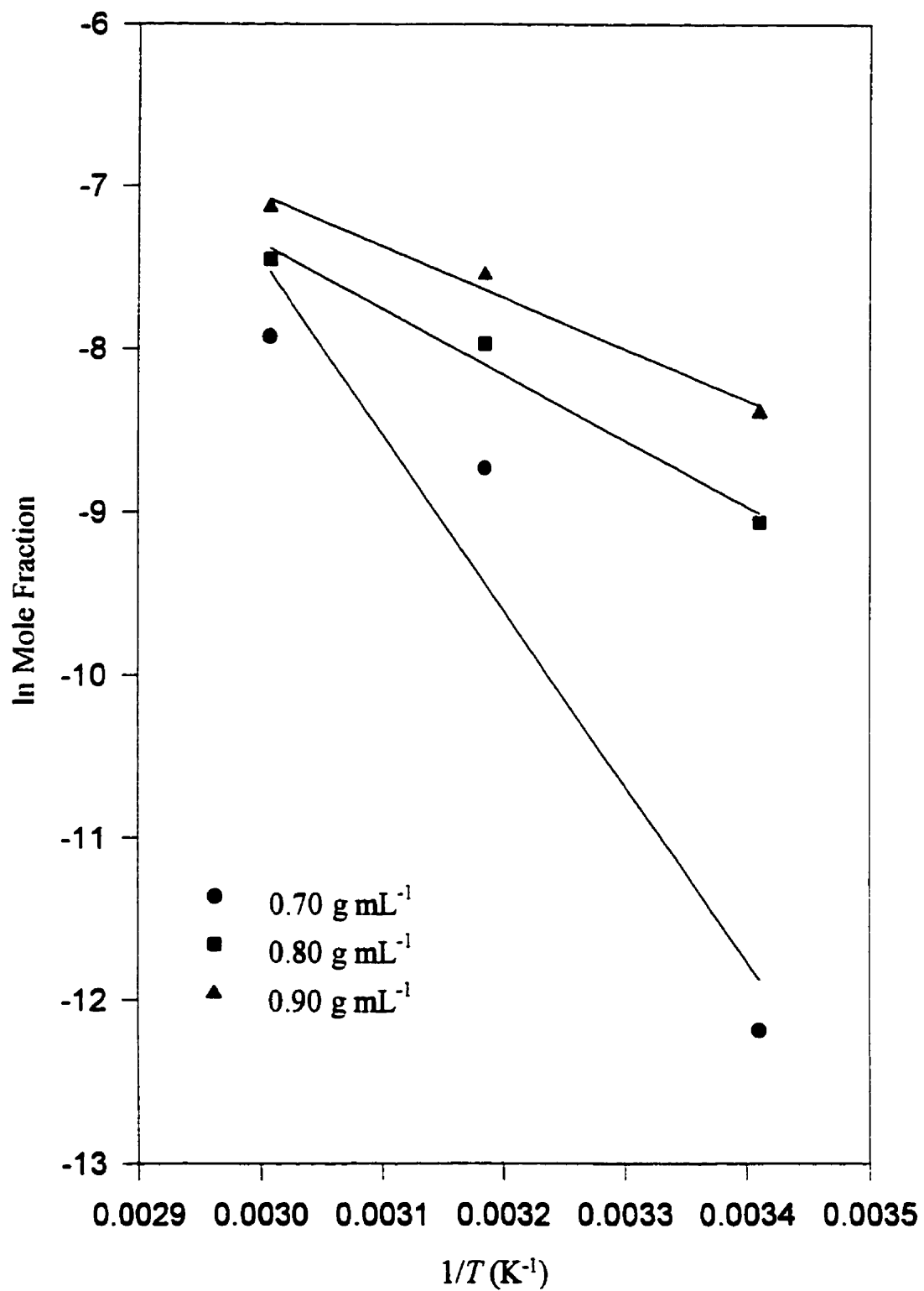
Figure 4.2.9. ln Mole Fraction as a function of $1/T$ for PCP at 0.70, 0.80, and 0.90 g mL^{-1}

The entropies of solution of PCP in CO_2 were also calculated from the plots in Figure 4.2.9. As the density of CO_2 is increased, the entropy change of the solution process decreases. This result was expected as more CO_2 molecules solvate the solute at higher densities and thus the fluid system is more ordered.

The isopycnic solubilities of 2,4-D and PCP were calculated in CO_2 using the regressions for the isotherms in Figures 4.2.4 and 4.2.6 at a constant density of 0.80 g mL^{-1}. The data are compared in Figure 4.2.10 using plots of ln Mole Fraction versus $1/T$. The enthalpies of solution at 25°C are shown in Table 4.2.3. Pentachlorophenol is more soluble in CO_2 because it is less acidic and less polar than 2,4-D. Although dispersion interactions between PCP and CO_2 are likely weaker than those between 2,4-D and CO_2, the solute-solute interactions between PCP molecules are also weaker. Intermolecular hydrogen bonding does not occur to a great extent in PCP because intramolecular hydrogen bonds are strong between the ortho chlorines and the hydroxide group (Blackman et al, 1955). It is therefore reasonable that the solvation of PCP in CO_2 is less endothermic compared with 2,4-D.

Table 4.2.3 Enthalpies in CO_2 for Polar Solutes at $\rho = 0.80$ g mL^{-1}

Compound	$\Delta H_{solution}$ (kJ mol^{-1})
2,4-D	48 ± 10
PCP	34 ± 5
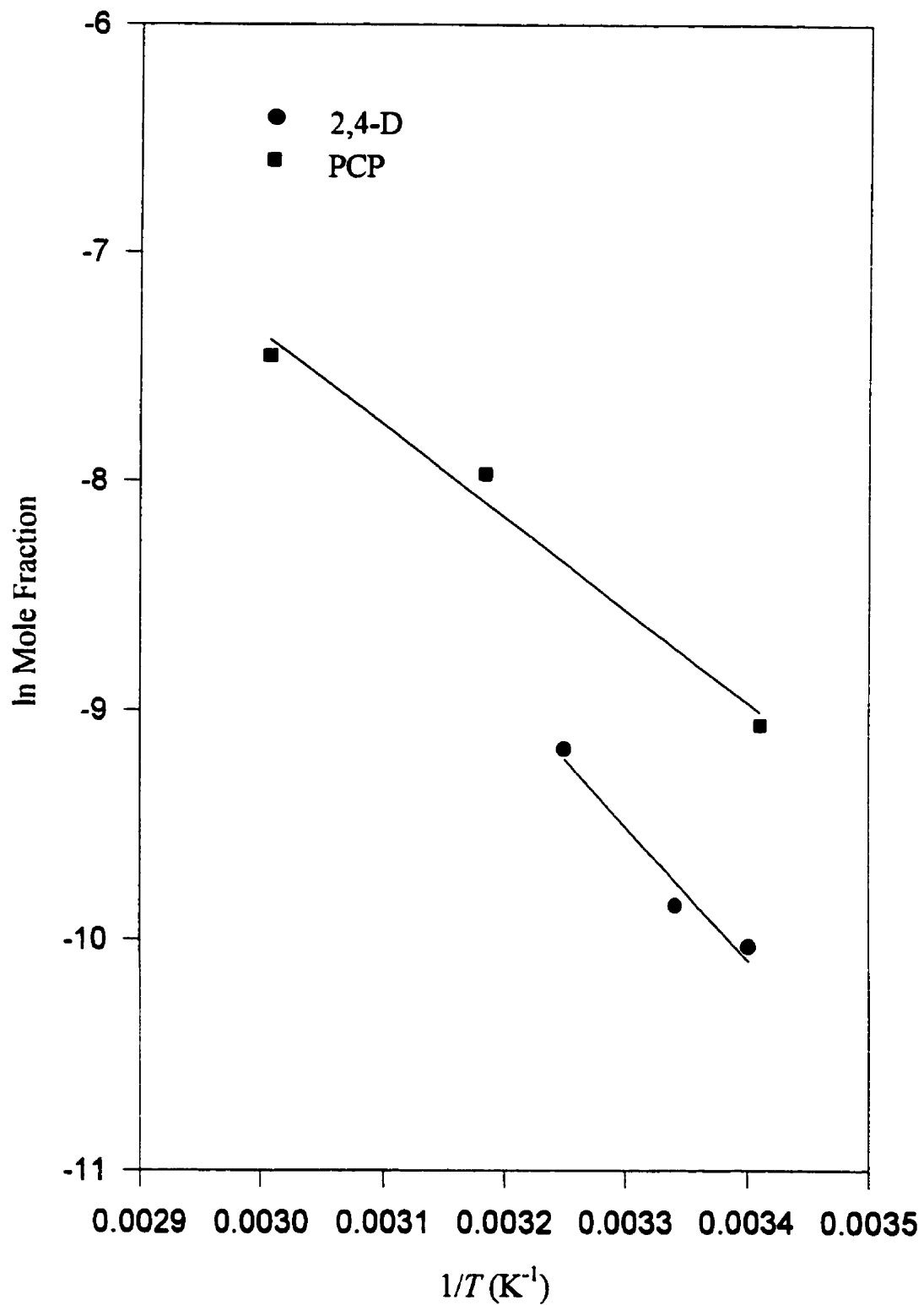
Figure 4.2.10. ln Mole Fraction of 2,4-D and PCP in CO_2 as a function of $1/T$ at 0.80 g mL^{-1}

4.2.2 Solubility in Water-Saturated CO$_2$

The solubilities of pentachlorophenol in carbon dioxide saturated with water shown in Figure 4.2.11 were determined at 19.1, 39.6, and 59.6°C. These conditions were similar to those used during subsequent CO$_2$-water extractions. Not surprisingly, the solubility of PCP in this "CO$_2$-rich phase" was similar to its solubility in pure CO$_2$. The majority of solute-solvent interactions in the CO$_2$-rich phase are apparently between PCP and CO$_2$ molecules and do not involve water.

It is likely most of the water fraction in the CO$_2$-rich phase reacts with CO$_2$ to form small amounts of carbonic acid, or at least aqueous CO$_2$. Little water thus remains for dissociation of carbonic acid to bicarbonate ions, thus making ionic interactions insignificant. In water-saturated CO$_2$ where little free water exists, hydrolysis of PCP should be negligible. In section 4.4, evidence is presented that there are very few ionized species, if any, in the CO$_2$-rich phase. Hydrogen bonding would also be minimal in this phase as pentachlorophenol has chlorines in both ortho positions to the hydroxide group. The only interactions which may be unique to water-saturated CO$_2$ are dipole-dipole interactions between PCP and carbonic acid. However, the fact remains that adding water had essentially no effect on the solubility of PCP.

The error is expressed either as the standard deviation of 3 or more points, or as the spread between two values. The curving lines in Figure 4.2.11 were obtained by calculating third order regressions.
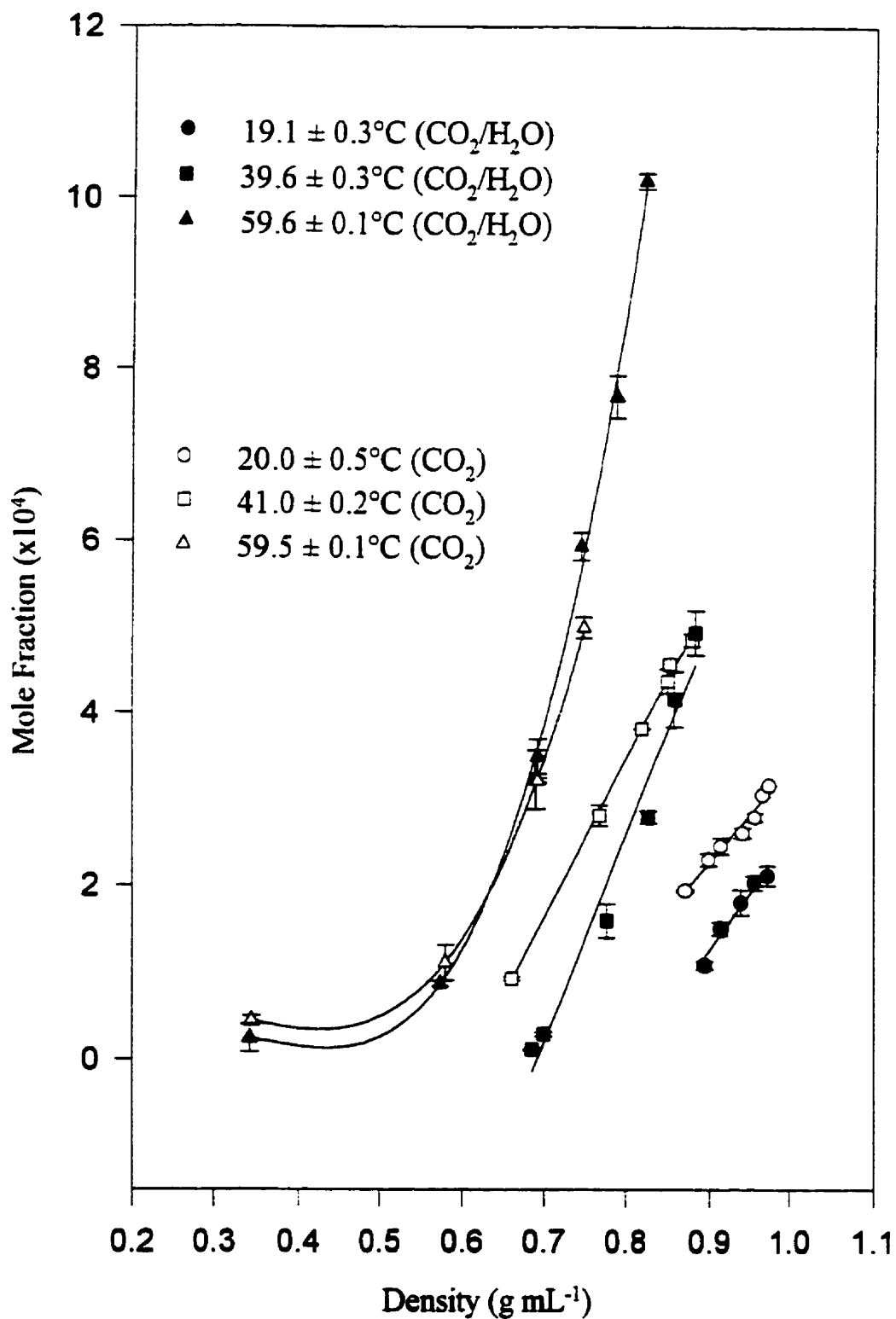
Figure 4.2.11. Solubility of PCP in CO_2 and CO_2 saturated with water as a function of density

4.2.3 Solubility in Water

The solubilities of several solutes were determined in water at atmospheric pressure and ambient temperatures. The data are presented in Table 4.2.4. This work yielded a mole fraction value of 9.0×10^{-7} ($13.4 \ \mu g \ mL^{-1}$) for the solubility of PCP in water at 1 atm. This value is in the same range as the data reported in the literature in section 1.4.2. Data has been reported in the range of 9.4×10^{-7} to 1.3×10^{-6} mole fraction (Freiter, 1979) and as 1.2×10^{-6} mole fraction at 27 °C (Carswell and Nason, 1938) for the solubility of PCP in water.

Table 4.2.4 Solubilities of Pentachlorophenol, Pentachlorobenzene, 2,3,4,5-tetrachlorophenol, and 2,4-dichlorophenoxyacetic Acid in Water at 1 atm and Ambient Temperatures

Compound	Solubility (Mole Fraction)
Pentachlorobenzene	1.0×10^{-8}
Pentachlorophenol	9.0×10^{-7}
2,3,4,5-tetrachlorophenol	6.4×10^{-6}
2,4-dichlorophenoxyacetic acid	6.2×10^{-5}

Pentachlorobenzene is almost insoluble in water as it does not have a hydroxide group for hydrogen bonding and is also non-polar. The solubility of 2,3,4,5-tetrachlorophenol in water was almost an order of magnitude higher than that of pentachlorophenol due to the removal of an ortho chlorine from PCP. 2,4-dichlorophenoxyacetic acid was the most soluble solute as it is the strongest acid and likely has a bigger dipole moment.

The solubility of pentachlorophenol in unbuffered water initially at equilibrium with air at 1 atm was measured at 23.6°C at pressures from 1 to 170 atm; a data point obtained at 20.5°C and 210 atm is also included in the plot in Figure 4.2.12. At the time of analysis, the system could not be regulated to a constant temperature at
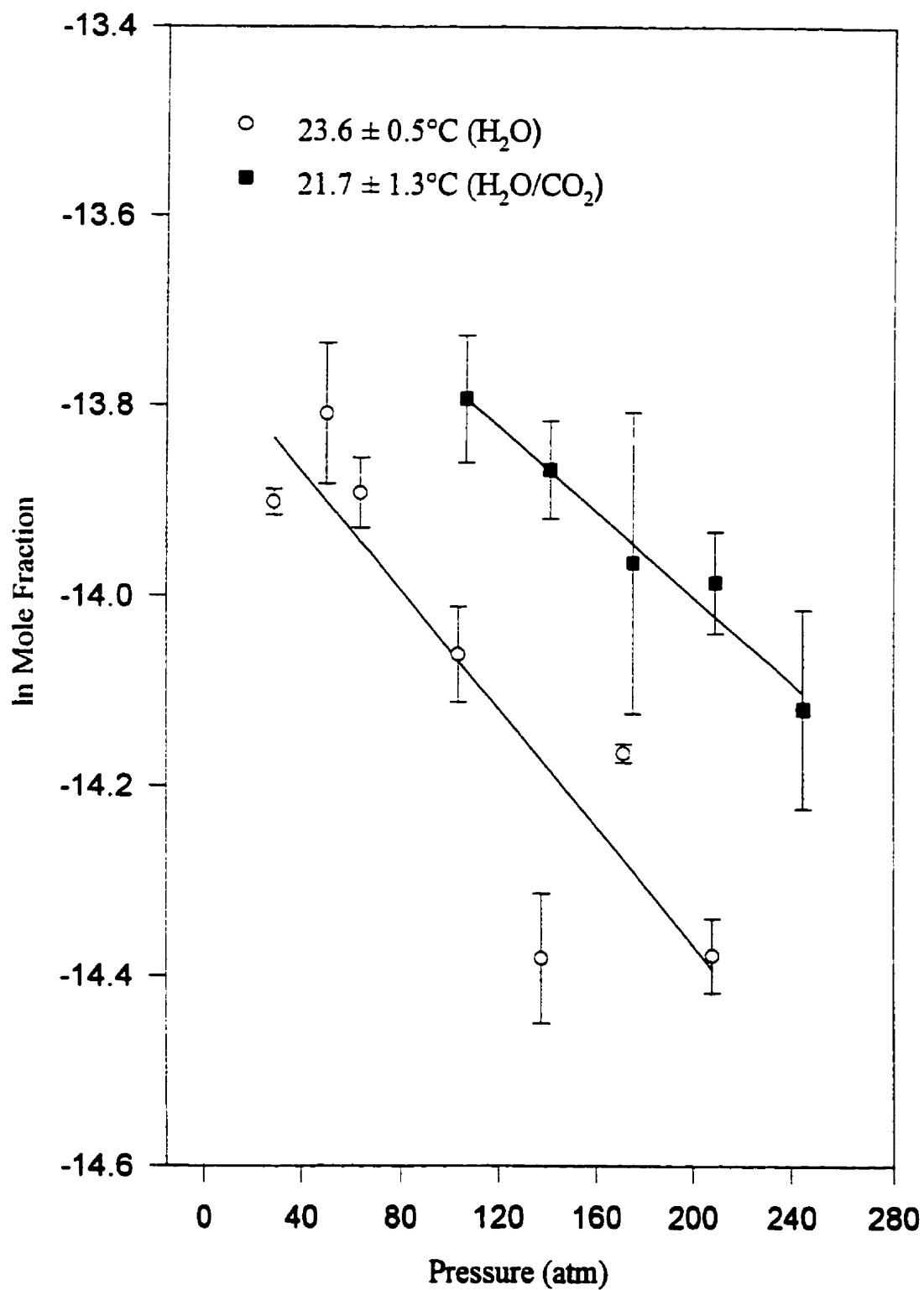
Figure 4.2.12. In Mole Fraction of PCP in water and water saturated with CO_2 at ambient temperatures

ambient conditions. Nonetheless, variation in this temperature range was expected to have only a limited effect on solubility as evidenced by the small variation in solute vapour pressure in Table 4.2.1. The results show a fairly linear decrease in solubility over the range of 1 - 210 atm, suggesting a positive volume change upon solution, ΔV, of PCP in water. From the slope of Figure 4.2.12 and using equation (2.5.7), ΔV has been calculated as $66 \text{ cm}^3 \text{ mol}^{-1}$. Hydrated PCP thus appears to have a compressibility similar to that of the non-solvated solid, giving it a volume change upon solution that is positive. Compression of the analyte in aqueous solution thus caused PCP to precipitate out of solution with increased pressure.

4.2.4 Solubility in CO_2-saturated water

The solubilities of PCP in water saturated with carbon dioxide presented in Figure 4.2.12 are only slightly larger than those in pure water (note the expanded y-axis scale in the figure). The volume change upon solution is similar to that in pure water and has a value of $54 \text{ cm}^3 \text{ mol}^{-1}$. PCP solubility increases slightly when water is saturated with CO_2, yet the extent of solute hydrolysis is decreased at pH 3. At this pH, the dissociation of pentachlorophenol to pentachlorophenoxide anion is almost negligible; the ratio [PCP$^-$]/[PCP] is about 0.02. The solubility of pentachlorophenol is therefore mostly a result of intermolecular interactions between unionized PCP and water. The higher amount of ions in solution apparently makes water a better solvent for PCP when it is saturated with CO_2. However, this conclusion is tenuous as the solubility data are comparable between the two plots in Figure 4.2.12.

4.2.5 Summary of Solute Solubilities

The solubilities of non-polar and polar solutes in carbon dioxide increased with increasing pressure. Solute solubilities also increased with increases in temperature due to the positive effect of temperature on solute vapour pressure. Cross-over regions were observed for the solubility of pentachlorophenol in CO_2 as a function of pressure. The solvation of PCP in CO_2 was less endothermic at higher densities, and was less endothermic than the solvation of 2,4-D.

Naphthalene had the highest solubility in carbon dioxide as it was the most volatile solute. Chrysene had the lowest solubility. Pentachlorophenol was more soluble than 2,4-D as it has weak intermolecular bonds due to the presence of chlorine atoms in both ortho positions to the hydroxide group. Pentachlorophenol solubilities in CO_2 saturated with water were not significantly different from solubility measurements in pure CO_2. The majority of the interactions in the CO_2-rich phase were between PCP and CO_2.

Pentachlorophenol was sparingly soluble in water as it does not form strong hydrogen bonds. 2,4-D had the highest solubility in water as it was the strongest acid tested. The solubility of pentachlorophenol in water decreased as the pressure was increased as PCP has a positive volume change upon solution. Similar results were observed for PCP in water saturated with carbon dioxide. The solubility of PCP in water was mostly a result of intermolecular interactions between unionized PCP and water.

4.3 Partitioning

4.3.1 Mass balance

The mass balance of pentachlorophenol in the partitioning experiments was determined by comparing the areas obtained for PCP in each phase to the appropriate calibration curves. On-line HPLC analysis of the CO_2-rich fraction required calibration standards of PCP in CO_2, as it was determined that at analytical concentrations a solvent effect on chromatography existed. Peak areas for the CO_2 standards were significantly greater than for standards prepared in either methanol or water. Standard peak areas were the same in CO_2 and CO_2 saturated with water. Chromatograms for PCP aliquots in the water- and CO_2-rich phases are shown in Appendix 2. The mass balance calculation accounted for the volume of water removed from the cell at each pressure increment of an isotherm. Knowledge of the mole fraction of CO_2 in the water-rich phase (King et al, 1992; Wiebe and Gaddy, 1940; Wiebe, 1941) allowed for the determination of the volume of the aqueous solution according to the apparent molar volume of $CO_{2(aq)}$ (Hnedkovský et al, 1996). The calculation used to determine the volume of the water phase at each pressure increment during an extraction is shown as follows:

$$V_A = V_{H_2O_{(l)}} + (n_{CO_2} \times V_{mCO_2(aq)}) \qquad (4.3.1)$$

where $V_{mCO_2(aq)} = 33.5 \ cm^3 \ mol$, $V_{H_2O_{(l)}}$ is the volume of liquid water measured in the cell, and

$$n_{CO_2} = \frac{\left(V_{H_2O(l)} \times \rho_{H_2O(l)} \right)}{18.02 \mathrm{gmol}^{-1}} \times x_B \qquad (4.3.2)$$

To determine the amount of solute (i) in either phase the following calculations were used:

$$M_i^A = V_A \times C_i^A \qquad (4.3.3)$$

$$M_i^B = (V_T - V_A) \times C_i^B \qquad (4.3.4)$$

where the total system volume (V_T) was 105 mL and C is the concentration of solute (i) in the water (A) or CO_2 (B). The mass balance was then calculated as $\dfrac{M_i^A + M_i^B}{M_T} \times 100$ where M_T was the total mass of solute originally introduced via the water phase.

The mass balances obtained for PCP partitioning experiments were between 80 and 110%. Sampling problems were frequently encountered for the first few injections of the water-rich fraction at low pressures. The areas obtained were inordinately large and the points were excluded from the partitioning plots as K would be very small.

4.3.2 Saturated Solution

The partitioning of pentachlorophenol from solute-saturated water (11.6 μg mL^{-1}) to CO_2 at sub- and supercritical conditions is quantified in Figure 4.3.1 as a function of pressure and temperature. The error on each value was calculated as a standard deviation for 3 or more points, or as the spread between two points. The limit of detection for the analysis of the water-rich fractions was 0.08 and 0.1 μg mL^{-1}, respectively, using the 112 and 10 μL sample loops. This allowed for a maximum K value of about 240 to be determined.
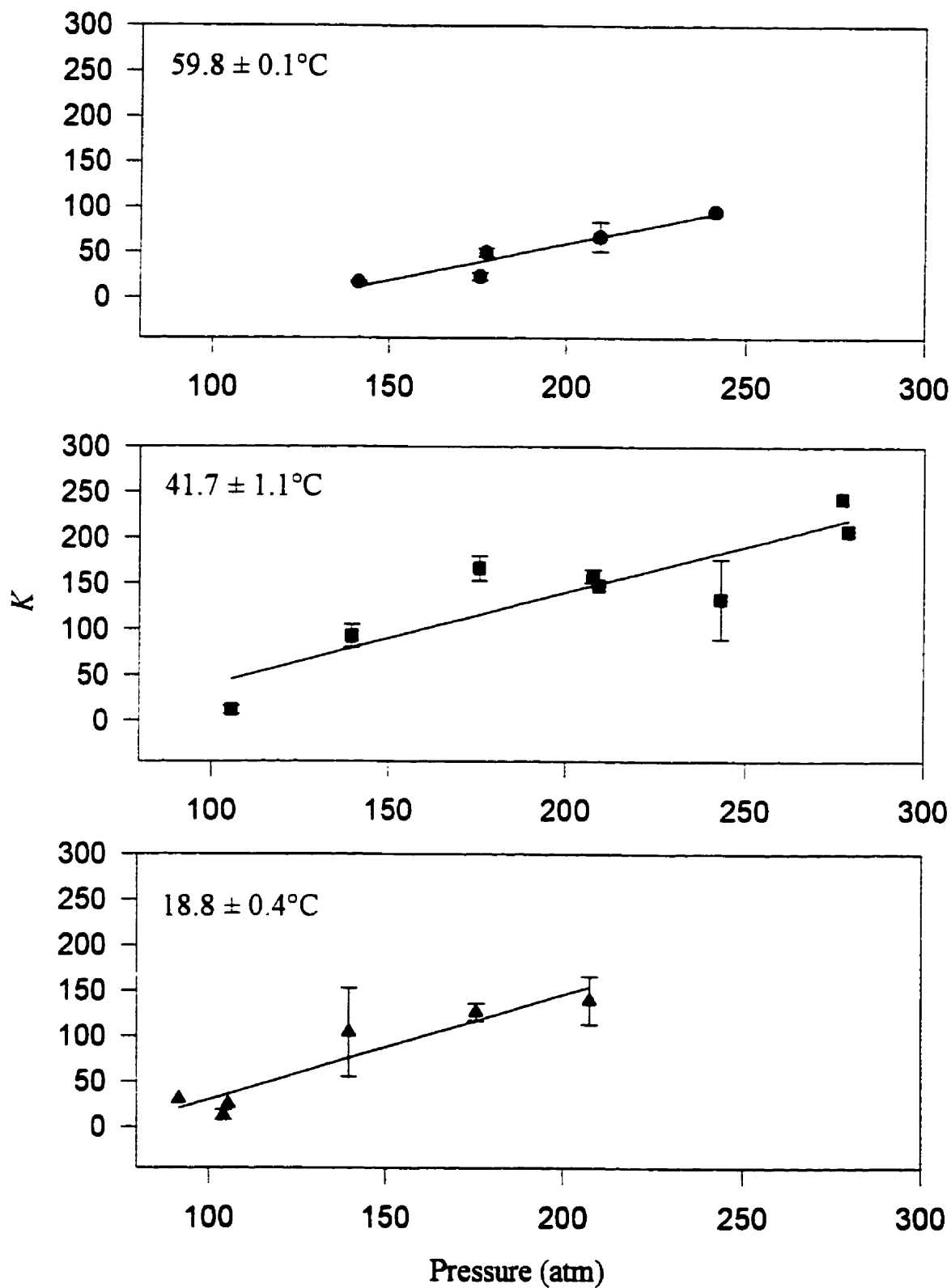
Figure 4.3.1. K for pentachlorophenol between CO_2 and water initially saturated in PCP

As the pressure, and thus the solvent density, increases along all isotherms in Figure 4.3.1, K shows a consistent increase on all plots due to enhanced solvation of PCP in CO_2. The positive effect of pressure was observed previously for solubility experiments and is consistent with the theory presented in section 2.5.2. The enhancement factor E for the solubility of a solid solute in a compressed gas increases as the pressure is increased; the solute mole fraction is a function of E.

Linear regressions were calculated for each set of data in Figure 4.3.1. The data are summarized in Table 4.3.1. Increasing the temperature causes the partitioning of pentachlorophenol (from the initially saturated solution) to drop significantly as a function of pressure. The slopes for the isotherms at 18.8, 41.7, and 59.8°C decrease as temperature is increased. This result has been observed for the partitioning of other phenolic compounds (reviewed in section 1.5.2) from water to carbon dioxide

Table 4.3.1. Linear Regression Slopes for the Partitioning of Pentachlorophenol from Saturated Solution as a Function of Pressure

Temperature (°C)	Slope of the Regression (atm^{-1})	r^2
18.8	1.16	0.887
41.7	1.00	0.788
59.8	0.81	0.910

It is likely more than one variable contributes to the reduction in K as the temperature is increased. Increasing the temperature from 18.8 to 41.7°C causes partitioning to increase as shown in Figure 4.3.2. In this temperature range, the effect of T on solute vapour pressure is more important than its effect on solvent density. However, there is no further increase in K as the temperature is raised above 41.7°C. The points for the isotherms at 41.7 and 59.8°C overlap at densities up to 0.75 g mL^{-1}. At 59.8°C,
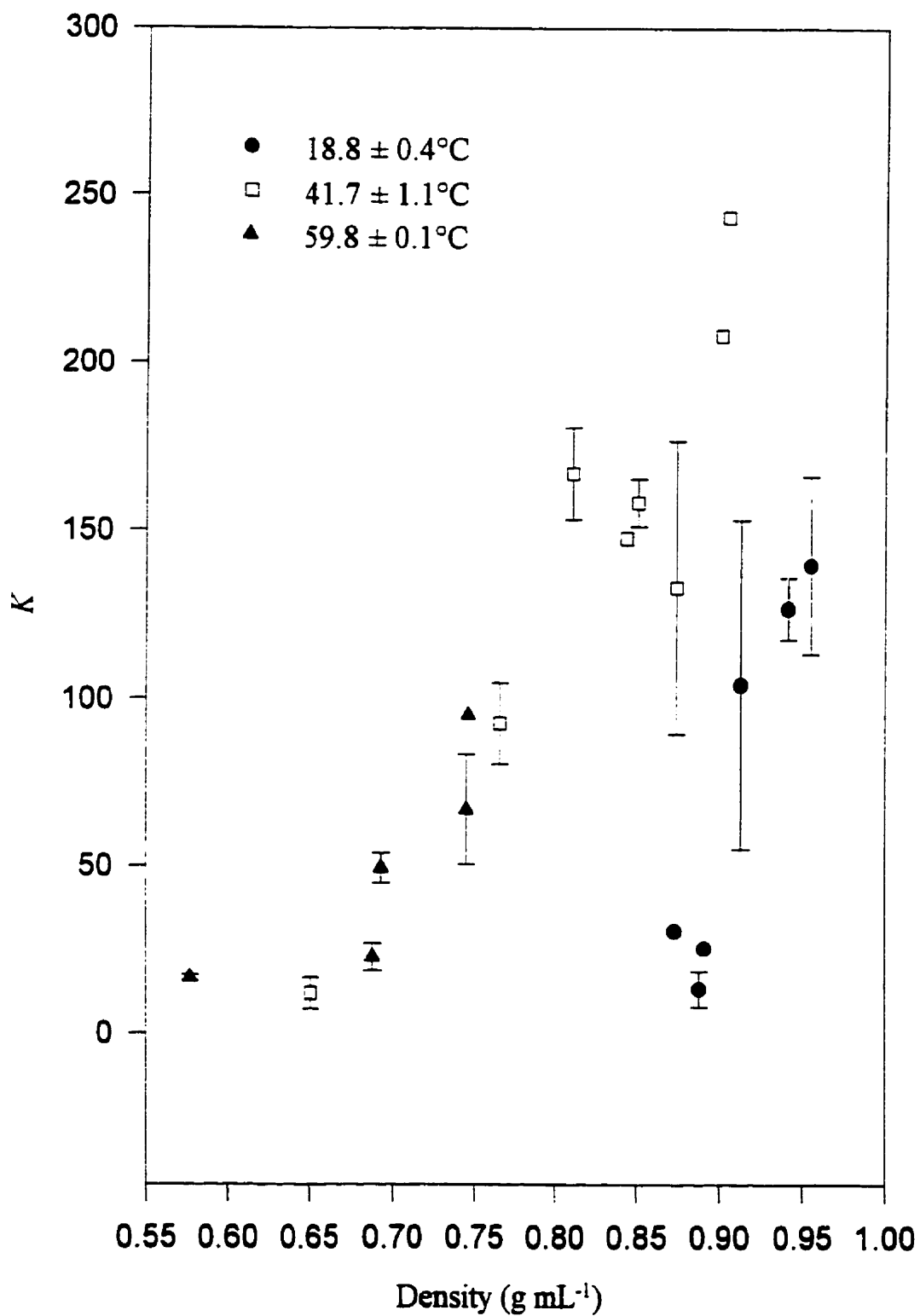
Figure 4.3.2. K as a function of density from water initially saturated with PCP

the reduced density of CO_2 apparently dominates the effect of temperature on solute vapour pressure.

The change in entropy for the partitioning process is not expected to vary significantly at constant density as the solvation of PCP in CO_2 does not change to a great extent. For the isotherms at 41.7 and 59.8°C, the distribution coefficient has the same value at densities up to 0.75 g mL^{-1} (Figure 4.3.2). As the change in free energy is the same for the partitioning process at both temperatures, partitioning must be more endothermic at the higher temperature. Referring to the same figure, partitioning at 18.8°C is smaller than at 41.7°C. For example, at about 0.9 g mL^{-1}, K at 18.8°C is 25 compared with a value of 240 at 41.7°C. The change in free energy for the partitioning process is lower at the higher temperature. This may be caused by an increase in the entropy term ($T\Delta S$). As well, partitioning at 18.8°C may be more endothermic.

Although K is higher at 41.7°C than at 18.8°C as a function of density, partitioning is smaller as a function of pressure. It is therefore assumed that other variables influence the partitioning of pentachlorophenol as the temperature is increased. Either (1) the interactions in the CO_2 phase become less significant or (2) the interactions in the water phase become more important. As the interactions in the CO_2-phase are not expected to change significantly during an extraction (for the reasons discussed in section 4.2.2), it is likely there are interactions in the water which are functions of temperature. One variable to consider is the change in the dissociation constant of pentachlorophenol. According to Gibb's free energy relationship, the pK_a of a solute decreases as the temperature is increased:

$$\Delta G = -RT \ln K = 2.303 RT pK_a \qquad (4.3.5)$$

The pK_a of pentachlorophenol was calculated at the three temperatures in Figure 4.3.1 and the data are presented in Table 4.3.2. Included in this table are the precentage of pentachlorophenoxide ions at each temperature at the pH of the aqueous phase (3.0).

Table 4.3.2. *pK$_a$* of Pentachlorophenol and the Percent of Pentachlorophenoxide Ions at pH 3

Temperature (°C)	pK$_a$ (calculated)	Percent Ions (PCP⁻)
18.8	4.77	1.7%
41.7	4.45	3.4%
59.8	4.2	5.9%

Increasing the temperature from 18.8 to 59.8°C has caused the number of pentachlorophenoxide anions in the water-rich phase to increase. As discussed in the theory, a solute will only partition to carbon dioxide in its unionized form. The distribution coefficient is therefore expected to decrease as the number of ions increases. As well, the data reported by Toews et al (1995) indicate that the pH of the water-rich phase increases slightly as the temperature is increased during a CO_2-water extraction due to the reduction of CO_2 solubility in water. For example, at a constant pressure of 100 atm, the pH increases from 2.83 to 2.95 as the temperature is raised from 25 to 70°C. A further increase in the number of pentachlorophenoxide ions is therefore expected at higher temperatures due to the pH effect.

4.3.3 Dilute Solution

Figure 4.3.3 demonstrates the effect on partitioning of reducing the initial concentration of pentachlorophenol in water from 11.6 to 1.3 µg mL⁻¹. The distribution coefficient is plotted as a function of pressure at 42.2 and 59.9°C for the dilute solution. The lower concentration more closely resembles contamination levels in natural water sources. The error bars are given as the standard deviation of several points.
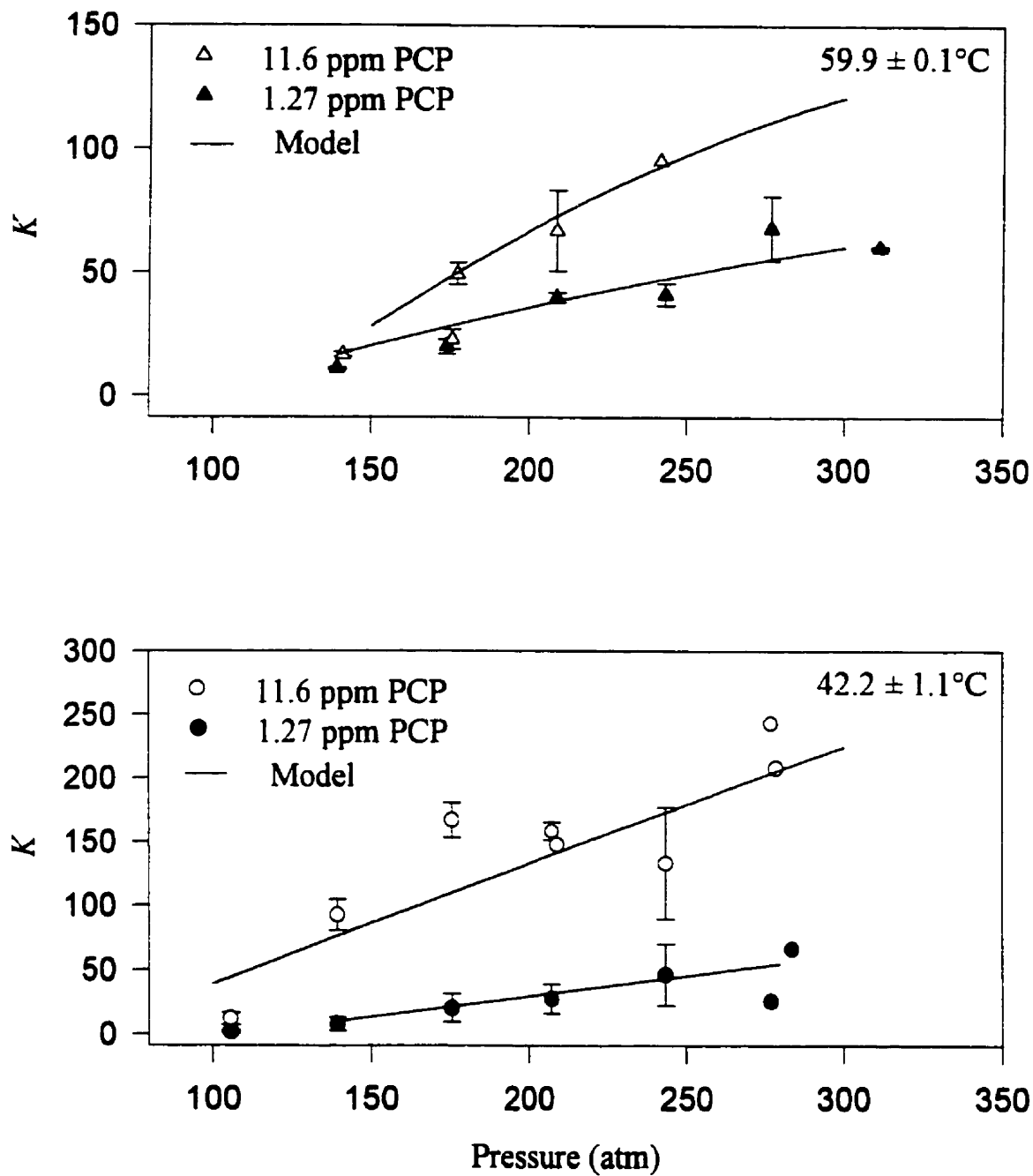
Figure 4.3.3. K for pentachlorophenol between water and CO_2 from dilute and saturated solutions

Partitioning to the CO_2-rich phase is smaller at the lower concentration. The theory in section 2.7.2 predicts the distribution coefficient is not a constant but depends on solute composition for moderately non-ideal solutions. Although the activities of the solute in either phase are equal at equilibrium, the activity coefficients are not equal and are functions of the mole fractions of the solute in CO_2 and water. For the partitioning of pentachlorophenol, it is apparent that at the lower concentration the activity coefficient in CO_2 (γ_i^B) is larger than for PCP in saturated solution. This conclusion is supported by the definitions of the activity coefficients in equations (2.7.5) and (2.7.6). In general, $\ln \gamma = \alpha (1 - x)^2$, where α is an interaction constant and x is the solute mole fraction. The values for the interaction constants α in each phase should be similar in magnitude as they both depend on the fugacity ratio f_i^S / f_i^L in equations (2.7.9) and (2.7.10). The relation predicts the activity coefficient for PCP in CO_2 will increase significantly as the mole fraction is decreased if the interaction constant α is sufficiently small. In contrast, γ for PCP in H_2O is not expected to vary to a large extent as the mole fraction of pentachlorophenol in water (x_i^A) is very small at all times (between 10^{-9} to 10^{-7} mole fraction). However, it is noted that both pentachlorophenol solutions (saturated and dilute) extracted in this work were very dilute. Theoretically, the distribution coefficient may be constant in the limiting case where $x \ll 1$ in both phases if the interaction constant α is large.

Another explanation for the increase in K as the initial concentration of PCP is increased (for which no data has been obtained) is presented as follows. Solute-solute bonding between PCP molecules is likely to be more important in a more concentrated solution and may result in the formation of dimers. Dimers would be less soluble in the polar water-rich phase as they would be non-polar. Pentachlorophenol dimers would more readily partition to CO_2 as a consequence of fewer and weaker solute-solvent (H_2O) interactions.

No effect of temperature on the partitioning of PCP from dilute solution was observed. Linear regressions, as well as 95% confidence intervals for the regressions, are plotted for the isotherms at 42.2 and 59.9°C in Figure 4.3.4. Error bars were omitted for the purpose of clarity. It can be seen that, although the slope of the regression at the higher temperature is slightly larger than that at 42.2°C (0.32 versus 0.28), the confidence intervals overlap.

The distribution coefficients have been presented thus far as the mole fraction of pentachlorophenol in CO_2 divided by its mole fraction in water. However, it is often convenient to express K as a ratio of concentrations. At 60°C and at a CO_2 density of 0.85 g mL^{-1}, $K_{concentration}$ is about 22. Therefore, 95% of PCP can be removed from water with a single extraction for a sample with a concentration near 1 μg mL^{-1}. For a saturated solution, $K_{concentration}$ is near 35. The amount extracted thus increases to about 97%. It is evident that there is little practical advantage in optimizing K in this range of values.
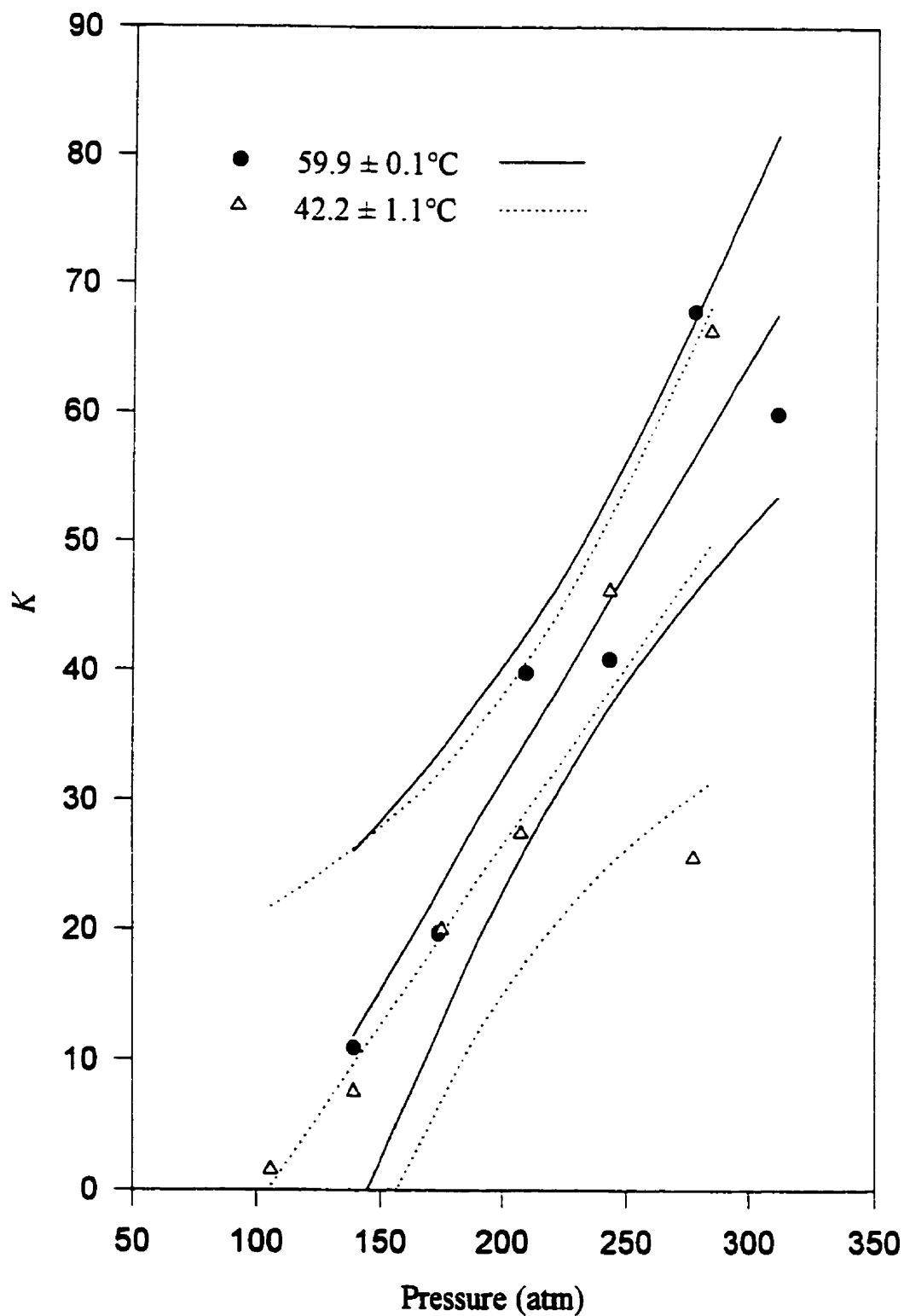
Figure 4.3.4. K for PCP between water and CO_2 from dilute solution (1.27 ppm) with a 95% confidence interval

4.3.4 Modelling

The data at both concentrations were modeled by the Peng-Robinson equation of state as outlined in section 2.7.3. The objective function minimized was $\Sigma[(y_i/x_i)_{calc} - (y_i/x_i)_{expt}]^2$, where y_i/x_i is the observed ratio of mole fractions of PCP in the aqueous and CO_2 phases respectively, and the quotient $(y_i/x_i)_{calc}$ is equal to the inverse of the ratio of activity coefficients, which were calculated via equation 2.7.16. The interaction parameters yielding the smallest objective function are listed in Table 4.3.3. The H_2O-CO_2 kij and kji values are from Panagiotopoupos and Reid (1986); all other values were fit to the experimental data. The saturation vapor pressure of PCP (required to evaluate ω in equation 2.7.14) was calculated from the Antoine constants given by Cross and Akgerman (1998).

Table 4.3.3. Interaction Parameters

i	j	k_{ij}	k_{ji}	
H_2O	CO_2	0.160	-0.198	
H_2O	PCP	0.190	-0.200	
PCP	CO_2	0.200	<u>11.6 ppm</u>	<u>1.27 ppm</u>
			0.48 (41.7°C)	0.55 (42.2°C)
			0.45 (59.8°C)	0.49 (59.8°C)

The objective function was most affected by the interaction parameters k_{ji} between PCP and CO_2. The actual value found for k_{ji} varied slightly depending on concentration of PCP and temperature. The only physical significance of this number is that the mixed values for the 'a' parameter in the Peng-Robinson equation are most significantly affected by the PCP-CO_2 interaction.

4.3.5 Solubility ratio

The ratio of the solubility of a solid solute in CO_2 to that in water (the "solubility ratio") provides a good measure of its partitioning behaviour. It was therefore expected that K would be high for pentachlorophenol as it is poorly soluble in water yet is moderately solubility in carbon dioxide (10^{-4} mole fraction). The solubility of pentachlorophenol in water is low compared with other phenols. A mole fraction of 9.0×10^{-7} was obtained in this work for PCP at 1 atm at ambient temperatures. The low solubility is largely a result of minimal hydrogen bonding between PCP and water which is caused by the presence of chlorine atoms in both ortho positions to the hydroxide group. This effect was reviewed in the theory (section 2.7.4). Measurement of the solubility of 2,3,4,5-tetrachlorophenol in water supports this conclusion. 2,3,4,5-tetrachlorophenol has the same structure as pentachlorophenol minus one chlorine atom ortho to the hydroxide group. The data obtained in this work indicated that removing the chlorine atom causes the solubility in water to increase an order of magnitude to 6.4×10^{-6} mole fraction.

To predict K for PCP, solubility ratios were calculated at ambient temperatures between pure water and pure CO_2, and then between water- and CO_2-rich phases. The latter is a better model as the interactions encountered in a water extraction are reproduced in both phases, that is, the water phase is saturated with CO_2 and the CO_2-rich phase is saturated with water. The solubility ratios and partitioning data at ambient temperatures are compared in Figure 4.3.5. Best fit lines were determined for each set of solubility data in Figures 4.2.6, 4.2.11, and 4.2.12 and the solubility ratio as a function of pressure was calculated. The solubility lines are curved
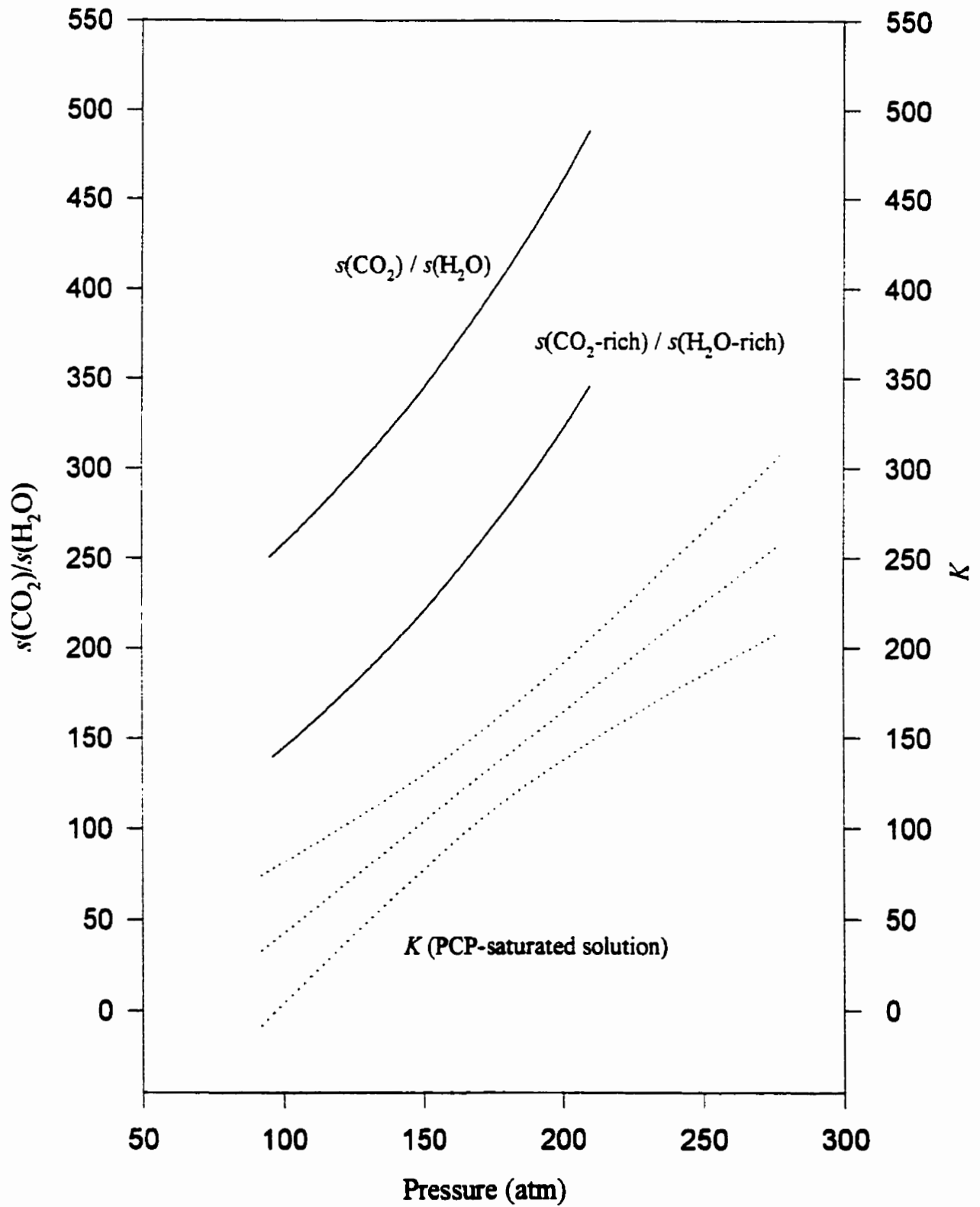
Figure 4.3.5. Comparison of the solubility ratios with the partitioning coefficient

upwards as PCP has a positive volume change upon solution in water while the solubility in CO_2 is coincidentally increasing. K for PCP from saturated solution at 18.8°C is also plotted. To facilitate the comparison, the distribution line was obtained by extrapolating the best fit line through the data points in Figure 4.3.1. The 95% confidence interval was calculated for the distribution line to show it is significantly different from the solubility ratios. The ratio of PCP solubility between the saturated phases is lower than between the pure phases. This is because the measurements for the solubility of PCP in water saturated with CO_2 were slightly higher than in pure water. As well, the solubility of PCP in the CO_2-rich phase was slightly smaller than in pure CO_2.

It is evident from the plots in Figure 4.3.5 that the distribution coefficient is smaller than the values predicted by the solubility ratios. At 160 atm, the solubility ratio between the water- and CO_2-rich phases is 240 while the value for K from a saturated solution of pentachlorophenol is 114. This difference is not surprising if the theory discussed in section 4.3.2 is considered. It is recalled that K is equal to the ratio of activity coefficients γ_i^A / γ_i^B. The activity coefficients are related to the solute composition via the relation $\ln \gamma = \alpha (1 - x)^2$. The values for the interaction constants α in each phase should be similar in magnitude as they both depend on the fugacity ratio f_i^S / f_i^L in equations (2.7.9) and (2.7.10). For carbon dioxide saturated with pentachlorophenol, x is of the order of 10^{-4} mole fraction and drops to 10^{-6} mole fraction during partitioning experiments. The activity coefficient for PCP in CO_2 will increase significantly as the mole fraction is decreased if the interaction constant α is sufficiently small. In contrast, γ for PCP in H_2O is not expected to vary to a large extent as the mole fraction is very small at all times, between 10^{-9} to 10^{-7} mole fraction.

Differences between the magnitudes of the solubility ratio and the distribution coefficient have been observed for other solutes. The results for p-chlorophenol and 2,4-dichlorophenol are shown in Table 4.3.4. In these cases, K was about one third to one half the size of the value predicted by the solubility ratio.

Table 4.3.4. Solubilities and Distribution Coefficients for *p*-chlorophenol and 2,4-dichlorophenol in Water and Carbon Dioxide

Compound	Solubility in Water[a] (Mole Fraction)	Solubility in CO_2[b] (Mole Fraction)	Solubility Ratio	K
p-chlorophenol	3.8×10^{-3}	2.043×10^{-2} 46°C; 163 atm	5.38	2.75^c 50°C; 163 atm
2,4-dichlorophenol	4.9×10^{-4}	7.583×10^{-2} 46°C; 163 atm	154.6	32.5^d 46°C; 163 atm

[a]Van Leer and Paulaitis, 1980; [b]Perry and Chilton, 1973; [c]Ghonasgi et al. 1991b; [d]Akgerman and Carter, 1994

4.3.5 Effect of pH

Figure 4.3.6 illustrates the effect of aqueous phase pH on the partitioning of pentachlorophenol from water to CO_2 at a density of 0.86 g mL^{-1}. The concentrations of PCP in the water samples were between 1.9 and 4.3 μg mL^{-1}. The temperature was about 40°C for all experiments; the temperature used for each experiment is noted on the figure. Solutions with pH < 3 were prepared using hydrochloric acid. Solutions with pH > 3 were prepared by adding appropriate amounts of sodium bicarbonate to form a bicarbonate-carbonic acid buffer. The amounts of buffer required were calculated using the Henderson-Hasselbalch equation and are listed in Table 4.3.5. Henry's constant at 298K (3.4×10^{-2} mol L^{-1} atm^{-1}) was used to estimate the amount of carbonic acid in the water phase. Samples without buffer or added acid had a pH of about 3 during partitioning experiments (Toews et al, 1995).
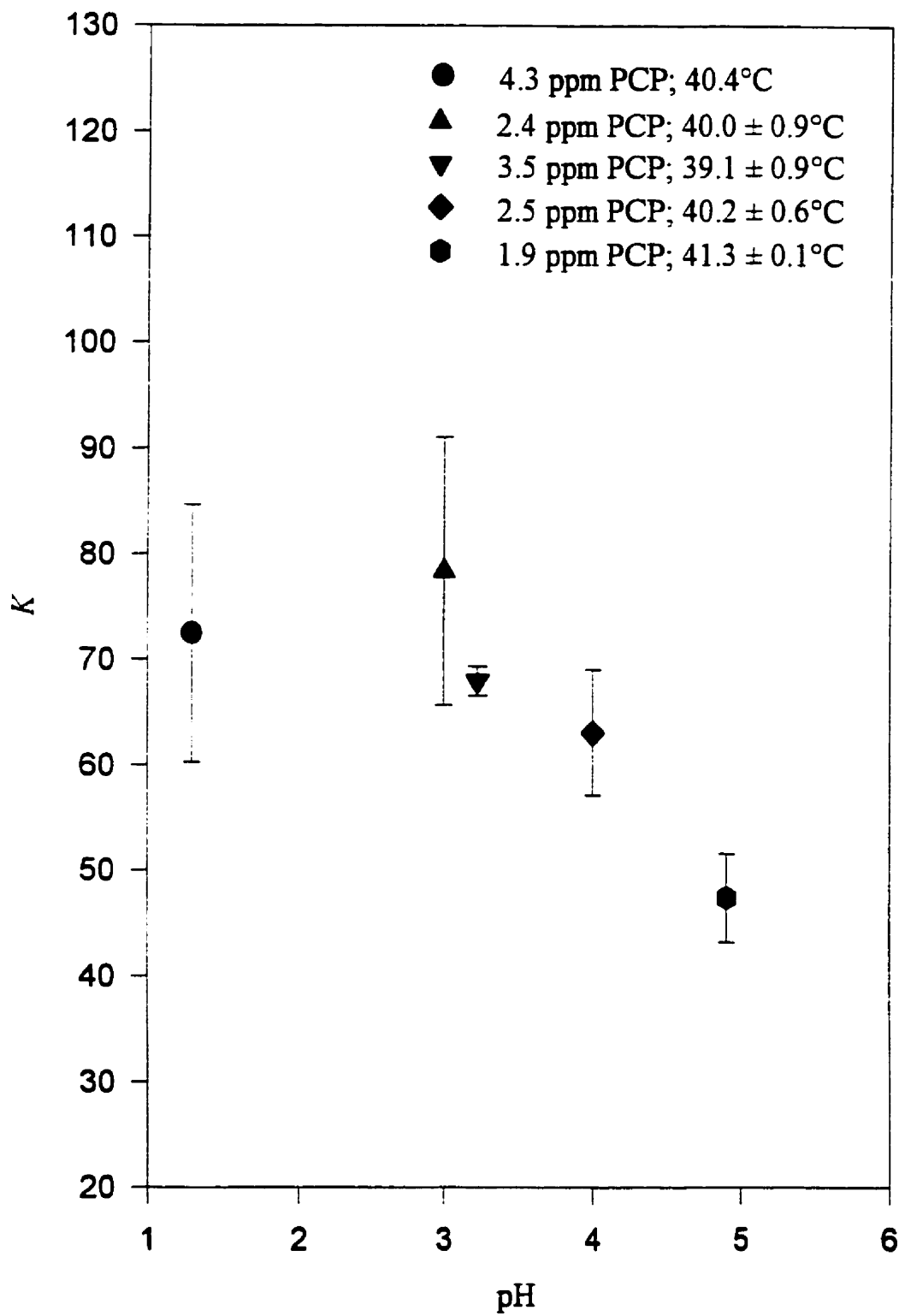
Figure 4.3.6. K as a function of solution pH for pentachlorophenol (0.86 g mL^{-1} CO$_2$)

Table 4.3.5. Concentrations[a] of Sodium Bicarbonate Buffer Used for Partitioning Experiments

Concentration of Sodium Bicarbonate [M]	Solution pH
5.0×10^{-3}	3.2
3.0×10^{-2}	4.0
2.4×10^{-1}	4.9

[a] Calculated with the Henderson-Hasselbalch equation: $pH = pK_a + \log[\text{base}] / [\text{acid}]$, where [acid] = $(3.4 \times 10^{-2} \text{ mol L}^{-1} \text{ atm}^{-1})(207.5 \text{ atm}) = 7.055 \text{ mol L}^{-1}$, [base] = $[HCO_3^-]$ and $pK_a = 6.37$.

The water fractions at pH 4.9 had to be collected off-line and acidified with HCl prior to analysis by HPLC. Except at pH 3.2, three or more measurements were made for K. In this case, two measurements were taken and the error was defined as the spread between values. Otherwise, standard deviation was calculated.

The data indicate that K increases as the pH is decreased for the partitioning of pentachlorophenol from water to carbon dioxide. This result was predicted by equation (2.7.23) which shows there are fewer pentachlorophenoxide anions in water at low pH. Pentachlorophenol will only partition to the CO_2 phase in its unionized form due to the low dielectric constant of CO_2. Neglecting for the moment the hydrolysis equilibrium, the maximum partition coefficient results when all of the unionized PCP partitions into the CO_2, leaving only the ionized form in the water phase:

$$K \approx \frac{[PCP_{CO_2}]}{[PCP^-_{(aq)}]} \tag{4.3.6}$$

$[PCP_{CO_2}]$ is equal to the original concentration of the unionized PCP in the water, $[PCP_{(aq)}]$. The proportion of PCP that is not hydrolyzed can be calculated using its acid hydrolysis constant:

$$[PCP_{(aq)}] = \frac{[PCP^-_{(aq)}][H_3O^+_{(aq)}]}{K_a} \qquad (4.3.7)$$

Introducing a CO_2 phase will have two effects. First, some of the unionized form of the PCP will partition into the CO_2 phase. However, the hydrolysis reaction will re-equilibrate as a result of the partitioning of (most of) the unionized PCP into the CO_2 phase, producing more unionized $PCP_{(aq)}$ and less $PCP^-_{(aq)}$. This will cause a shifting of the partition equilibrium towards the organic phase, and so the actual partition coefficient will be higher than that predicted. This effect is observed for the data in Table 4.3.6. Except at pH 1.3, the values of K measured in these experiments were higher than what would be predicted based solely on the percent ionization of the PCP. At the low pH it is likely K was too large to be measured accurately due to detection limit problems in the water phase.

Table 4.3.6. Percent of Pentachlorophenoxide Ions and Predicted and Actual K at Different pH at 40°C

pH	Percent Ions (PCP$^-$)	Predicted K^a (see text)	Measured K
1.3	0.1	1420	72 ± 12
3.0	3.4	28.4	78 ± 12
3.2	5.3	16.8	68 ± 1
4.0	26.2	2.8	63 ± 6
4.9	73.8	0.36	47 ± 4

[a]These K values were calculated assuming only the unionized PCP partitioned into the CO_2, leaving only ionized PCP in the water.

4.3.7 Effect of Ionic Strength

Figure 4.3.7 illustrates the effect of added salt on partitioning. Three water samples were prepared with concentrations ranging from 5.0×10^{-3} to 1 M NaCl. The concentration of pentachlorophenol in each solution was between 3.2 - 3.5 $\mu g \ mL^{-1}$. Partitioning experiments were performed with CO_2 at a density of 0.86 g mL^{-1} at about 40°C. K is slightly higher for PCP from a solution containing 5.0×10^{-2} M NaCl compared with 5.0×10^{-3} M NaCl. The data at both molarities are in close proximity to K for PCP from dilute solution. However, a substantial increase in salt concentration (to 1.0 M NaCl) caused the distribution coefficient for pentachlorophenol to increase to a value of 190 for a sample with 1.0 M NaCl. At this concentration, 98.5% of PCP was extracted from water with an equal volume of CO_2.

The activity coefficients for ionic species in the NaCl solutions were calculated using the Debye-Hückel limiting law. The data are presented in Table 4.3.7.

Table 4.3.7. Activity Coefficients in Sodium Chloride Solutions

NaCl Concentration [M]	γ^a
5.0×10^{-3}	0.92
5.0×10^{-2}	0.77
1.0	0.31

[a] Calculated with the Debye-Hückel limiting law: $\log \gamma_\pm = -|z_+ z_-| A \ I^{1/2}$ where $A = 0.509/(mol \ kg^{-1})^{1/2}$.

The value used for A was for an aqueous solution at 25°C. As well, the law can fail at concentrations above 0.1. Therefore, although the data in Table 4.3.7 indicates the trend for γ as a function of concentration, there is a level of uncertainty associated with it.
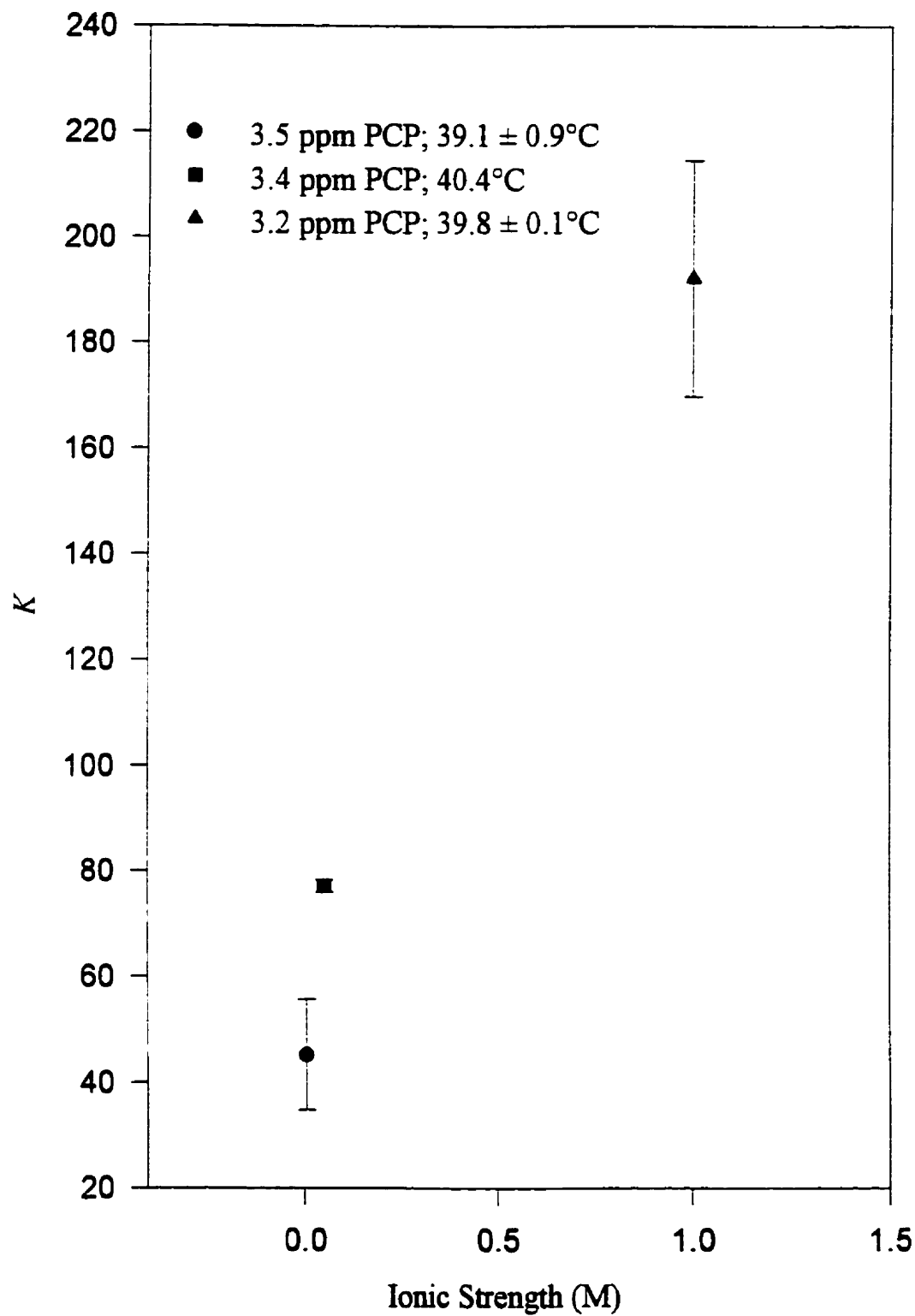
Figure 4.3.7. K as a function ionic strength (added NaCl) for pentachlorophenol
(0.86 g mL^{-1} CO$_2$)

As the ionic strength of the water phase is increased, the activity coefficient for ionic species in solution decreases. The decrease in γ should cause the concentration of pentachlorophenoxide anion to increase due to the secondary ion effect. However, this work has shown the value of K to increase significantly as the ionic strength of the water is increased, indicating the interactions between PCP and an ionic solution are less favourable. Because K is largely dependent on the partitioning of unionized PCP, the increase in the amount of pentachlorophenoxide anion was not significant. The overall result is that K is large for a solution with a sufficiently high ionic strength.

4.3.8 Other solutes

Partitioning data for 2,4-dichlorophenoxyacetic acid between water and CO_2 are presented in Figure 4.3.8. Experiments were performed at 40.2°C from an aqueous solution with a 2,4-D concentration of 0.77 μg mL^{-1}. The solute concentration was measured only in the water phase during partitioning experiments. To calculate K, material balance of the solute in the two phases was assumed. For the first two points in Figure 4.3.8 (at about 0.6 g mL^{-1} CO_2) 95% of the solute was apparently in the water phase at equilibrium. This amount decreased to 16% at a density of 0.9 g mL^{-1}.

The distribution coefficient was approximately an order of magnitude smaller for 2,4-D than for pentachlorophenol. This seems reasonable as the solubility of 2,4-D in carbon dioxide is also an order of magnitude smaller. Water is a good solvent for 2,4-D. This solute is a stronger acid than PCP and is more readily hydrolyzed. As well, ion-dipole interactions and hydrogen bonding between water and 2,4-D are expected to be stronger.

Partitioning experiments were performed for pentachlorobenzene between water and carbon dioxide at about 40°C. This solute was investigated to determine the effect of removing the hydroxide group from pentachlorophenol. Because the solubility of pentachlorobenzene is very low in water, solid (8.5 mg) was placed in the cell with 50 mL of water. A large amount of solid was used with the hope that the solute could be detected in both phases at equilibrium. However, pentachlorobenzene could not be detected in the water phase. The amount detected in the CO_2 phase was 100% or greater, indicating K is very high. Based on the limit of detection in the water phase (0.4 μg mL^{-1}), it was calculated that $K > 1000$.
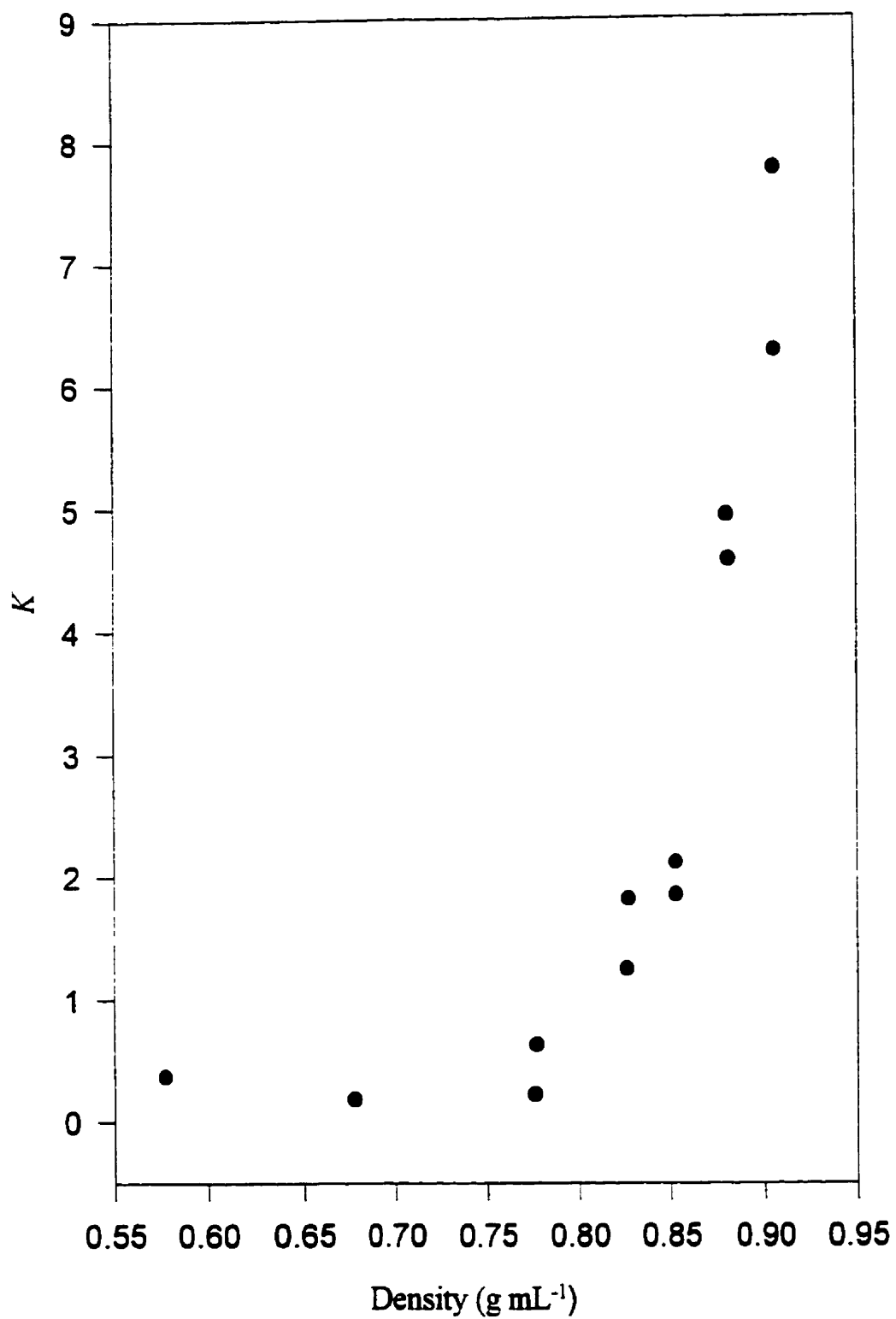
Figure 4.3.8. K for 2,4-D between water and CO_2 from dilute solution (0.77 μg mL^{-1}) at 40.2 ± 1.0°C

Partitioning coefficients were determined for 2,3,4,5-tetrachlorophenol between water and CO_2 at 41.0°C from an aqueous solution with an initial concentration of 2.1 µg mL^{-1}. The data are presented with values for pentachlorophenol from dilute solution in Figure 4.3.9. The fact that the values of K are so close to each other indicates that removing one chlorine atom from PCP (in the ortho position) did not have a significant effect on partitioning as the density of CO_2 was increased. However, this conclusion is tentative. As shown in Table 4.2.4, the solubility of PCP in water is almost an order of magnitude smaller than for 2,3,4,5-tetrachlorophenol. It is therefore expected that K should be higher for PCP. As well, the mass balance for the partitioning of 2,3,4,5-tetrachlorophenol was between 50 – 60 %.

● 2,3,4,5-tetrachlorophenol; $41.0 \pm 1.0°C$; $2.1\ \mu g\ mL^{-1}$
□ PCP; $42.2 \pm 1.1°C$; $1.3\ \mu g\ mL^{-1}$

K

Density $(g\ mL^{-1})$
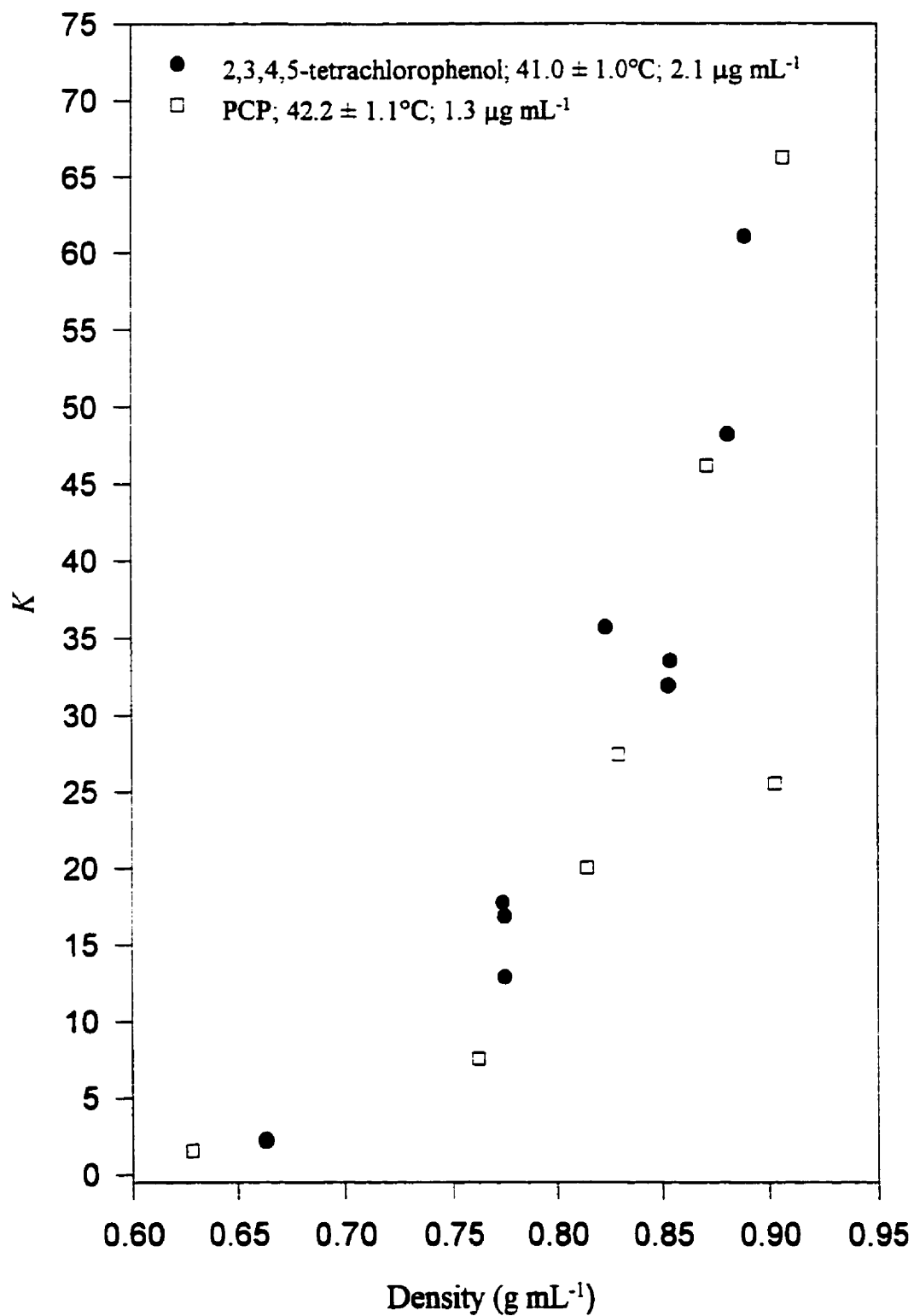
Figure 4.3.9. K for 2,3,4,5-tetrachlorophenol and pentachlorophenol from dilute solution

4.4 Impedance Measurements

The impedance of carbon dioxide in equilibrium with water was measured using the method described in section 3.2.5. Data obtained using an AC impedance meter were discarded as constant readings could not be obtained. Readings from a DC impedance meter did not fluctuate significantly over time, and thus could be taken after an equilibration time of only a few seconds.

The impedance of a 0.1M solution of sodium chloride was measured as 36.9Ω. The cell constant C ($= l/A$) was calculated as 0.362 cm^{-1} with the following equation using the value 9.8×10^{-3} Ω^{-1} cm^{-1} for κ^{*} (HCP, 1977):

$$\kappa = \frac{l}{RA}$$

(4.4.1)

If the molar concentration is c, then the molar conductivity is:

$$\Lambda_{m} = \frac{\kappa}{c}$$

(4.4.2)

Pure CO_2, CO_2 saturated with water, and the CO_2 phase during a PCP partitioning experiment all had impedances greater than 20 MΩ. The minimum number of ions in CO_2 was estimated using equations (4.4.1) and (4.4.2). Assuming the impedance of CO_2 was at least 20 MΩ and the conductivity of a hypothetical solution 1M in $H_3O^{+}_{(aq)}$ and 1 M in $HCO_3^{-}_{(aq)}$ was 390 Ω^{-1} cm^2 mol^{-1} (the sum of these ions' conductivities), the concentration of ions in CO_2 was calculated to be less than 10^{-12} mol L^{-1}. However, in one litre of carbon dioxide in equilibrium with water, there is approximately 0.1 mol of water, that is, 0.1 mol of carbonic acid. This concentration of acid in a water rich phase normally yields a concentration of ions of the order of 10^{-8} mol L^{-1}. The data therefore indicate the hydrolysis of carbonic acid to protons

and bicarbonate ions is negligible in the CO_2 saturated with water. The above calculation also indicates there is likely a negligible concentration of pentachlorophenoxide anions in CO_2 during a partitioning experiment, since there is no free water in the CO_2 phase to hydrolyze the PCP.

4.5 Ion Pairs in Carbon Dioxide

It is unlikely pentachlorophenol is solvated as an ion pair in CO_2. This conclusion is derived from the results obtained during a solubility experiment of pentachlorophenol sodium salt (Na-PCP) in carbon dioxide.

The apparent solubility of Na-PCP in CO_2 was 1.3×10^{-4} mole fraction at about 40°C and 135 atm. (This value compared reasonably well with the solubility of pentachlorophenol (2.8×10^{-4} mole fraction) at the same temperature and pressure.) Upon completion of the Na-PCP solubility experiment, a portion of the CO_2 phase was collected in a small amount water. The water was saturated with solute as evidenced by a visible amount of precipitate. However, analysis of the water by atomic emission spectroscopy showed no sodium in the sample (see Appendix 3). This result was unexpected as the solubility of Na-PCP in water was measured at 590 μg mL^{-1} and the limit of detection for the AES method was 1 μg mL^{-1}. The likely conclusion is that the carbon dioxide used in the solubility experiment contained a sufficient amount of water to hydrolyze Na-PCP to pentachlorophenol. Only 25 μL of water would have been required for the hydrolysis to occur. This amount is equal to the amount of water required to saturate the volume of CO_2 in the extraction cell.

To confirm the Na-PCP ion pair was not solvated in CO_2, NMR proton spectra were measured of the precipitate collected during the solubility experiment, for pure pentachlorophenol, and for pentachlorophenol sodium salt. Each sample was run at the same concentration in deuterated acetone. Looking at all three spectra in Appendix 4, it is evident that both PCP and the precipitate collected during the solubility experiment possess a hydroxide group as evidenced by the proton chemical shifts near 10 δ. The shift is not present on the spectra for Na-PCP. This result confirms that the solute dissolved in CO_2 during Na-PCP solubility experiments was pentachlorophenol.

4.6 Summary of Partitioning Results

The partitioning of pentachlorophenol from water initially saturated with PCP to carbon dioxide was higher as the pressure was increased. However, increasing the temperature caused the partitioning of PCP to drop significantly. K for PCP was also a function of the initial concentration of solute in the water sample. The partitioning coefficient was smaller for a solution with a lower initial concentration. Temperature did not significantly affect partitioning of PCP from dilute solution.

The data for pentachlorophenol was modeled with the Peng-Robinson equation of state using a concentration dependent mixing rule. The interaction parameter between CO_2 and PCP was sensitive to both PCP concentration and temperature. The partitioning data were also predicted by calculating the solubility ratio, which was higher than K. The activity coefficient for PCP in CO_2 was high for partitioning experiments from dilute solutions.

The partitioning of pentachlorophenol from water to carbon dioxide decreased as the pH was increased. However, the partitioning coefficient increased significantly from a solution with a high ionic strength.

The distribution coefficient was an order of magnitude smaller for 2,4-D than for PCP. K for pentachlorobenzene was almost 2 orders of magnitude higher than all other solutes tested as it was almost insoluble in water. The partitioning of 2,3,4,5-tetrachlorophenol was equal to that of PCP. It is noted, however, that K was predicted to be higher for PCP than 2,3,4,5-tetrachlorophenol as pentachlorophenol was less soluble in water. The partitioning of 2,3,4,5-tetrachlorophenol had a poor mass balance.

CHAPTER FIVE
CONCLUSIONS

1. Apparatus

A high pressure stainless steel extraction cell was constructed for static solubility and partitioning experiments in water and in liquid and supercritical carbon dioxide. On-line monitoring by HPLC allowed for accurate determination of the solute-solvent equilibrium during solubility experiments. Using on-line detection minimized sample loss and interference from impurities. As well, each of the water and CO_2 phases could be analyzed separately during water extractions to monitor the partitioning equilibrium and to measure partitioning coefficients. A variable wavelength detector made the system amenable to the analysis of solutes of different compositions and concentrations.

Use of the apparatus was validated by measuring the solubility of naphthalene, a solute which is well characterized in the literature. As well, mass balances of 80% or better were obtained for PCP partitioning experiments.

2. Solubilities in CO_2

The solubilities of non-polar (naphthalene and chrysene) and polar (pentachlorophenol and 2,4-D) solutes in carbon dioxide were determined as functions of temperature and pressure. The solubilities of all solutes increased with increasing pressure as compressed CO_2 has a higher solvent power. The solvation of PCP was less endothermic at higher densities. As well, the entropy change of the solution process decreased with increases in pressure as more CO_2 molecules solvated the solute at higher densities. Solute solubilities also increased with increases in temperature (despite the decrease in solvent density) due to the positive effect of temperature on solute vapour pressure. Cross-over regions were observed for the

solubility of pentachlorophenol in CO_2 as a function of pressure due to the interplay of these two temperature effects.

Naphthalene had the highest solubility in carbon dioxide as it was the most volatile solute tested. Chrysene had the lowest solubility as it has a high molecular weight and is likely characterized by strong intermolecular bonds. Pentachlorophenol was more soluble than 2,4-D as it has weak intermolecular bonds due to the presence of chlorine atoms in both ortho positions to the hydroxide group. The solvation of PCP in CO_2 was shown to be less endothermic than 2,4-D.

Pentachlorophenol solubilities in CO_2 saturated with water were not significantly different from solubility measurements in pure CO_2. Most of the water in CO_2 likely reacted to form carbonic acid, which could not dissociate to carbonate ions as there was no free water. PCP did not form strong bonds with carbonic acid and there were essentially no ions in the CO_2 phase for ion-dipole interactions, as determined by impedance measurements. Therefore, the majority of the interactions in the CO_2-rich phase were between PCP and CO_2.

3. Solubilities in water

Pentachlorophenol was sparingly soluble in water at atmospheric pressure as it did not form strong hydrogen bonds, again due to the chlorine atoms in both ortho positions to the hydroxide group. Removing one chlorine from the ortho position caused the solubility of 2,3,4,5-tetrachlorophenol to be an order of magnitude higher than for PCP. Pentachlorobenzene was almost insoluble in water as it does not have a hydroxide group. 2,4-D had the highest solubility in water as it was the strongest acid tested.

The solubility of pentachlorophenol in water decreased as the pressure was increased as PCP had a positive volume change upon solution. Similar solubilities were

measured in water saturated with carbon dioxide. The solubility of PCP in water is mostly a result of intermolecular interactions between unionized PCP and water.

4. Partitioning

The partitioning of pentachlorophenol from water initially saturated with PCP to carbon dioxide was higher as the pressure was increased. Compressing CO_2 to higher densities enhanced the solvation of all solutes in this work. However, increasing the temperature caused the partitioning of PCP to drop significantly. Several variables contributed to this temperature effect. Increasing the temperature caused the density, and thus the solvent power, of CO_2 to decrease. As well, the pK_a of PCP decreased with increasing temperature. This meant there were more pentachlorophenoxide ions in solution at higher temperatures; PCP cannot partition to CO_2 in an ionized form.

The partitioning of PCP was a function of the initial concentration of solute in the water sample. The partitioning coefficient was smaller for a solution with a lower initial concentration. Lowering the initial concentration of PCP in water caused the activity coefficient for PCP in CO_2 to increase. It is also likely solute-solute bonding between PCP molecules was more important in the more concentrated solution, thus reducing the number of interactions between PCP and water. Temperature did not significantly affect partitioning of PCP from dilute solution.

The data for pentachlorophenol was modeled with the Peng-Robinson equation of state using a concentration dependent mixing rule. The interaction parameter between CO_2 and PCP was sensitive to both PCP concentration and temperature. The partitioning data were also predicted by calculating the solubility ratio, which was about 2 times higher than K. The activity coefficient for PCP in CO_2 was higher for partitioning experiments than for solubility experiments as the mole fraction of solute was lower.

The partitioning of pentachlorophenol from water to carbon dioxide decreased as the pH was increased as there were more pentachlorophenoxide anions in water at high pH. Except at pH 1.3, K was higher than expected overall as the hydrolysis reaction for PCP was continually re-equilibrating as the extraction proceeded. K was large from a solution with a high ionic strength. The partitioning coefficient was about 4 times higher from a solution with a concentration of 1M NaCl. The effect of lowering the pH may also be due to an increase of ionic strength.

The distribution coefficient was an order of magnitude smaller for 2,4-D than for PCP. 2,4-D was less soluble than PCP in CO_2, and more soluble in water. K for pentachlorobenzene was almost 2 orders of magnitude higher than all other solutes tested as it was almost insoluble in water. The partitioning of 2,3,4,5-tetrachlorophenol was equal to that of PCP; apparently, removing a chlorine atom ortho to the hydroxide group on PCP did not affect its partitioning. It is noted, however, that K was predicted to be higher for PCP as it was less soluble in water than 2,3,4,5-tetrachlorophenol. It is also noted 2,3,4,5-tetrachlorophenol did not have a mass balance better than 60% during partitioning experiments.

4. Analytical applications

Partitioning experiments with the extraction cell constructed in this work indicate 95% of pentachlorophenol can be extracted from a 1 ppm aqueous solution with an equal volume of CO_2. The recovery increases to 98.5% for extractions from water with a high ionic strength. Because solute recovery is already high, the experimental method does not need to be further "optimized" using pressures and temperatures exceeding those tested in this work.

As well, using an equal volume of carbon dioxide, 95% of 2,3,4,5-tetrachlorophenol and 89% of 2,4-D can be removed from water with a single static extraction. The extraction method is therefore suited to the extraction of an acid with a pK_a as low as

3.89 (that of 2,4-D). Increasing the volume of the CO_2 phase, or decreasing the volume of the water phase, will improve solute recovery if this is necessary for acidic species. The amount of pentachlorobenzene remaining in the water phase following a CO_2 extraction would be almost negligible (however, due to its low solubility in water, it is unlikely a water sample would contain a significantly high concentration of pentachlorobenzene).

The extraction cell used in this work is suitable for extractions from samples with a volume of 50mL or less. The system is best suited as an analytical method. At present, the extraction method is not suited to sample clean up or water remediation. To satisfy this purpose, a method would need to be devised which allowed the water to be continually flowed through the extraction cell.

The results obtained in this work indicate using supercritical CO_2 for the extraction of water samples containing acidic compounds is a good alternative to current methodologies. Only one hour is required for the extraction and analysis of pentachlorophenol using a static system. A complete extraction with a minimal volume of CO_2 would also be possible with a dynamic system if the CO_2 flow rate is optimized to achieve equilibrium. The number of steps required during SF extractions are minimal compared with conventional liquid-liquid and solid phase extractions. The on-line method used in this work combined sample extraction, separation, and detection while minimizing the risk of sample loss and contamination. The limit of detection in this work was near 0.1 ppm in both phases for most solutes. Other on-line detection methods may detect lower concentrations. As well, sample concentration may be possible with a dynamic method. Finally, one could use several small volumes of CO_2 to preconcentrate the analytes.

The initial start-up cost for a supercritical fluid method is expensive as high pressure equipment is required. However, the cost is minimal once the necessary equipment has been purchased as large volumes of organic solvents and solid-phase cartridges are not required, and the time required for the extraction step is small.

CHAPTER SIX

REFERENCES

Akgerman, A., Carter, B.D. "Equilibrium Partitioning of 2,4-Dichlorophenol between Water and Near-Critical and Supercritical Carbon Dioxide" J. Chem. Eng. Data **39**(3), 510 (1994)

Alzaga, R., Durand, G., Barceló, D., Bayona, J.M. "Comparison of Supercritical Fluid Extraction and Liquid-Liquid Extraction for Isolation of Selected Pesticides Stored in Freeze-Dried Water Samples" Chromatographia **38**(7/8), 502 (1994)

Arcand, Y., Hawari, J., Guiot, S.R. "Solubility of Pentachlorophenol in Aqueous Solutions: The pH Effect" Wat. Res. **29**(1), 131 (1995)

Atkins, P.W. **Physical Chemistry**, 4th ed.; W.H. Freeman and Company: New York, (1990)

Barceló, D., Hennion, M-C. "On-Line Sample Handling Strategies for the Trace-Level Determination of Pesticides and their Degradation Products in Environmental Waters" Analytica Chimica Acta **318**, 1 (1995)

Barna, L., Blanchard, J.-M., Rauzy, E., Berro, C. "Solubility of Fluoranthene, Chrysene, and Triphenylene in Supercritical Carbon Dioxide" J. Chem. Eng. Data **41**(6), 1466 (1996)

Barnabas, I.J., Dean, J.R., Hitchen, S.M., Owen, S.P. "Supercritical Fluid Extraction of Organochlorine Pesticides from an Aqueous Matrix" J. Chromatogr. A **665**, 307 (1994a)

Barnabas, I.J., Dean, J.R., Hitchen, S.M., Owen, S.P. J. Chromatogr. Sci. **32**, 547 (1994)

Blackman, G.E., Parke, M.H., Garton, G. "The Physiological Activity of Substituted Phenols. II. Relationships between Physical Properties and Physiological Activity" Archs Biochem. Biophys. **54**, 55 (1955)

Brewer, S.E., Kruus, P. "Direct Supercritical Fluid Extraction from Water" J. Environ. Sci. Health **B28**(6), 671 (1993)

Brudi, K., Dahman, N., Schneider, H. "Partition Coefficients of Organic Substances in Two-Phase Mixtures of Water and Carbon Dioxide at Pressures of 8 to 30 Mpa and Temperatures of 313 to 333 K" J. Supercrit. Fluids **9**(3), 146 (1996)

Bunce, N. **Environmental Chemistry**; Wuerz Publishing Ltd.: Winnipeg, (1991)

Carswell, T.S., Nason, H.K. "Properties and Uses of Pentachlorophenol" Ind. Eng. Chem. **30**(6), 622 (1938)

Chang, C.J., Huang, I. "Separation of Phenolic Pollutants from Dilute Solutions Using Supercritical Carbon Dioxide and Nitrous Oxide" Sep. Sci. Tech. 30(5), 683 (1995)

Combs, M.T., Ashraf-Khorassani, M., Taylor, L.T. "pH Effects on the Direct Supercritical Fluid Extraction of Phenols from Aqueous Matrices" J. Supercrit. Fluids 9(2), 122 (1996)

Cooper, A.I., Londono, J.D., Wignall, G., McClain, J.B., Samulski, E.T., Lin, J.S., Dobrynin, A., Rubinstein, M., Burke, A.L.C., Fréchet, J.M.J., DeSimone, J.M. "Extraction of a Hydrophilic Compound from Water into Liquid CO_2 Using Dendritic Surfactants" Nature 389, 368 (1997)

Croft, M.Y., Murby, E.J., Wells, R.J. "Simultaneous Extraction and Methylation of Chlorophenoxyacetic Acids from Aqueous Solution Using Supercritical Carbon Dioxide as a Phase Transfer Solvent" Anal. Chem. 66(24), 4459 (1994)

Cross, W.M. Jr., Akgerman, A. "Single-Component and Mixture Solubilities of Hexachlorobenzene and Pentachlorophenol in Supercritical Carbon Dioxide" Ind. Eng. Chem. Res. 37(4), 1510 (1998)

Daneshfar, A., Barzegar, M., Ashraf-Khorassani, M., Levy, J.M. "Supercritical Fluid Extraction of Phenoxy Acids from Water" J. High Resol. Chromatogr. 18, 446 (1995)

Ehntholt, D.J., Thrun, K., Eppig, C. "The Concentration of Model Organic Compounds Present in Water at Parts-per-Billion Levels Using Supercritical Fluid Carbon Dioxide" Intern. J. Environ. Chem. 13, 219 (1983)

Freiter, E.R. Kirk-Othmer's Encyclopedia of Chemical Technology, 3rd ed.; John Wiley and Sons: New York, Vol. 5 (1979)

Ghonasgi, D., Gupta, S., Dooley, K.M., Knopf, F.C. "Measurement and Modeling of Supercritical Carbon Dioxide Extraction of Phenol from Water" J. Supercrit. Fluids 4(1), 53 (1991a)

Ghonasgi, D., Gupta, S., Dooley, K.M., Knopf, F.C. "Supercritical CO_2 Extraction of Organic Contaminants from Aqueous Streams" AIChE Journal 37(6), 944 (1991b)

Green, L.A., Akgerman, A. "Supercritical CO_2 Extraction of Soil-Water Slurries" J. Supercrit. Fluids 9(3), 177 (1996)

Gupta, S., Ghonasgi, D., Dooley, K.M., Knopf, F.C. "Supercritical Carbon Dioxide Extraction of a Phenolic Mixture from an Aqueous Waste Stream" J. Supercrit. Fluids 4(3), 181 (1991)

Harned, H.S., Davis, Jr., R. "The Ionization Constant of Carbonic Acid in Water and the Solubility of Carbon Dioxide in Water and Aqueous Salt Solutions from 0 to 50°" J. Solution. Chem. 65, 2030 (1943)

Hawthorne, S.B., Miller, D.J., Nivens, D.E., White, D.C. "Supercritical Fluid Extraction of Polar Analytes Using in Situ Chemical Derivatization" Anal. Chem. 64(4), 405 (1992)

HCP: CRC Handbook of Chemistry and Physics, 58th ed.; CRC Press, Inc.: Cleveland, (1977)

Hedrick, J., Taylor, L.T. "Quantitative Supercritical Fluid Extraction/Supercritical Fluid Chromatography of a Phosphonate from Aqueous Media" Anal. Chem. 61(17), 1986 (1989)

Hedrick, J.L., Mulcahey, L.J., Taylor, L.T. "Supercritical Fluid Technology", A.C.S. Symposium Series 488, 206 (1992)

Hedrick, J.L., Taylor, L.T. "Direct Supercritical Fluid Extraction of Nitrogenous Bases From Aqueous Solution" J. High Res. Chrom. 15, 151 (1992)

Hedrick, J.L., Taylor, L.T. "Supercritical Fluid Extraction Strategies of Aqueous Based Matrices" J. High Res. Chrom. 13, 132 (1990)

Hnedkovský, L., Wood, R.H., Majer, V. "Volumes of Aqueous Solutions of CH_4, CO_2, H_2S, and NH_3 at Temperatures from 298.15 K to 705 K and Pressures to 35 Mpa" J. Chem. Thermodynamics 28, 125 (1996)

Johnston, K.P., Harrison, K.L., Clarke, M.J., Howdle, S.M., Heitz, M.P., Bright, F.V., Carlier, C., Randolph, T.W. "Water-in-Carbon Dioxide Microemulsions: An Environment for Hydrophiles Including Proteins" Science 271, 624 (1996)

King, M.B., Mubarak, A., Kim, J.D., Bott, T.R. "The Mutual Solubilities of Water with Supercritical and Liquid Carbon Dioxide" J. Supercrit. Fluids 5(4), 296 (1992)

King, J.W., Johnson, J.H., Eller, F.J. "Effect of Supercritical Carbon Dioxide Pressurized with Helium on Solute Solubility during Supercritical Fluid Extraction" Anal. Chem. 67(13), 2288 (1995)

Laintz, K.E., Wai, C.M., Yonker, C.R., Smith, R.D. "Extraction of Metal Ions from Liquid and Solid Materials by Supercritical Carbon Dioxide" Anal. Chem. 64(22), 2875 (1992)

Mackay, D., Shiu, W.Y. "A Critical Review of Henry's Law Constants for Chemicals of Environmental Interest" J. Phys. Chem. Ref. Data 10(4), 1175 (1981)

Macnaughton, S.J., Foster, N.R. "Solubility of DDT and 2,4-D in Supercritical Carbon Dioxide and Supercritical Carbon Dioxide Saturated with Water" Ind. Eng. Chem. Res. 33(11), 2757 (1994)

Madras, G.M., Erkey, C., Akgerman, A. "A New Technique for Measuring Solubilities of Organics in Supercritical Fluids" J. Chem. Eng. Data 38(3), 422 (1993)

McHugh, M., Paulaitis, M.E. "Solid Solubilities of Naphthalene and Biphenyl in Supercritical Carbon Dioxide" J. Chem. Eng. 25(4), 326 (1980)

Miller, D.J., Hawthorne, S.B., Clifford, A.A. "Solubility of Chlorinated Hydrocarbons in Supercritical Carbon Dioxide from 313 to 413 K and at Pressures from 150 to 450 bar" J. Supercrit. Fluids 10, 57 (1997)

Ong, C.P., Lee, H.K., Li, S.F.Y. "Direct Coupling of Supercritical Fluid Extraction-Supercritical Fluid Chromatography for the Determination of Selected Polycyclic Aromatic Hydrocarbons in Aqueous Environmental Samples" Environ. Monit. Assess. 19(1-3), 63 (1991)

Panagiotopoulos, A.Z., Reid, R.C. "New Mixing Rule for Cubic Equations of State rf Highly Polar, Asymmetric Systems" ACS Symp. Series 300, 571 (1986)

Peng, D-Y., Robinson, D.B. "A New Two-Constant Equation of State" Ind. Eng. Chem. Fundam. 15(1), 59 (1976)

Perry, R.H.,, Chilton, C.H. Chemical Engineer's Handbook, 5th ed.; McGraw-Hill: New York (1973)

Prausnitz, J.M., Lichtenthaler, R.N., de Azevedo, E.G. **Molecular Thermodynamics of Fluid-Phase Equilibria**, 2nd ed.; Prentice-Hall, Inc.: New Jersey, (1986)

Ramsey, E.D., Minty, B., McCullagh, M.A., Games, D.E., Rees, A.T. "Analysis of Phenols in Water at the ppb Level Using Direct Supercritical Fluid Extraction of Aqueous Samples Combined On-line With Supercritical Fluid Chromatography-Mass Spectrometry" Analytical Communications 34(3-6), 3 (1997)

Read, A.J. "The First Ionization Constant of Carbonic Acid from 25 to 250°C and to 2000 bar" J. Solution Chem. 4(1), 53 (1975)

Roop, R.K., Akgerman, A. "Distribution of a Complex Mixture between Water and Supercritical Carbon Dioxide" J. Chem. Eng. Data 35(3), 257 (1990)

Roop, R.K., Akgerman, A. "Entrainer Effect for Supercritical Extraction of Phenol from Water" Ind. Eng. Chem. Res. 28(10), 1542 (1989)
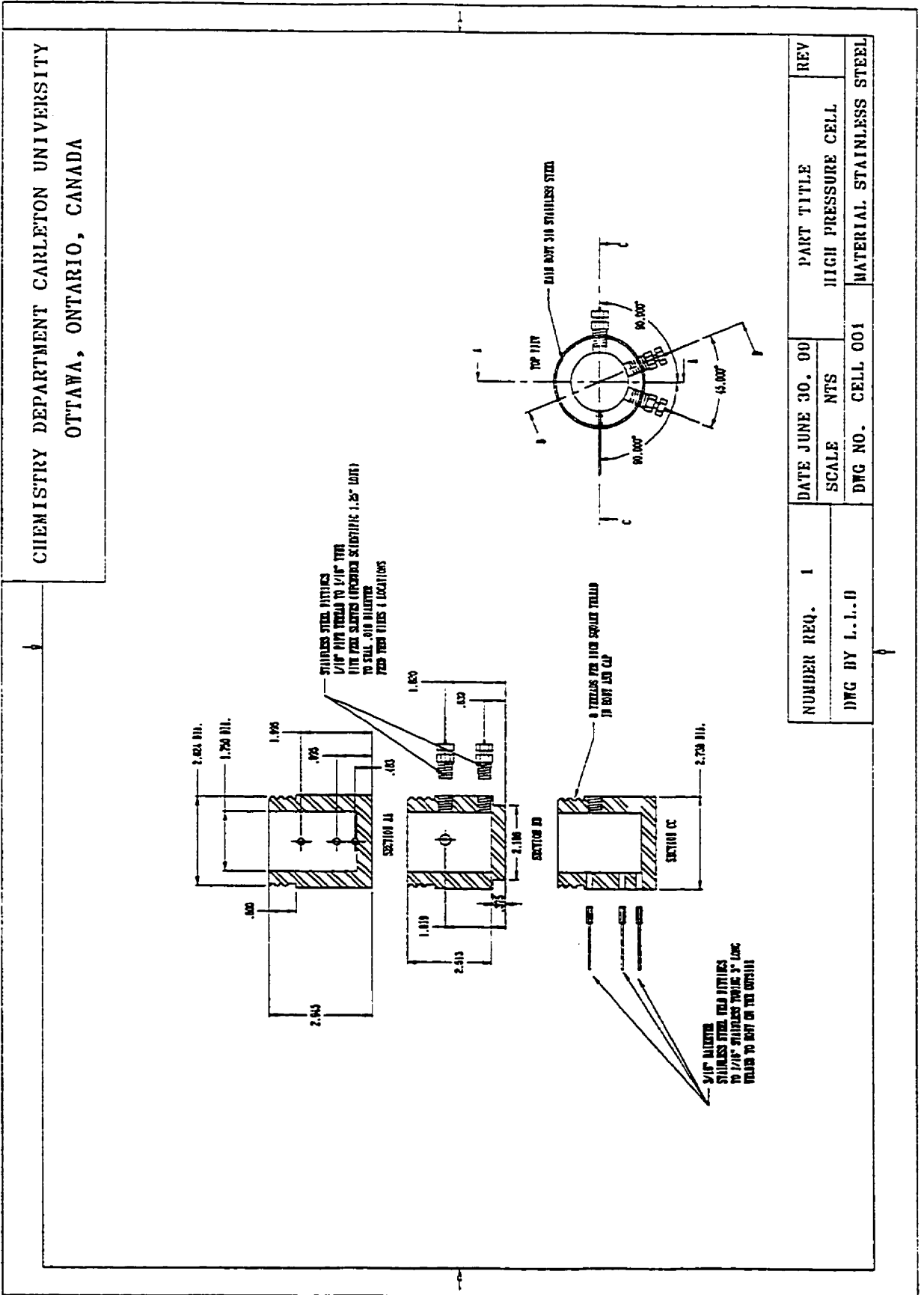
Roop, R.K., Akgerman, A., Dexter, B.J., Irvin, T.R. "Extraction of Phenol from Water with Supercritical Carbon Dioxide" J. Supercrit. Fluids 2(2&3), 51 (1989)

Sawamura, S., Kitamura, K., Taniguchi, Y. "Effect of Pressure on the Solubilities of Benzene and Alkylbenzenes in Water" J. Phys. Chem. 93(12), 4931 (1989)

Sawamura, S., Tsuchiya, M., Ishigami, T., Taniguchi, Y., Suzuki, K. "Effect of Pressure on the Solubility of Naphthalene in Water at 25°C" J. Solution Chem. 22(8), 727 (1993)

Schäfer, K., Baumann, W. "Solubility of Some Pesticides in Supercritical CO_2" Fresenius Z Anal. Chem. 332, 122 (1988)

Schneider, G.M. "Physico-Chemical Properties and Phase Equilibria of Pure Fluids and Fluid Mixtures at High Pressures" NATO ASI Series E: Applied Sciences (Supercritical Fluids Fundamentals for Application) 273, 91 (1994)

Skoog, D.A., West, D.M. Fundamentals of Analytical Chemistry, 4th ed.; CBS College Publishing: New York, (1982)

Suárez, J.J., Medina, I., Bueno, J.L. "Diffusion Coefficients in Supercritical Fluids: Available Data and Graphical Correlations" Fluid Phase Equilibria 153, 167 (1998)

Tang, P.H.-T., Ho, J.S. "Liquid-Solid Disk Extraction Followed by Supercritical Fluid Elution and Gas Chromatography of Phenols from Water" J. High Resol. Chromatogr. 17, 509 (1994)

Taylor, L.T. Supercritical Fluid Extraction; John Wiley and Sons, Inc.: New York, (1996)

Thiebaut, D., Chervet, J.-P., Vannoort, R.W., De Jong, G.J., Brinkman, U.A.Th., Frei, R.W. "Supercritical-Fluid Extraction of Aqueous Samples and On-Line Coupling to Supercritical-fluid Chromatography" J. Chromatogr. 477, 151 (1989)

Toews, K.L., Shroll, R.M., Wai, C.M. "pH-Defining Equilibrium between Water and Supercritical CO_2. Influence on SFE of Organics and Metal Chelates" Anal. Chem. 67(22), 4040 (1995)

Van Leer, R.A., Paulaitis, M.E. "Solubilities of Phenol and Chlorinated Phenols in Supercritical Carbon Dioxide" J. Chem. Eng. Data 25(3), 257 (1980)

Wenzel, H., Rupp, W. "Calculation of Phase Equilibria in Systems Containing Water and Supercritical Components" Chem. Eng. Sci. 33, 683 (1978)

Wiebe, R. "The Binary System Carbon Dioxide-Water Under Pressure" Chem. Revs. 29, 475 (1941)

Wiebe, R., Gaddy, V.L. "The Solubility of Carbon Dioxide in Water at Various Temperatures from 12 to 40° and at Pressures to 500 Atmospheres. Critical Phenomena." J. Am. Chem. Soc. **62**, 815 (1940)
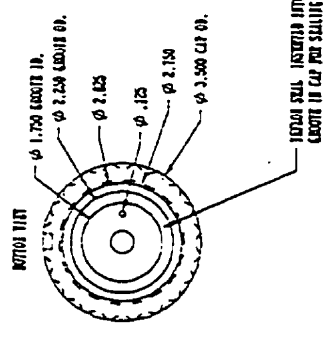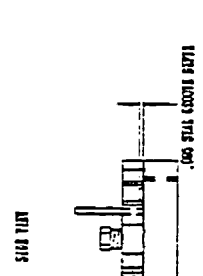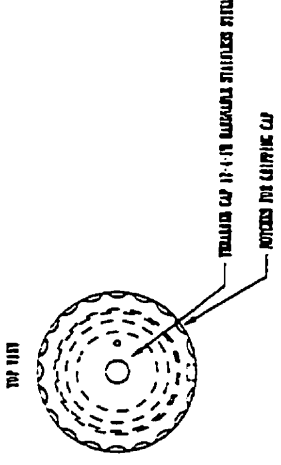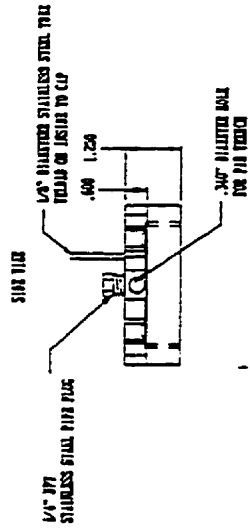
Wiebe, R., Gaddy, V.L. "Vapor Phase Composition of Carbon Dioxide-Water Mixtures at Various Temperatures and at Pressures to 700 Atmospheres" J. Am. Chem. Soc. **63**, 475 (1941)

Yeo, S-D., Akgerman, A. "Supercritical Extraction of Organic Mixtures from Aqueous Solutions" AIChE Journal **36**(11), 1743 (1990)

# Appendix 1. Engineering diagram of the extraction cell used in this work

CHEMISTRY DEPARTMENT CARLETON UNIVERSITY
OTTAWA, ONTARIO, CANADA

SIDE VIEW

.080 STEEL SHIELD PLATE

BOTTOM VIEW

ϕ 1.750 GROOVE I.D.
ϕ 2.250 GROOVE O.D.
ϕ 2.425
ϕ .75
ϕ 3.500 CAP O.D.

INDIUM SEAL INSERTED INTO GROOVE IN CAP FOR SEALING

SIDE VIEW

1/8" DIAMETER STAINLESS STEEL TUBE WELDED OR BRAZED TO CAP

1.250
.400

THREADED FILL HOLE FOR SCALING PLUG

3/4"

1/8" NPT STAINLESS STEEL PIPE PLUG

TOP VIEW

THREADED CAP 12-4-70 DURIRON STAINLESS STEEL

NOTCHES FOR GRIPPING CAP

PART TITLE		REV
HIGH PRESSURE CELL		
MATERIAL STAINLESS STEEL		

DATE JUNE 30, 00	
SCALE NTS	
DWG NO. CELL 001	
NUMBER REQ. 1	
DWG BY L.L.B	

Appendix 2. Chromatograms for pentachlorophenol in carbon dioxide and water during partitioning experiments
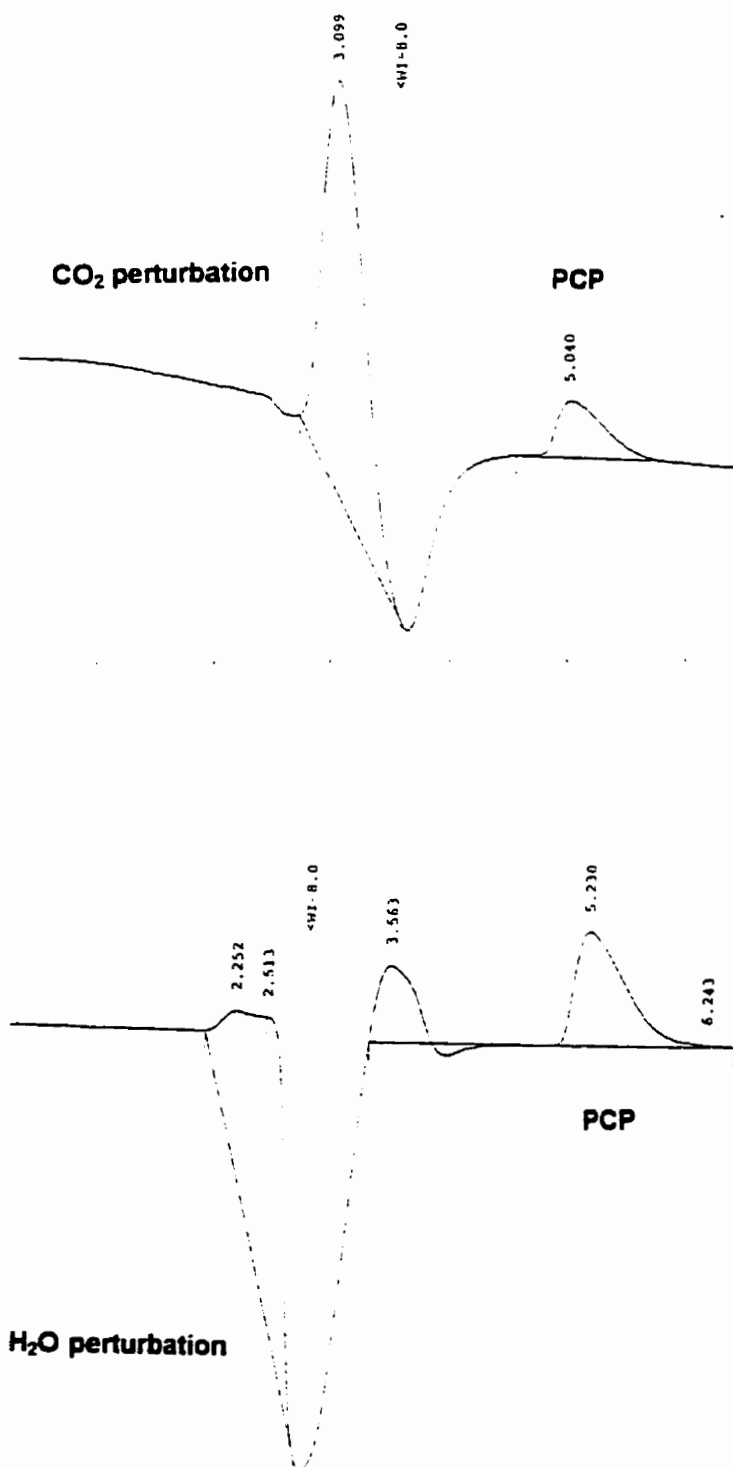
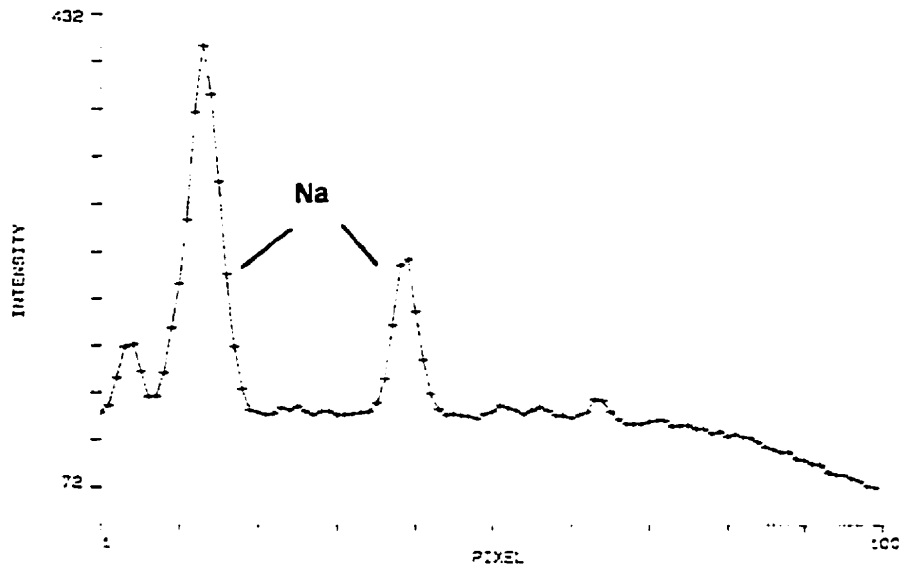## Appendix 3. Atomic emission spectra for sodium analysis

149

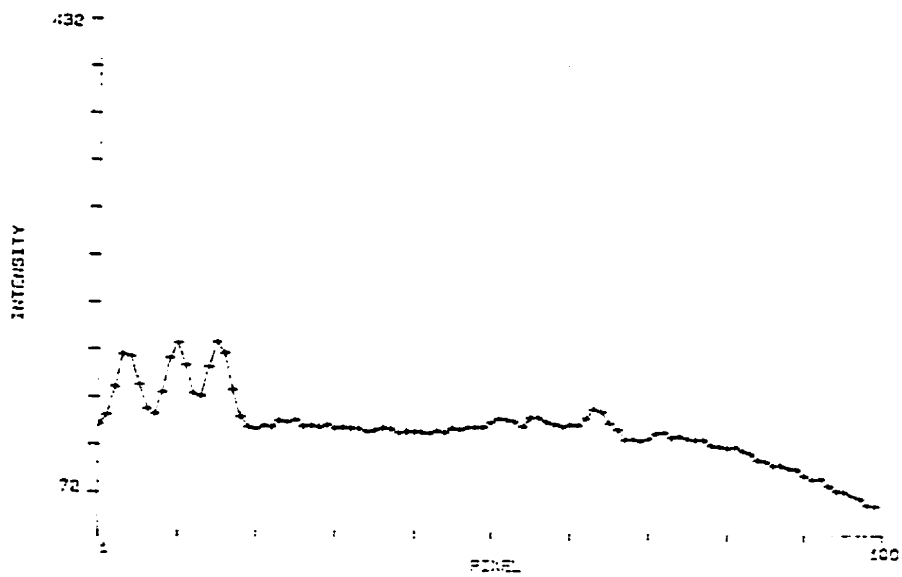IT= 60.000   LINEAR   SD590610.103

Sample

432

INTENSITY

72

PIXEL   100
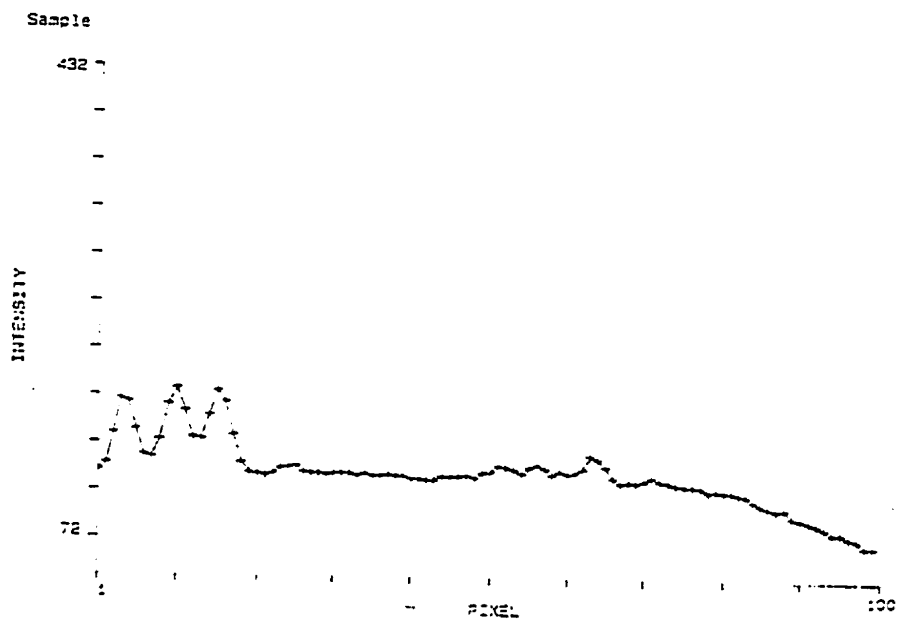
Appendix 4. Nuclear magnetic resonance spectra

Pentachlorophenol

Pentachlorophenol sodium salt

Sample